AEDC-TMR-95-P1

DEVELOPMENT AND OPERATION OF THE AEDC HIGH TEMPERATURE WALL LABORATORY (HTWL)

G. R. Beitel

Micro Craft Technology/AEDC Operations

April 1995

Approved for public release; distribution is unlimited.

ARNOLD ENGINEERING DEVELOPMENT CENTER
ARNOLD AIR FORCE BASE, TENNESSEE
AIR FORCE MATERIEL COMMAND
UNITED STATES AIR FORCE

Report Documentation Page

Form Approved
OMB No. 0704-0188

1. REPORT DATE **APR 1995**	2. REPORT TYPE	3. DATES COVERED **00-00-1995 to 00-00-1995**
4. TITLE AND SUBTITLE **Development And Operation Of The AEDC High Temperature Wall Laboratory (HTWL)**		5a. CONTRACT NUMBER 5b. GRANT NUMBER 5c. PROGRAM ELEMENT NUMBER
6. AUTHOR(S)		5d. PROJECT NUMBER 5e. TASK NUMBER 5f. WORK UNIT NUMBER
7. PERFORMING ORGANIZATION NAME(S) AND ADDRESS(ES) **Micro Craft Technology/AEDC Operations,Arnold Air Force Station,TN,37389**		8. PERFORMING ORGANIZATION REPORT NUMBER
9. SPONSORING/MONITORING AGENCY NAME(S) AND ADDRESS(ES)		10. SPONSOR/MONITOR'S ACRONYM(S) 11. SPONSOR/MONITOR'S REPORT NUMBER(S)

12. DISTRIBUTION/AVAILABILITY STATEMENT
Approved for public release; distribution unlimited

13. SUPPLEMENTARY NOTES

14. ABSTRACT
see report

15. SUBJECT TERMS

16. SECURITY CLASSIFICATION OF:			17. LIMITATION OF ABSTRACT	18. NUMBER OF PAGES	19a. NAME OF RESPONSIBLE PERSON
a. REPORT **unclassified**	b. ABSTRACT **unclassified**	c. THIS PAGE **unclassified**	**Same as Report (SAR)**	**115**	

Standard Form 298 (Rev. 8-98)
Prescribed by ANSI Std Z39-18

APPROVAL STATEMENT

This report has been reviewed and approved.

Jerry F. Fairchild

JERRY FRANK FAIRCHILD
Flight Dynamics Technology
Applied Technology Division
Test Operations Directorate

Approved for publication:

FOR THE COMMANDER

Robert T. Crook

ROBERT T. CROOK
Asst Chief, Applied Technology Division
Test Operation Directorate

SUMMARY

Backside water cooling is used extensively to transfer heat from critical elements in high heat flux devices such as hypersonic test facilities and nuclear reactors. IN such devices, efficient cooling is accomplished with high heat transfer coefficients resulting form the transition of the coolant from single phase convection to nucleate boiling at higher heat flux. Analytical modeling of the heat transfer mechanisms for the design of complex configurations becomes difficult in the boiling regime, especially at the critical heat flux (CHF) condition. Experimental investigation of the cooling process can provide the means to study the heat transfer mechanisms, evaluate parametric trends, and develop working correlations for the cooling configuration of interest. A flow boiling apparatus, called the High Temperature Wall Laboratory (HTWL), has been developed at the USAF/Arnold Engineering Development Center (AEDC) to perform experimental investigation of the cooling processes encountered in high-pressure, electric arc heater facilities. A summary of the development and operation of the apparatus and a discussion of initial experimental work using the apparatus is contained in this report.

TABLE OF CONTENTS

ILLUSTRATIONS

TABLES

NOMENCLATURE

A_{CS}	Test section cross sectional area, m^2 or ft^2
A_S	Test section outside surface area, m^2 or ft^2
B	Bias limit
CHF	Critical heat flux, W/m^2 or Btu/ft^2 sec
D_h	Hydraulic diameter, mm or in.
dT_{sub}	Degree of subcooling, °C or °F (T_{sat} - T_b)
E	Energy, kW
G	Mass velocity, kg/m^2 sec or lbm/ft^2 sec
h	Heat transfer coefficient, W/m^2 °C or Btu/ft^2 sec °F
HTL	High Temperature Laboratory
HTWL	High Temperature Wall Laboratory
I	Current, amps
I_{d-c}	d-c current, amps
I_{rms}	rms current, amps
L	Test section length, m or ft
p_{exit}	Test section exit pressure, bar or psi
$p_{suction}$	Back pressure on the high pressure demineralized water pump, bar or psi
$\dot{q}$	Heat flux, W/m^2 or Btu/ft^2 sec
$\dot{q}_{CALC}$	Calculated heat flux from temperature distribution finite difference routine W/m^2 or Btu/ft^2 sec
$\dot{q}_{SYS}$	Heat flux computed from temperature rise of coolant, W/m^2 or Btu/ft^2 sec
$\dot{q}_{TOT}$	Total heat flux computed from rectifier current and voltage, W/m^2 or Btu/ft^2 sec
$\dot{q}_{TS}$	Heat flux computed from rectifier current and test section voltage drop W/m^2 or Btu/ft^2 sec
R	Resistance, ohms
S	Standard deviation
T_b	Bulk coolant temperature, °C or °F
T_{sat}	Coolant saturation temperature, °C or °F
T_{wall}	Test section outside wall temperature, °C or °F
U_{RSS}	Root sum of squares uncertainty
V	Voltage, volts
V_{drop}	Test section voltage drop, volts
ρ_e	Electrical resistivity , ohm-m or ohm-ft

1.0 INTRODUCTION

The work reported herein was performed by Arnold Engineering Development Center (AEDC), Air Force Materiel Command (AFMC), under Program Element 65807F. The Air Force Program Managers were Capt. D. G. Burgess, Maj. H. Martin, and Capt. P. Zeman, DOT. The work was performed by Micro Craft Technology, support contractor for aerodynamic testing at AEDC, AFMC, Arnold Air Force Base, Tennessee. The work was performed in the Aerospace Systems Facility (ASF) and the Technology and Development Facility (TDF) under AEDC Project Number DD01 (Job Number 0115). The work was conducted during the period between 1 October 1989 and 30 September 1994.

Electric arc heaters have been used at the AEDC for the simulation of reentry flight heating at pressures up to 150 atm and mass average enthalpy of 4.65 - 9.3 x 10^6 J/kg (2000 - 4000 Btu/lbm) in air. Corresponding heat flux levels to the wall of the arc heater nozzles are as high as 9 x 10^7 W/m^2 (8,000 Btu/ft^2 sec), and future test conditions will require nozzles to survive 200 atm (Ref. 1) at heat flux levels up to 1.25 x 10^8 W/m^2 (11,000 Btu/ft^2 sec). Backside subcooled, forced convection cooling with high-pressure demineralized water is currently used to balance the heat load originating from the high temperature gas flowing through the nozzle (Fig. 1). In order to accommodate the higher heat loads, there is current interest in exploiting the backside water cooling concept to the limit of its capability. In addition to air-side heating prediction and favorable material characteristics, the thermostructural design of advanced nozzle concepts requires reasonable estimates of cooling heat transfer coefficients and limitations (i.e., burnout limit or critical heat flux condition) of water cooling as discussed in Ref. 2.

Efficient cooling of arc heater nozzles is accomplished with high heat transfer coefficients resulting from the transition of the coolant from single phase convection to nucleate boiling at higher heat flux. Analytical modeling of the heat transfer mechanisms for the design of complex configurations becomes difficult in the boiling regime, especially at the critical heat flux (CHF) condition. Experimental investigation of the cooling process can provide the means to study the heat transfer mechanisms, evaluate parametric trends, and develop working correlations for the cooling configuration of interest. A flow boiling apparatus, called the High Temperature Wall Laboratory (HTWL), has been developed at the USAF/AEDC to perform experimental investigation of the cooling processes encountered in high-pressure, electric arc heater facilities. A summary of the development and operation of the apparatus and a discussion of initial experimental work using the apparatus is contained in this report.

2.0 BACKGROUND

Once a cooling process has transitioned into boiling, theoretical approaches for determining heat transfer characteristics have limited application because of difficulties in obtaining interaction or interface properties of the two phases. Moreover, no theory has yet been created for forced convection, or flow, boiling burnout (Ref. 3). Many researchers have resorted to developing correlations based on microscopic bubble mechanisms, dimensional analysis, fairing of test data, or a combination of these. Reasonable confidence in predicting heat transfer information in the partial nucleate boiling and fully developed nucleate boiling regimes has been shown by Bergles and Rohsenow, Ref. 4, and Rohsenow, Ref. 5, respectively (see also Guglielmini, et al., Ref. 6); however, considerable disagreement between the large number of CHF correlations exists. Gambill (Ref. 7) compared several CHF correlations for water flow in a tube and found that prediction of CHF at higher coolant velocity using the correlations varied by nearly a factor of four and by a factor of two at lower velocity. Factors of two or greater between correlation predictions at higher coolant mass velocity have also been noted by Zeigarnik, et al. (Ref. 8) and Boyd (Ref. 9), and the disagreement tends to worsen as mass velocity increases. A recent comparison (Ref. 10) of fifty flow boiling CHF correlations at conditions anticipated in HTWL demonstrated the lack of agreement (factors of ten and greater between correlation predictions) and limitations of currently accepted CHF correlations. It should be pointed out that empirical CHF correlations typically have been derived for a specific range of experimental conditions, and extrapolation of a correlation outside the specific range can lead to very large errors. In addition, a given analytical CHF correlation typically has enough "adjustable" constants in the predictive equations to permit an acceptable correlation of a specific data set; however, general application of the correlation to various configurations or test conditions may result in significant errors (Ref. 11). As recommended in Refs. 10 and 12, among the more appropriate CHF correlations for subcooled, forced convection water flow are those proposed by Bernath (Ref. 13), Van Huff and Rousar (Ref. 14), Rousar (Ref. 15), Yagov and Puzin (Ref. 16), Levy (Ref. 17), and Labuntsov (Ref. 18). Many of the heat transfer correlations, from pure convection to burnout, have been incorporated in various computer models at AEDC.

Various flow boiling experiments performed in the past have provided insight to the boiling heat transfer mechanisms and parametric trends which have aided in the development of working correlations. Resistance heating, or Joule heating, has been used by boiling heat transfer researchers for a number of years to produce the necessary heat flux from a surface to be cooled (Ref. 12). The heat flux level is more easily determined from a simple energy balance in a Joule heating configuration, where other heating techniques such as secondary fluid heating (e.g., steam) or cartridge heaters introduce more complex energy conversion. Though numerous external flow boiling experiments have been performed (Ref. 3), boiling heat transfer is sensitive to the coolant flow geometry and heated wall configuration; therefore, internal flow boiling data on configurations closely representing arc heater nozzle cooling passages are more appropriate for the analysis of cooling processes in an arc heater configuration. Internal flow boiling has been studied primarily with tubes and annuli, where significant differences in heat transfer data have been noted between tubes and annuli of the same length and equivalent diameter (e.g., Refs. 19 and 20). In addition, more than 20 parameters have been identified that affect the CHF in flow boiling (Ref. 21). Further flow boiling experimentation is required because of the sensitivity of boiling heat transfer data to geometry and test conditions, and the large uncertainty resulting from the extrapolation of current boiling heat transfer correlations to the arc heater cooling requirements.

3.0 EXPERIMENTAL APPARATUS

In order to verify the predictive approaches and, if necessary, develop a more appropriate CHF correlation for the arc heater nozzle cooling conditions, an experimental boiling apparatus, called the High Temperature Wall Laboratory (HTWL), was developed at the AEDC. The desired heat flux at the surface/coolant interface on the inner wall of an annulus is achieved by passing high current through a thin-walled tubular metallic test section, thereby producing Joule heating. The annular configuration was selected for the experimental studies since it represents the coolant flow geometry of the current arc heater nozzles. Heat flux levels as high as 2×10^8 W/m^2 (18,000 Btu/ft^2 sec) are desired in the apparatus for the study of future nozzle concepts. This maximum heat flux level, coolant flow requirements anticipated in advanced nozzle concepts, instrumentation requirements for the definition of operating conditions, and reasonable machining size limitations dictate the overall size and configuration of the test section and support systems. A schematic of the apparatus and support systems is shown in Fig. 2. The AEDC engineering drawings for the HTWL are:

Electrical System	VU351559,VU351689,VUF51122, PY007294,PYT03801.52
Demineralized and Raw Water Systems	PY208422,PY208431,PY208484, PY208571,PY208648
Test Section Assembly	PY208423,PY208564,PY208632
Instrumentation	SKVY50475

Rapid Power Technologies Drawing No. 20712-W148 provides a schematic of the high energy power supplies used in the HTWL and discussed in the following section.

3.1 POWER REQUIREMENTS AND ELECTRICAL SYSTEM

The peak heat flux occurs near the throat of an arc heater nozzle where, for the baseline nozzle configuration under consideration, the inner diameter of the annular cooling channel is approximately one inch (Ref. 1). By selecting a low-cost, machinable, low electrical conductance metal such as 304 stainless steel (material properties given in Appendix 1), and following the computation approach outlined in Appendix 2, the power supply requirements necessary to achieve up to 2×10^8 W/m^2 (18,000 Btu/ft^2 sec) in a 25.4-mm (1-in.), 19-mm (0.75-in.), and a 12.7-mm (0.5-in.) diam tube are approximated as shown in Fig. 3[1]. As pointed out in Ref. 12, the heated wall material has been shown to have a possible effect on boiling heat transfer; therefore, consideration of the actual copper-zirconium (Amzirc®) nozzle material should be included. Because copper and its alloys have very high electrical conductivity, the materials require very high power in resistance heating to reach the heat flux levels identified above. Figure 4 illustrates the high power requirements for a 25.4-mm (1-in.), 19-mm (0.75-in.), and a 12.7-mm (0.5-in.) diam Amzirc tube.

Experimental results have shown that the type of power source (a-c vs. d-c) can significantly affect the boiling process (Ref. 12). Therefore, two 16,000-amp d-c rectifiers

---

[1]This analysis assumes a mean material temperature that is computed from the HTWL data reduction program discussed in Section 3.5 Data Reduction. The computation of the mean temperature requires an energy balance of the heated wall and cooling fluid, which is accounted for in the heat transfer data reduction. This mean temperature is used here to determine reasonable values of the material resistivity. Note that the same mean temperature is used for the different materials, i.e., no material effects on the heat transfer process is assumed.

manufactured by Rapid Power Technologies were selected for the HTWL test section heating. The rectifiers, when operated in a parallel mode, would provide up to 32,000 amps at 100 volts (3.2 MW) for heating of the HTWL test section. Specifically, the high heat flux condition discussed previously could be achieved with a 25.4-mm (1.0-in.) diam 304 stainless steel tube with a 0.76-mm (0.030-in.) thick wall (Fig. 3a). Material effects would be evaluated with 12.7-mm (0.5-in.) diam, 0.25-mm (0.010-in.) thick tubes[2] of various materials including Amzirc (Fig. 4c) and stainless steel (Fig. 3c). One disadvantage of the rectifiers is that peak performance is achieved when the rectifiers are operated at the peak voltage output of 100 volts. The test section length to be heated, material type, and internal temperature drives the voltage drop in the system; therefore, an optimum test section length of 150 mm (6.0 in.) was selected and an adjustable water-cooled ballast resistor bank was added to the electrical system to allow operation of the rectifiers at peak voltage output for improved power accuracy. When test sections with low voltage drop are used (e.g., Amzirc and copper), an additional voltage drop is set at the ballast resistor bank to operate the rectifiers near 100 volts. The actual uncertainty of the power levels provided by the rectifiers is discussed in Section 5.0 Performance and Data Uncertainty. Current loss into the cooling water of the resistor bank was determined to be negligible (less than 1 mA with raw water cooling). The rectifiers are routinely operated up to 100 percent (1.6 MW) power in the current control mode. Rectifier output from 1.6 MW to 3.2 MW requires operation in the voltage control mode with limited duration.

The mezzanine of the High Temperature Lab (HTL) was selected as the site for HTWL primarily because of the proximity of the 6900-v electrical feed required by the rectifiers and the high pressure demineralized water system in the building. Figure 5 shows the layout of the HTWL equipment positioned on the HTL mezzanine. The 6900-v electrical feed provides power to the rectifiers through a pad mounted switch which allows switching of the 6900-v feed between the HTWL rectifiers and the HTL spin coil rectifiers also located on the mezzanine. Power for the rectifier controls is supplied by the building 480-v system. The high current, low voltage power provided by the rectifiers is fed to the ballast resistor bank and test section assembly through eight 38-mm (1.5-in.) diam, 777.7 MCM insulated cables. The ballast resistor bank is made up of eight tubes (four for each rectifier) made of standard 19-mm (0.75-in.) diam Sch-40 304 stainless steel pipe. The insulated power cables are attached to the tube elements with copper lugs. Copper jumper plates between pairs of the tubes allow the length to be varied from zero to 2.75 m (9 ft). Such an arrangement allows voltage drops in the elements from zero to 80 volts to be set. Each pipe is electrically isolated from ground by Plexiglas® supports and high-pressure flexible hoses at the inlet and exit. The tube elements are cooled by low-pressure (7 bar or 100 psi) raw water through upstream and downstream manifolds. Details of the ballast resistor bank are shown in Fig. 6.

A ground fault protection system prevents the rectifiers from being started should a ground fault be present anywhere in the high energy electrical system. In addition, the ground fault system will phase back and shut down the rectifiers during operation if a ground fault occurs at any power setting. For example, during initial testing of a large diameter test section

[2]Extremely thin tubes (less than 0.25-mm thick wall) are difficult to instrument, easily damaged, and have higher voltage requirements than are capable with the selected rectifiers and are, therefore, not considered.

which had a small coolant flow annulus, the test section failed at burnout and bent against the stainless steel water jacket. Because the test section shell, and hence the water jacket, were grounded through the test stand (isolated later with Plexiglas spacers), a ground path for the high electrical energy occurred. The ground fault protection system detected the fault and shut down the rectifiers before significant damage to the hardware could occur. Because small current paths to ground typically exist in the HTWL circuit (e.g., conductance through the demineralized water adjacent to the energized test section) and the fact that the level changes with rectifier power setting, an adjustable trigger point for the ground fault system is provided.

3.2 COOLANT REQUIREMENTS AND DEMINERALIZED WATER SYSTEM

The existing closed loop high-pressure demineralized water system used by the AEDC arc facilities is capable of very high volumetric flows (2500 liters per min or 650 gpm) at a pressure up to 100 bar (1500 psi). Coolant velocity at the throat of the baseline nozzle configuration is approximately 30.5 m/s (100 fps) with a total mass flow rate of approximately 5 kg/sec (11 lbm/sec) or 300 liters per min (80 gpm). Future pumping requirements may necessitate higher pressure coolant flow; however, the high cost for such a system in a continuous flow facility will probably limit operation in the foreseeable future to coolant pressure below 100 bar. Therefore, the closed-loop high-pressure demineralized water system is adequate for constant coolant inlet temperature studies in the HTWL.

The closed loop circuit (Fig. 2a) incorporates an existing Bingham high pressure pump (Fig. 7) and heat exchanger located in the HTL, and connection to the high-pressure loop for HTWL supply/return is below the mezzanine near the H2 Arc Heater Facility. Because the existing closed loop water system pumps approximately 2500 liters per min (650 gpm), a bypass loop in the HTWL system allows mass flow variation over a broad range with the velocity being set at the test section by the annular flow area. Strainers with 0.254-mm (0.01-in.) mesh are located upstream and downstream of the test section to prevent contaminates from entering the test section or returning to the pump. Isolation valves in the HTWL/H2 flow loops permit quick changeover between the two installations. The entire circuit is constructed of 304 stainless steel except for short sections of high-pressure flexible hose used to electrically isolate the HTWL test section. A 51-mm (2-in.) diam throttling valve (Annin Co. globe valve) and Grove pressure regulator upstream of the test section and a 51-mm (2-in.) diam flow control valve (Kent Introl Ltd. globe valve with pneumatic positioner) downstream are use to adjust flow conditions at the test section and maintain flow stability in the circuit (see discussion in Ref. 12 concerning flow loop instabilities). A 51-mm (2-in.) diam Hoffer Flow Controls turbine flowmeter is installed upstream of the coolant pressure regulator and inlet manifold. High-pressure pump capabilities permit run times up to 30 minutes. The bulk coolant temperature is fixed at approximately room temperature and the water conductivity is limited to approximately 100 μS/cm. The dissolved oxygen content is typically 4 ppm or 31.5 percent of saturation. The water quality and temperature limitations of the existing closed loop system prompted consideration of a separate blowdown system for future testing in the HTWL. Such a system would allow for additional water treatment and control of the bulk coolant temperature so that subcooling could be held constant over a given pressure range.

The blowdown circuit (Figs. 2b and 5) incorporates two 2500-liter (650 gallon), stainless steel demineralized water storage tanks (Figs. 8a and 8b) that are pressurized by high pressure gaseous nitrogen from the HTL nitrogen bottle farm (Fig. 8c). The water storage tanks and nitrogen bottles are located outside the south wall of the HTL. Processed water provided by the facility demineralized water system is further processed by a separate Culligan DB Series water deionizer (Fig. 8d), permitting the water conductivity to be varied down to approximately 0.1 μS/cm. The deionizer is used to process the water as it is introduced at low pressure into the water storage tanks, and low conductivity is maintained until the run by recirculating the water through the deionizer and back to the tanks. The bulk coolant temperature may be varied from room temperature up to 95 °C (200 °F) through the use of a 30-kW submersible Chromalox (Model TMIS 6305E4) heater in each of the water tanks, which also provides a method to degas the water. The blowdown circuit, like the closed loop circuit, is constructed of 304 stainless steel except for short sections of high-pressure flexible hose used to electrically isolate the test section. The cooling water, upon exiting the test section and outlet manifold, is discharged into the large overhead sump line in the HTL building which terminates at the underground sump tank.

Run times in the blowdown circuit as long as 25 minutes are possible; however, they are limited to less than 10 minutes at flow rates above 8 kg/sec (18 lbm/sec). Coolant pressure may be varied up to 100 bar (1500 psi). As with the closed loop circuit, a significant pressure drop (i.e., larger than the test section pressure drop) is maintained just upstream of the test section assembly to provide flow stability. The blowdown circuit was not used during initial HTWL testing where data were obtained to provide for the definition of the performance envelope and operating characteristics of various support systems. Therefore, blowdown circuit operating characteristics and data are not discussed in this report.

3.3 TEST SECTION ASSEMBLY

The HTWL test section assembly (Fig. 9a) currently in use simulates the annular flow arrangement that is incorporated in the cooling passage of an arc heater nozzle. The actual arc heater nozzle and associated cooling passages are converging/diverging by design (Fig. 1), and, consequently, parameters such as the coolant mass velocity, static pressure, subcooling, acceleration, and heat flux distribution vary along the length of the nozzle. Because more than 20 parameters have been shown to influence flow boiling heat transfer and CHF (Refs. 12 and 21), the test section assembly in HTWL was designed such that individual parametric trends could be evaluated. Figure 9b shows a cutaway of the test section assembly, revealing the heated horizontal tubular test section and annular flow channel.

Electrical energy enters the assembly by way of eight large electrical cables clamped to four copper tabs on one end of the test section assembly. The energy passes through a copper flange and test section end piece to the test section which is electron beam welded to the copper end pieces. The electrical energy passes out of the assembly through a copper flange and cable attachments similar to the way it enters. All electrical conducting components of the test section assembly, except the test section tube, are fabricated from electrolytic tough-pitch copper. The nonconducting portions of the assembly are fabricated from 304 stainless steel and are insulated from the conducting components by Micarta® and C-11 glass/epoxy insulating materials. In addition, the entire test section assembly is insulated from the test stand/support structure by Plexiglas spacers. Cool-Amp Silver Plating Powder and Burndy Penetrox A Anti-Oxidation Coating are used where slip fit/electrical contact assembly is required. As shown in Fig. 9b, the downstream test section end piece includes a piston assembly to allow for test section thermal expansion which, in some cases, can be as large as 2.5 mm (0.1 in.).

The water coolant flow enters the test section assembly from high-pressure flexible hoses at four fittings spaced between the electrical connections (see Fig. 9b). The flow channels transition into a horizontal annular flow configuration that includes an entry length of at least ten hydraulic diameters for fully developing the flow prior to reaching the heated test section. Interchangeable water jacket sleeves (an example is shown in Fig. 10a) allow the annulus gap to be varied. Hydraulic diameters[3] of 3.8 mm to 7.1 mm (0.15 in. to .28 in.) were selected based on the test section sizes discussed in the following paragraph and a velocity range requirement of 15 to 61 m/s (50 to 200 fps). The water jacket sleeves are fabricated of 304 stainless steel or Delrin® AF resin/Teflon® fiber composite. The composite water jacket is used primarily for the small hydraulic diameter where arcing across the water gap may be possible. The coolant exits the test section assembly similar to the way it enters. A pressure relief valve connected to the annular flow channel protects the assembly from over-pressurization when large vapor voids are generated at test section burnout.

Three size test section tubes are currently in use: a 26-mm (1.024-in.) diam tube with a 0.76-mm (0.03-in) thick wall, a 19-mm (0.75-in.) diam tube with a 0.51-mm (0.02-in.) thick wall, and a 12-mm (0.45-in) diam tube with a 0.25-mm (0.01-in) thick wall. The smallest test sections are used primarily to evaluate the previously discussed wall material effects where copper and its alloys are much more difficult to electrically heat. Materials of interest include Amzirc, OFHC copper, Inconel® 600, and 304 stainless steel. Material properties of these materials are included in Appendix 1. The electrical resistivity of the materials from material property reference manuals was verified at elevated temperature in the AEDC Precision Measurement Equipment Laboratory. The largest diameter test sections (fabricated from 304 stainless steel) allow for assessment of cooling characteristics on test sections with diameters approximating actual arc nozzle throat diameters. To prevent continuous operation of the rectifiers at the high power conditions required by these two test section sizes, the intermediate size test sections (fabricated from 304 stainless steel) are used for a bulk of the HTWL parametric studies. The test sections are typically 150-mm (6-in.) long, although shorter lengths can be used to assess length effects. The intermediate size test sections are fabricated from stock tubing. All other test section tubes are fabricated using the EDM (electrical discharge machining) process at AEDC. A uniform surface finish between the test sections is maintained to prevent differing contributions of surface roughness on heat transfer. Typical rms roughness (measured with a Taylor-Hobson Surtronic 3P Surface Roughness Machine) on the outside surface of the tubes is approximately 0.76 to 0.91 μm (30 to 36 μin.). Wall thickness variations are determined with a Zeiss Coordinate Measurement Machine. Typical standard deviation for a

[3]For an annulus, the hydraulic diameter is defined as two times the annular gap, or the outer diameter minus the inner diameter.

24-point measurement on the 19-mm (0.75-in.) diam tube with a 0.51-mm (0.02-in.) thick wall is 0.005 mm (0.0002 in.). Each test section is filled with the low thermal conductivity epoxy, Sauereisen® 31, to prevent structural deformation due to the high water pressure, and to protect the internal instrumentation.

The tubular test sections are press fit onto the copper end pieces approximately 7.6 mm (0.3 in.). The initial method of using high temperature silver solder to attach the test section tubes to the copper end pieces was found to be unsuccessful when damage to internal instrumentation and leaks from the joints were noted in early testing. Subsequent joints made with the AEDC electron beam welding technique yielded satisfactory results. A hydrostatic pressure test bottle is used to leak check the test section welds prior to installation in the HTWL apparatus. Figure 10a shows a 19-mm (0.75-in.) diam, stainless steel test section welded to the electrolytic tough pitch copper end pieces, and a closeup of the electron beam weld is shown in Fig. 10b.

3.4 INSTRUMENTATION AND DATA ACQUISITION

Generally, the most important measurements to be made in a flow boiling apparatus are the coolant conditions, the energy dissipated at the test section, and the surface temperature of the test section. Instrumentation in the HTWL to monitor and record coolant temperature, pressure, and flow rate at various points in the flow circuit allows determination of the coolant conditions. This instrumentation includes absolute temperature (type T thermocouples) and pressure (0-2000 psi Viatran pressure transducers) measurements in the inlet and outlet coolant manifolds and differential temperature measurements between the manifolds. Coolant flow rate is determined from a 51-mm (2-in.) diam Hoffer Flow Controls turbine flowmeter installed upstream of the coolant pressure regulator and inlet manifold. In addition, the total flow rate and inlet/outlet pressures of the high-pressure demineralized water pump are monitored in the HTL main control room during a closed-loop HTWL run. When the blowdown circuit is used in the HTWL, the water temperature at three locations (top, middle, and bottom) in each of the two demineralized water storage tanks and the gaseous nitrogen supply pressure are recorded during a run. Absolute pressure of the coolant is measured with 0-2000 psi Teledyne Tabor pressure transducers at various axial locations (at the outside wall of the annulus) along the length of the test section. Coolant pressure drop (Statham Pressure Transducer) and a high speed pressure measurement (Kulite® Pressure Transducer) are also recorded at the test section.

Several methods are used to determine the power or energy existing at the test section. A discussion of the actual approaches used in determining various energy balances is included in Section 3.5 Data Reduction. Instrumentation used to support the energy balance computations include d-c current (internal rectifier shunt) and voltage for each rectifier, the total power produced by each rectifier (measured with a Ohio Semitronics Model PC8 Watt Transducer), the true rms current and voltage for each rectifier (measured with a Ohio Semitronics Model VT8 Variable Frequency Voltage Transducer), and the test section d-c voltage drop. The test section rms voltage drop is proportional to the average rms voltage for the rectifiers.

Probably the most difficult measurement is the surface temperature of the test section. Ideally, a surface temperature at the heated wall and coolant interface is desired for heat transfer analyses. In reality, an intrusive measurement would affect the wall heat transfer or disrupt the coolant flow pattern, and a non-intrusive measurement of surface temperature at the interface is very difficult, if not impossible, to make. In the HTWL test sections, no. 30 (0.25-mm or 0.01-in. diam) type K thermocouples are attached to the inside wall of the test section at various stations along its length permitting the coolant/wall interface temperature (on the opposite side of the wall) to be determined analytically. A discussion of the inferred coolant/wall interface temperature computations is included in the next section and Appendix 3. The thermocouples are typically spot welded to the wall of the larger diameter test sections and glued with the high thermal conductivity epoxy, Eastman P-10, in the smaller, thin-walled (0.25-mm thick wall) test sections. In both installations, one leg of the thermocouple is attached directly to the surface, and the junction is made approximately 0.75-mm (0.03-in) above the surface as recommended by Hughes in Ref. 22. This arrangement prevents erroneous temperature indications from a voltage drop produced by the current flow in the test section. No separation of the thermocouple wires from the tube surface caused by thermal expansion of the test section has been noted in posttest inspections. Steady-state temperature response from epoxied and spot-welded thermocouples on a representative test section compared within 1.1 °C (2 °F) in a laboratory oven up to 480 °C (900 °F). In addition, only a slight conduction effect due to the presence of the thermocouples was verified using the 2-D axisymmetric heat conduction program TRAX (Ref. 23). Teflon insulated thermocouples were used during initial testing; however, internal test section temperatures exceeded the vaporization temperature of the Teflon, and shorting of the thermocouple wires was experienced. The problem was alleviated by switching to braided glass insulated thermocouples, although, care had to be exercised when using the thermocouple wire in a damp environment. As mentioned previously, each test section is filled with the low thermal conductivity epoxy, Sauereisen 31, to provide additional protection to the internal thermocouple wires.

The critical heat flux in a flow boiling apparatus typically occurs at the most downstream location of the heated test piece, and surface temperature, therefore, is of primary interest at that location. Conduction heat transfer effects in the tubular test sections, caused by the presences of the copper end pieces, necessitate analytical modeling of the configuration for the determination of the best placement of the thermocouples near the ends of the test section for accurate temperature measurement. The 3-D thermostructural computer code, ANSYS®, is used to model the conduction heat transfer effects in the test sections of different size and material at various power levels. The code also allows for the inclusion of temperature sensitive material properties such as the thermal and electrical conductivities. Figure 11 shows a typical temperature distribution of a HTWL test section with the copper end pieces. It was found that placement of the thermocouples at least 10 mm (0.4 in.) from the ends of the heated portion of the test sections reduced the conduction effect to an acceptable level.

Additional instrumentation in the HTWL includes type T thermocouples on each ballast element. The thermocouples are electrically isolated from the current carrying ballast elements with thin mica sheets. Type T thermocouple probes in the raw water supply and return manifolds for the ballast resistor bank provide cooling water temperature monitoring. Analog pressure gages located in the demineralized water and raw water manifolds allow for quick assessment of water pressure conditions. Because of the high water pressure and high electrical energy present in the apparatus, a modular control room was installed on the HTL mezzanine near the HTWL apparatus (Figs. 5 and 12) to protect the HTWL data acquisition system, ground fault protection system, and personnel. Remote control of the rectifiers and operation of the HTWL flow control devices are possible from the control room. The thermocouple harnesses are twisted (approximately three turns per inch) and shielded between the apparatus and the control room to reduce interference caused by the proximity of the high current flow in the test section and electrical feed cables. In order to further isolate the test section thermocouple measurements, each signal is fed through a Preston Amplifier prior to sampling by the data acquisition system. Monitoring of the rectifier performance (a-c ripple effects) is accomplished with a rack-mounted Tektronix 8300 XWB Oscilloscope (Fig. 12) and a portable Tektronix 2445 Trigger Oscilloscope.

Approximately 60 channels of data are recorded during each run with a Neff Instrument Corp. Model 470 data acquisition system (Fig. 12). Steady-state data are typically recorded at 20 samples per sec for a 5-sec burst at each power setting. Thermocouple ice point references and system calibration are provided by the Neff, although external ice point references are required by the test section thermocouples since the Preston amplifiers are used. The raw data are converted to .PRN files by the Neff software for use in an external spreadsheet program. The Neff 470 also permits real time monitoring of pertinent measurements during a run. In addition, the Neff provides contact closures based on adjustable parameter limits for use as system interlocks. Currently, the Neff initiates rectifier shutdown if a low limit on demineralized water flow rate or a high limit on ballast resistor element temperatures are reached. A schematic of the data acquisition and monitoring systems is presented in Fig. 13.

3.5 DATA REDUCTION

HTWL data are reduced posttest on a Dell 425E personal computer and an IBM POWERstation work station. Each steady-state power setting data set is imported into a Microsoft® Excel spreadsheet using a command macro where running averages are performed on each of the measured parameters. An input file of the averaged values is then constructed for use in the FORTRAN data reduction program. The data reduction program, called HTWLDR, is used to compute various energy balances, demineralized water coolant conditions, total heat flux generated at the HTWL test section, and the steady-state internal temperature distribution in the test section.

Several methods are used to determine the power or energy introduced to the test section. One method involves an energy balance using the coolant mass flow and temperature rise measurements at the test section. Another method makes use of the current flow and the voltage drop across the test section. A slight variation of this method makes use of the test section material resistivity rather than the test section voltage drop. The actual power produced by each rectifier is measured with a Ohio Semitronics Model PC8 Watt Transducer for comparison with each of the energy computation methods mentioned. The heat flux based on the energy dissipated is then computed using the test section geometry.

An accurate calculation of the temperature distribution in the HTWL test section is required to determine the surface temperature at the test section wall/coolant interface. Initial methods used to compute the steady-state temperature distribution included a simple integration of the steady-state 1-D planar and radial conduction heat transfer equations with uniform volumetric heat generation. Because the methods assume constant material properties and little effect of the extreme convection boundary condition, a more appropriate 1-D axisymmetric finite difference approach was chosen to achieve higher accuracy. The approach allows for temperature dependent material properties (thermal and electrical conductivity), and hence, nonuniform internal heat generation. In addition, the flow of current is allowed to redistribute within the wall thickness depending on the local material resistance. An adiabatic wall is assumed on the inside surface of the test section where the low thermal conductance epoxy is present in the actual configuration. An initial estimate of the convective heat transfer coefficient on the outside surface of the test section is obtained from the boiling heat transfer program COOLWL. Gauss-Seidel iteration with relaxation is used to reach a steady-state temperature solution. Once a temperature distribution solution meeting the selected error criteria is reached, the convective heat transfer coefficient is adjusted until the computed inside surface temperature matches the experimentally measured wall temperature from the test section thermocouples. The coefficient adjustment procedure may be bypassed if the measured wall temperature is known to be in error.

Because of possible voltage losses in the actual HTWL hardware, an option is included in the HTWLDR program to adjust the input test section voltage drop such that the final calculated total current matches the measured current at a given power level from the HTWL experiment. An additional total heat flux value is computed from summation of the individual element heat fluxes in the finite difference temperature calculation. This heat flux value and the value computed from the energy balance using the coolant mass flow and temperature rise measurements at the test section are probably the most accurate heat flux calculations.

A more complete discussion of the data reduction equations and a listing of the HTWLDR program and input file are provided in Appendix 3. Sample tabulated raw data and reduced data are presented in Appendix 4.

4.0 TEST PROCEDURE

Installation and removal of the HTWL test section are relatively straightforward. The electrical contact surfaces of the test section copper end pieces (including the downstream piston assembly) are coated with Cool-Amp Silver Plating Powder and Burndy Penetrox A Anti-Oxidant to prevent arcing between the slip fit surfaces. The downstream end piece cap is then installed. Following the cleaning of the test section surface with denatured alcohol, the two halves of the water jacket are assembled around the test section. The assembly is then slipped into the test section assembly shell (Fig. 9b) assuring that the alignment pin hole in the water jacket is aligned with the alignment pin port on the shell. Once aligned, the alignment pin is installed with the appropriate o-ring. The stainless steel upstream cap and copper downstream cap are installed with the appropriate o-rings. Concentricity of the test section with the water jacket is verified by measuring the distance from selected instrumentation port faces to the test section with a depth gage. Hookup of the test section thermocouples to the permanent thermocouple patch panel completes the installation. Removal of the test section upon test completion is accomplished in the reverse order.

The HTWL demineralized water circuit is filled using the HTL 57 liters per min (15 gpm) makeup pump (Union Pump Co. Model TD-50) and venting air out of the circuit through the vent valves on top of the HTWL test section and inlet and outlet manifolds. Once the circuit is filled (water discharge from vent lines), the vent valves are closed and the circuit is pressurized to 34.5 bar (500 psi) using the makeup pump for leak check purposes. The ballast resistor bank is adjusted to the desired length based on the voltage drop anticipated at the test section. Low pressure raw water flow is established at the ballast resistor bank. The HTWL control room power, rectifier control power, data acquisition system, and computer are turned on, and instrumentation calibration is initiated using the Neff data acquisition system. Operation of the HTWL apparatus necessitates the evacuation of the HTL building and fenced area except for the HTWL and main control rooms.

A typical run sequence begins with the manual startup of the rectifier cooling fans. Water flow through the apparatus is established using the HTL high pressure demineralized water pump. The coolant flow rate and pressure at the test section are then adjusted to the planned test condition. The ground fault panel is then reset prior to rectifier startup. Electrical power to the test section is initiated by closing the power feed circuit breaker, starting each rectifier at a low output level, and slowly increasing power to the first set point. Following stabilization of various measurements, approximately 5 seconds of data are acquired with the Neff data acquisition system, after which the power is slowly increased to the next power set point. At least two power cycles are performed with each test section prior to burnout to assess aging effects or identify other data hysteresis. The estimated CHF (based on pretest predictions and data acquired previously at the same test conditions) is approached slowly with small increments in power until the test section fails at burnout. Test section failure is accompanied by a change in power demand from the rectifiers which, in turn, phases back the rectifiers to a negligible power setting prior to shutdown. The use of a burnout detector to prevent test section destruction is not possible because of the speed and intensity of the transition from nucleate to film boiling (Ref. 12). Demineralized water conductivity and dissolved oxygen content levels are recorded prior to and after each run with an Omega Engineering Inc. Model PHH-10 Conductivity/Temperature/PH Meter and a Cole Parmer Model 5946-70 Dissolved Oxygen Meter, respectively. The following list of procedures are used for the setup and operation of the HTWL apparatus:

OP-SC-C7PHT-WL-000001	Operating Sequence - Closed Loop
OP-SC-C7PHTWL-000002	Electrical Preop
OP-SC-C7PHTWL-000003	Demineralized Water System Preop - Closed Loop
OP-SC-C7PHTWL-000004	Ballast Resistor Low Pressure Raw Water Preop
OP-SC-C7PHTWL-000005	HTWL Electrical Postop

OP-SC-C7PHTWL-000006	Demineralized Water System Postop - Closed Loop
OP-SC-C7PHTWL-000007	Ballast Resistor Low Pressure Raw Water Postop
OP-SC-C7PHTWL-000008	Operating Sequence - Open Loop
OP-SC-C7PHTWL-000009	Nitrogen Pressurization Preop
OP-SC-C7PHTWL-000010	Demineralized Water System Preop - Open Loop
OP-SC-C7PHTWL-000011	Nitrogen Pressurization Postop
OP-SC-C7PHTWL-000012	Demineralized Water System Postop - Open Loop
OI-IC-00676-164901	Neff Data Acquisition System

5.0 SYSTEM PERFORMANCE AND DATA UNCERTAINTY

Initial test results obtained after shakedown and checkout of the HTWL aided in the definition of the performance envelope and operating characteristics of various support systems. As stated previously, all of the HTWL testing to date has been performed using the closed loop circuit and the HTL high pressure demineralized water pump. Figure 14 presents the flow performance envelope for the three test sections discussed in Section 3.3. The available volumetric flow rate at a given inlet manifold pressure measured just upstream of the HTWL test section is shown in Fig. 14a and at a given test section exit pressure (burnout location) in Fig. 14b. The water jackets selected for each test section provided for hydraulic diameters of 3.76 mm (0.148 in.) for the 26-mm (1.024-in.) diam tube, 5.08 mm (0.2 in.) for the 19-mm (0.75-in.) diam tube, and 7.06 mm (0.278 in.) for the 12-mm (0.45-in) diam tube. The optimum setting for the demineralized water bypass valve, which resulted in the highest mass flow achievable yet providing for safe starting and operation of the high pressure pump, was found to be one-fifth open. Generally, the highest output pressures from the HTL high pressure demineralized water pump are achieved with a makeup pump suction pressure of 48.3 bar (700 psi). Higher pressures are attainable at the higher flow rates; however, the pump is limited to operation below 124 bar (1800 psi) at the pump discharge or approximately 114 bar (1650 psi) at the inlet manifold.

Rectifier performance is presented in Fig. 15. Each of the two rectifiers was operated in the current control mode up to 100-percent power output by installing a solid copper test section and using the maximum available ballast resistor length. Shown in Fig. 15a are the d-c current output and rms current output (the actual output of each rectifier made up of the d-c signal with an a-c component riding on the d-c waveform) for each rectifier. Also included in the figure are the combined d-c and rms current outputs of the two rectifiers since power requirements typically necessitated the parallel operation of the rectifiers. Figure 15b shows the power output of the rectifiers up to 100-percent. Voltage limitation of the ballast resistor bank prevented the output of the full 1.6 MW of power at 100-percent for the solid test section. As mentioned previously, the rectifiers may be operated up to 200-percent for limited run times.

The ballast resistor voltage and surface temperature characteristics as a function of rectifier rms current are presented in Fig. 16. As in the rectifier performance checks, a solid copper test section with a negligible voltage drop was used to obtain the ballast resistor characteristics. The maximum voltage drop that can be obtained across the ballast resistor elements is 80 volts (Fig. 16a). Surface temperatures on the elements remain below 140°C (300°F) as shown in Fig. 16b.

Electromagnetic fields generated by the high power electrical systems were of concern for personnel safety and control room equipment reliability, and were evaluated during initial testing in HTWL. Magnetic flux density (MFD) measurements were performed with a F. W. Bell Model-9500 Gaussmeter in order to quantify the level of electromagnetic interference in the HTWL control room during rectifier operation. Figure 17 presents the a-c (unfiltered) and d-c MFD measurements as a function of total rectifier power. The a-c MFD did not change with rectifier operation or measurement location in the control room; however, d-c MFD measurements showed considerable effects of rectifier power level and location of the measurement within the control room. The maximum d-c MFD levels were recorded near the floor of the control room, and are shown in Fig. 17 along with the maximum values recorded at chest height throughout the room. No differences in the MFD levels were detected with the absence of 6900-v power fed to the HTL building and with 6900-v power to the rectifiers with zero output (i.e., no change in MFD levels with or without the presence of the 6900-v power feed).

Figure 18 presents typical data acquired in the HTWL for a 19-mm (0.75-in) diam, 304 stainless steel test section at the noted test conditions. The curve presented in Fig. 18a is a pretest prediction of the boiling curve using Kays and Leung (Ref. 24) correlation for pure forced convection, Bergles and Rohsenow (Ref. 4) correlation for transition from pure convection to fully developed nucleate boiling, and the Rohsenow (Ref. 5) nucleate boiling correlation in the boiling regime. As can been seen in Fig. 18a, lower wall temperatures have been noted in the experiments than are predicted by the above correlations; however, good agreement is shown near burnout. A possible cause for the discrepancy may be the inaccuracy in the wall temperature measurement. As noted previously, care had to be exercised in preventing the braided glass insulation from becoming wet. The presence of a small amount of moisture on the thermocouple leads resulted in considerable noise in the temperature measurements. A possible correction for the moisture problem would be to incorporate metallic sheathed thermocouple leads. Future tests in the facility will address the disagreement between the pretest prediction and test data. The CHF predictions from the correlations of Bernath (Ref. 13), Van Huff and Rousar (Ref. 14), Rousar (Ref. 15), Yagov and Puzin (Ref. 16), Levy (Ref. 17), and Labuntsov (Ref. 18) are also shown in Fig. 18a. The CHF occurred at the most downstream station of the test section, and therefore, the data presented in the figure were measured at that particular station. The correlations of Labuntsov and Rousar best predicted the CHF in this particular test; however, neither correlation included data from annular configurations. Redundant CHF data at the same conditions from future tests will aid in the evaluation of the current prediction capability.

Figure 18b shows a comparison of the various heat flux calculations. The total heat flux (subscript TOT) from the hardware is determined from the rms current and voltage measured at the rectifiers and, therefore, has the largest value because of energy losses in the electrical cables, ballast resistor, and attachments. The test section measured heat flux (subscript TS) is determined similarly to the total heat flux except that the rms voltage drop across the test section assembly is used instead of the rectifier voltage. The heat flux computed from the coolant temperature rise through the test section (subscript SYS) and the heat flux calculated from a summation of the element internal heat generation in the finite difference routine (subscript

CALC) are probably the most accurate and agree within 6 percent at all but the lowest power settings.

Typical dependance of the pressure drop across the test section assembly on heat flux is illustrated in Fig. 18c. As heat flux is initially increased, the pressure drop decreases because of decreasing friction factor (see Ref. 25). As boiling begins and becomes well established, the pressure drop increases. As can be seen in Fig. 18c, the pressure drop across the 150-mm (6-in.) long test section is small at the elevated pressure and velocity for the particular test.

The effects of boiling at elevated heat flux has not been detected in the form of pressure oscillations. Figure 18d presents typical high speed pressure measurements for low power settings where no boiling could exist and higher settings where boiling was suspected. Only slight differences between the nonboiling and boiling results can be seen in the figure.

Burnout of the test sections typically occurred at the most downstream location of the heated tube as shown in Fig. 19. Because the bulk fluid temperature is highest and the thermal boundary layer is largest at this location, it follows that the cooling would be less efficient thereby promoting burnout. However, during preliminary testing in the HTWL, a few burnouts occurred at the most upstream location on the test pieces. Typically, the upstream burnouts occurred at lower power settings indicating premature failure due to structural anomalies or an inadequate weld. Such problems would cause coolant leakage to the interior of the test piece, deterioration of the internal epoxy support, and eventual collapse and melting of the heated tube wall.

The rectifier ripple, or the a-c component which rides on the d-c output signal, contributes a significant amount to the uncertainty of the instantaneous power output of the rectifiers. The ripple for the two rectifiers was measured during the rectifier performance checks using the solid test section described previously. The measured ripple for each rectifier is shown in Fig. 20a, and the actual waveforms are presented in Fig. 20b. Because the rectifiers are operated near the maximum voltage output of 100 volts, the ripple accounts for approximately 5 to 7 percent uncertainty in the instantaneous power output. The uncertainty may be reduced to approximately 2 percent of reading at all voltage levels by the addition of a Rapid filter assembly to each rectifier. Use of rms values for rectifier current and voltage in the dissipated energy and heat flux equations minimize the effects of ripple on the time-averaged data uncertainty. Uncertainty in the rms current and voltage is primarily measurement device and data system inaccuracies.

Additional factors which contribute to the uncertainty in the energy dissipated at the test section include variations in the test section wall thickness and material properties. The wall thickness variations are determined by the AEDC Precision Inspection Laboratory as described in Section 3.3. The test section material density and electrical resistivity from literature were verified by personnel in the AEDC Precision Measurement Equipment Laboratory. Uncertainty of the test section wall thickness and material properties along with measurement uncertainty of other instrumentation used in the HTWL are included in Table 1a.

In general, instrumentation calibration and data uncertainty estimates were made using methods recognized by the National Institute of Standards and Technology (NIST). Measurement uncertainty is a combination of bias and precision errors defined as:

$$U_{RSS} = \pm [(B)^2 + (2S)^2/n]^{1/2}$$

where U_{RSS} is the root sum of squares uncertainty, B is the bias limit, S is the standard deviation about a mean value of the measurement process, "n" is the number of experiment periods from which the samples were used in determining the mean value (taken here to equal one), and the multiplier "2" assumes 10 or more samples associated with S and is used to ensure a 95-percent coverage for the uncertainty limits.

In addition to the uncertainty, the type and range of measuring device, the type of recording device, and the method of calibration for each measurement are provided in Table 1a. Propagation of the bias and precision errors of measured data through the calculated data was made in accordance with Ref. 26 and the results are presented in Table 1b.

6.0 CONCLUDING REMARKS

In conclusion, a new high heat flux, flow boiling apparatus for the study of cooling effectiveness has been developed at the AEDC. The current application of HTWL is for the evaluation of cooling processes encountered in high-pressure, electric arc heater facilities, particularly arc heater nozzles. The facility is capable of providing up to 3.2 MW of power to a metallic test section, simulating heat flux levels in excess of 2×10^8 W/m^2 (18,000 Btu/ft^2 sec), with a water flow rate up to 9 kg/sec (20 lbm/sec) at pressure up to 100 bar (1500 psi). The current test section configuration allows for the determination of parametric effects in annular flow, and a closed flow loop or blowdown circuit are available for various parameter ranges. Early heat transfer data from HTWL show some disagreement with pretest predictions in the fully developed nucleate boiling regime and at CHF. Therefore, additional testing in the HTWL is required such that more accurate prediction of cooling requirements for actual arc heater nozzles may be accomplished.

REFERENCES

1. Shope, F.L. "Conceptual Thermal Design of a 200-atm, Water-Cooled Arc Heater Nozzle," AIAA-93-2879, presented at the AIAA 28th Thermophysics Conference in Orlando, FL, July 1993.
2. Shope, F.L. "Conjugate Conduction/Convection/Nucleate-Boiling Heat Transfer with a High-Speed Boundary Layer," J. of Thermophysics and Heat Transfer, Vol 8, No 2, April-June 1994, pp. 275-281.
3. Lienhard, J.H. "Burnout on Cylinders," J. of Heat Transfer, Vol 110, November 1988, pp. 1271-1286.
4. Bergles, A.E. and Rohsenow, W.M. "The Determination of Forced-Convection Surface-Boiling Heat Transfer," J. Heat Transfer, Vol 86, August 1964, pp. 365-372.
5. Rohsenow, W.M. "Heat Transfer with Evaporation," Heat Transfer... A Symposium, Summer 1952, Chapter 4, Eng. Res. Inst., Univ. of Mich., Ann Arbor, published in 1953, pp. 101-149.
6. Guglielmini, G., Nannei, E., and Pisoni, C. "Survey of Heat Transfer Correlations in Forced Convection Boiling," Multiphase Transport - Fundamentals, Reactor Safety, Applications, edited by T.N. Veziroglu, Vol 1, 1980, pp. 845-861.
7. Gambill, W.R. "Burnout in Boiling Heat Transfer - Part II. Subcooled Forced-Convection Systems," Nuclear Safety, Vol 9 No 6, November-December 1968, pp. 467-480.
8. Zeigarnik, Yu.A., Privalov, N.P., and Klimov, A.I. "Critical Heat Flux with Boiling of Subcooled Water in Rectangular Channels with One-Sided Supply of Heat," Thermal Engineering, Vol 28 No 1, 1981, pp. 40-43.
9. Boyd, R.D. "Subcooled Flow Boiling Critical Heat Flux (CHF) and Its Application to Fusion Energy Components. Part II. A Review of Microconvective, Experimental, and Correlational Aspects," Fusion Technology, Vol 7, January 1985, pp. 31-52.
10. Beitel, G.R. "Estimation of Critical Heat Flux in the High Temperature Wall (HTWL) Experiment," Memo for Record dated 9 July 1992.
11. Bergles, A.E. "Burnout in Boiling Heat Transfer. Part II: Subcooled and Low-Quality Forced-Convection Systems," Nuclear Safety, Vol 18 No 2, March-April 1977, pp. 154-167.
12. Beitel, G.R. "Boiling Heat Transfer Processes and Their Application in the Cooling of High Heat Flux Devices," AEDC-TR-93-3 (ADA266086), May 1993.
13. Bernath, L. "A Theory of Local-Boiling Burnout and Its Application to Existing Data," Chem. Engng Progr. Symp. Series, Vol 56, No 30, 1960, pp. 95-116.
14. Van Huff, N.E. and Rousar, D.C. "Ultimate Heat Flux Limits of Storable Propellants," 8th Liquid Propulsion Symposium, CPIA Report 121, Vol II, 1966.
15. Rousar, D.C. "Correlation of Burnout Heat Flux for Fluids at High Velocity and High Subcooling Conditions," M.S. Thesis, Univ. of California Davis, 1966.
16. Yagov, V.V. and Puzin, V.A. "Burnout Under Conditions of Forced Flow of Subcooled Liquid," Thermal Engng, Vol 32, No 10, 1985, pp. 569-572.
17. Levy, S. "Prediction of the Critical Heat Flux in Forced Convection Flow," General Electric Report GEAP-3961, June 1962.

18. Labuntsov, D.A. "Critical Thermal Loads in Forced Motion of Water Which is Heated to a Temperature Below the Saturation Temperature," Sov. At. Energy, Vol 10, No 5, March 1962, pp. 516-518.

19. Becker, K.M. and Hernborg, G. "Measurement of Burnout Conditions for Flow of Boiling Water in a Vertical Annulus," J. Heat Trans., August 1964, pp. 393-407.

20. Zenkevich, B.A., Kirillov, P.L., Alekseev, G.V., Peskov, O.L., and Sudnitsyn, O.A. "Heat Transfer Burnout in Water Flow Through Round Tubes and Annuli," Proc. 4th Intl Heat Trans. Conf., Vol VI, Paper no. B6.13, 1970.

21. Boyd, R.D. "Subcooled Flow Boiling Critical Heat Flux (CHF) and Its Application to Fusion Energy Components. Part I. A Review of Fundamentals of CHF and Related Data Base," Fusion Technology, Vol 7, January 1985, pp. 7-30.

22. Hughes, T.G. "Critical Heat Fluxes for Curved and Straight Surfaces During Subcooled Flow Boiling," PhD Thesis Penn State Univ. TM-74-194 (AD/A-003 036), June 1974.

23. Rochelle, J.K. "TRAX-A Finite Element Computer Program for Transient Heat Conduction Analysis of Axisymmetric Bodies," MS Thesis, University of Tennessee, June 1973.

24. Kays, W.M. and Leung, E.Y. "Heat Transfer in Annular Passages - Hydrodynamically Developed Turbulent Flow with Arbitrarily Prescribed Heat Flux," Int. J. Heat Mass Trans., Vol 6, 1963, pp. 537-557.

25. Bergles, A.E. and Dormer, T., Jr. "Subcooled Boiling Pressure Drop with Water at Low Pressure," Int. J. Heat Mass Trans., Vol 12, 1969, pp. 459-470.

26. Abernethy, R.B. et al. and Thompson, J.W. "Handbook Uncertainty in Gas Turbine Measurements," AEDC-TR-73-5 (AD755356), February 1973.

27. Aerospace Structural Metals Handbook, Vol 4, Baitelle - Columbus Lab., Purdue Publishing, 1993.

28. ASM Handbook, Vol 2, Properties and Selection: Nonferrous Alloys and Special-Purpose Materials, ASM International, 1992.

29. Thermophysical Properties of Matter, Vol 1, Thermal Conductivity - Metallic Elements and Alloys, Plenum Publishing, New York, 1970.

30. Thermophysical Properties of Matter, Vol 4, Specific Heat - Metallic Elements and Alloys, Plenum Publishing, New York, 1970.

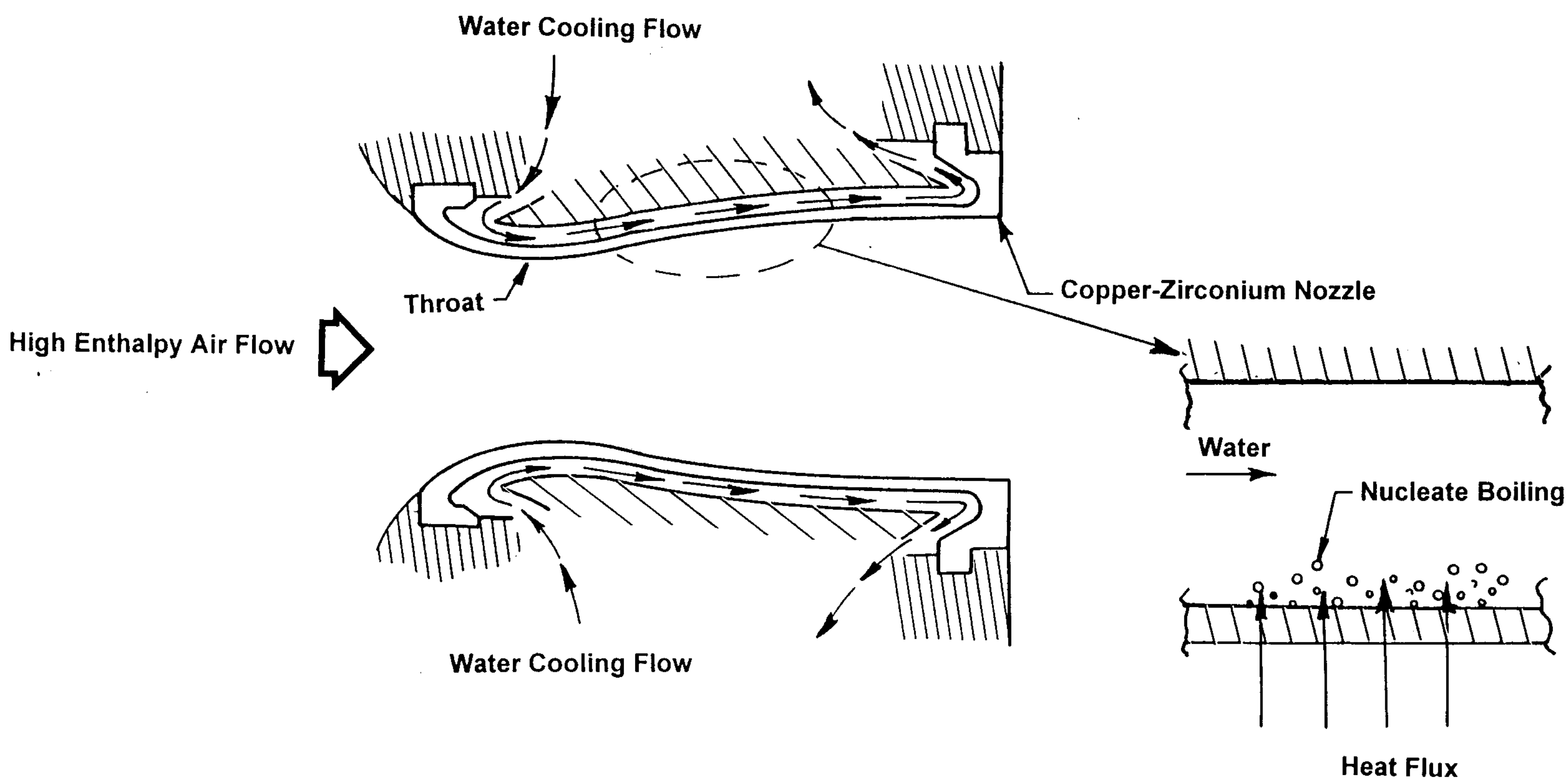

Figure 1. Arc Heater Nozzle Heating/Cooling

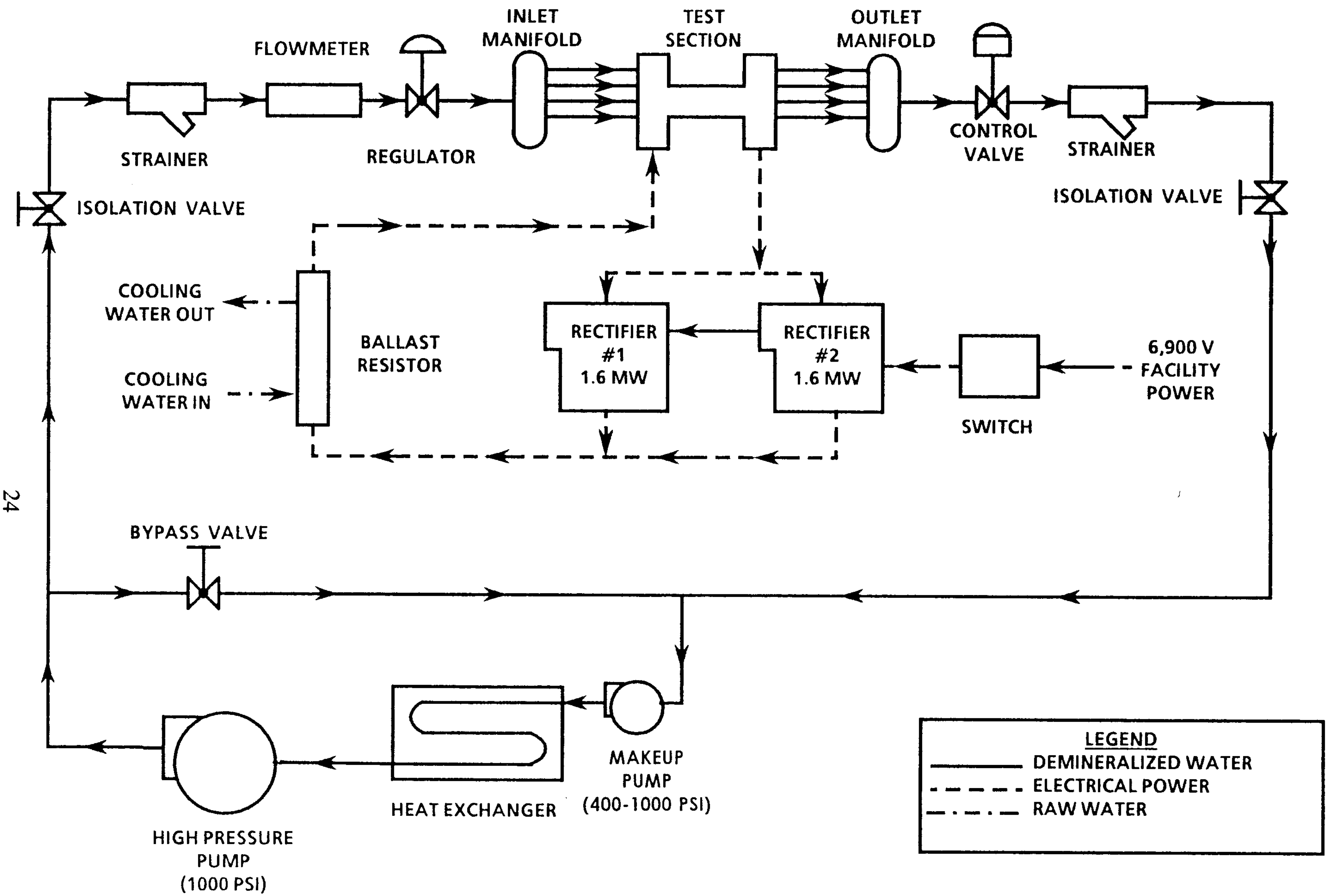

a. Continuous Flow Circuit

Figure 2. HTWL System Schematic

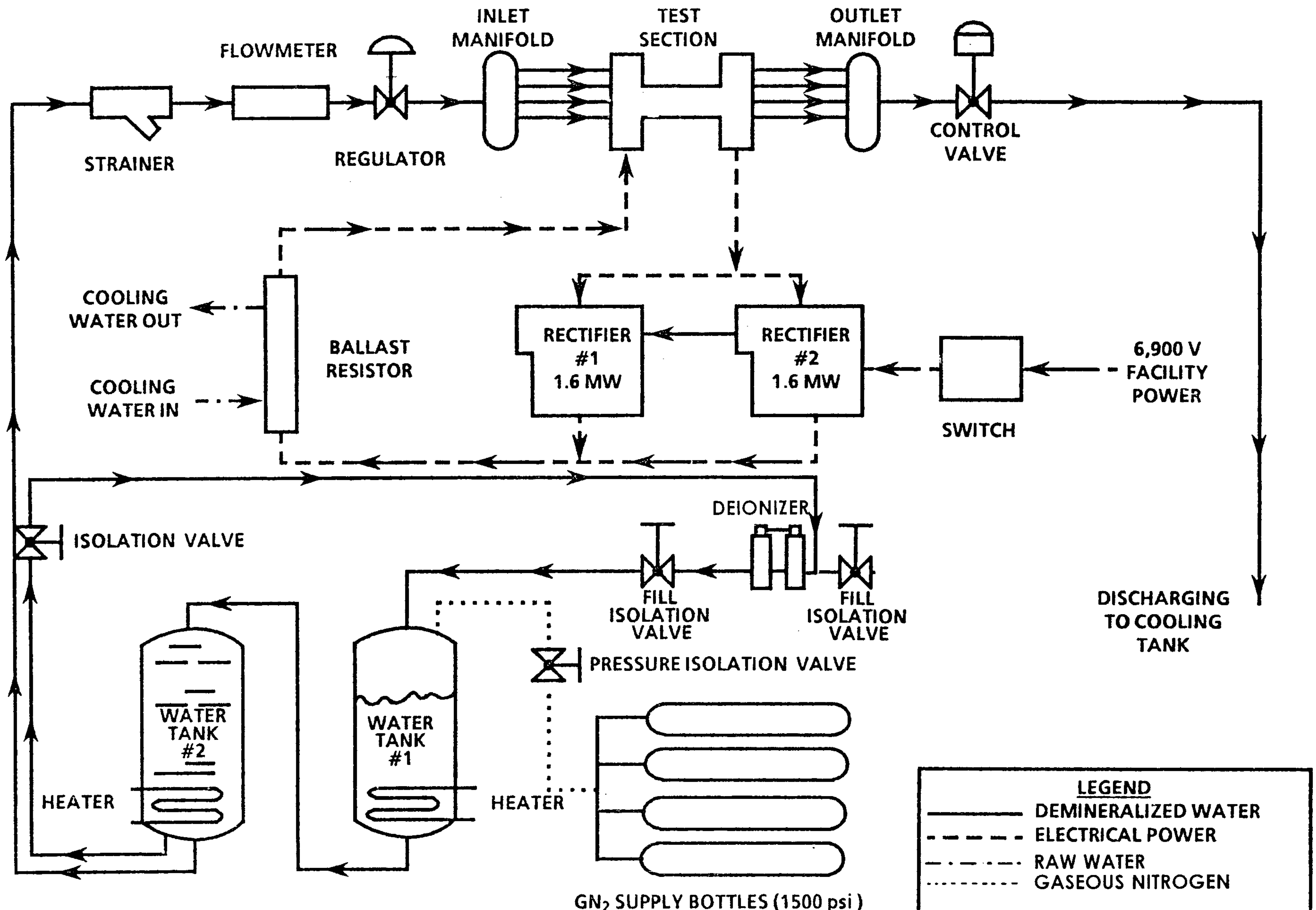

b. Blowdown Flow Circuit
Figure 2. Concluded

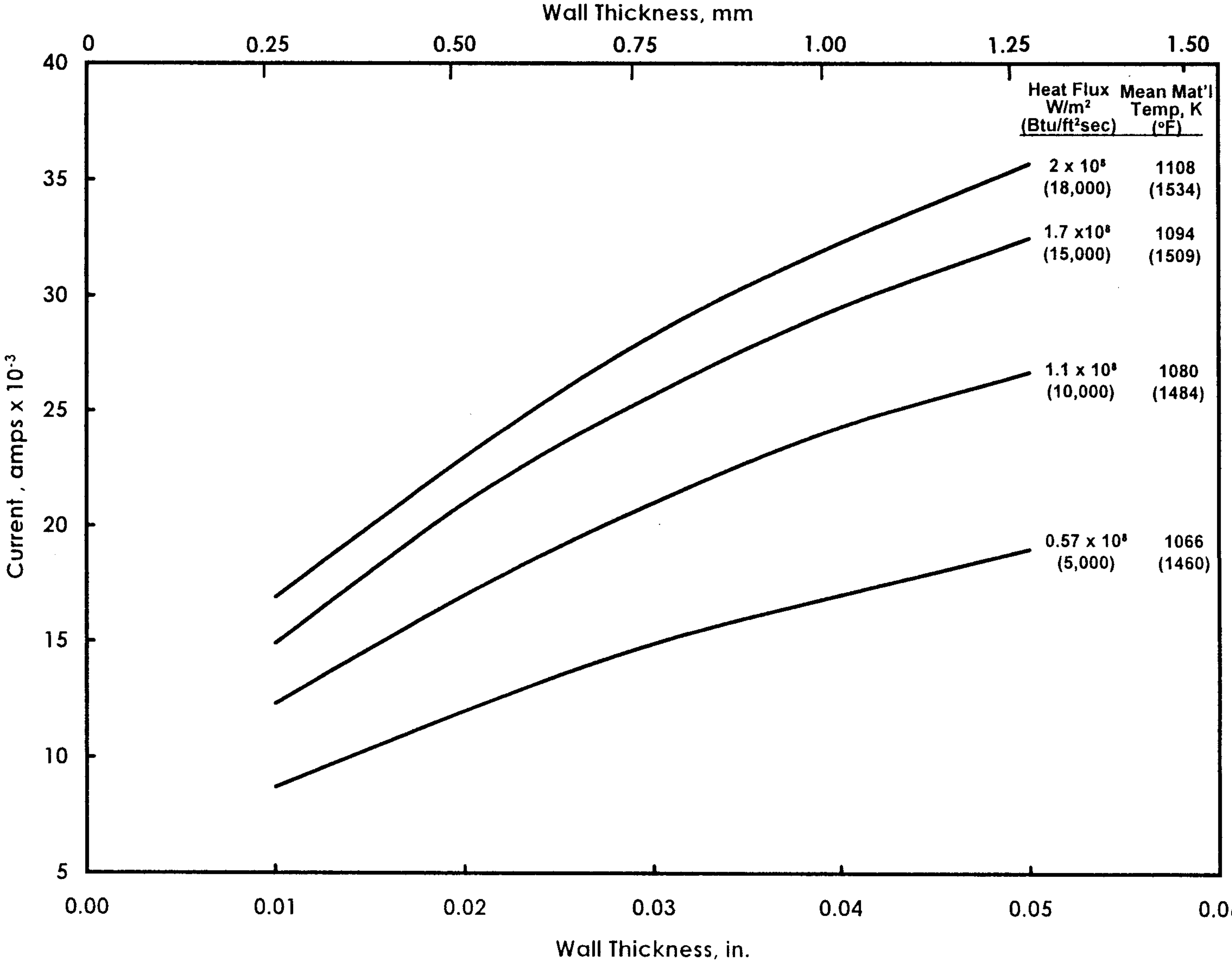

a. Outside Diameter of 1 in. (25.4 mm)

Figure 3. Power Supply Requirements for an Electrically-Heated Stainless-Steel Tube

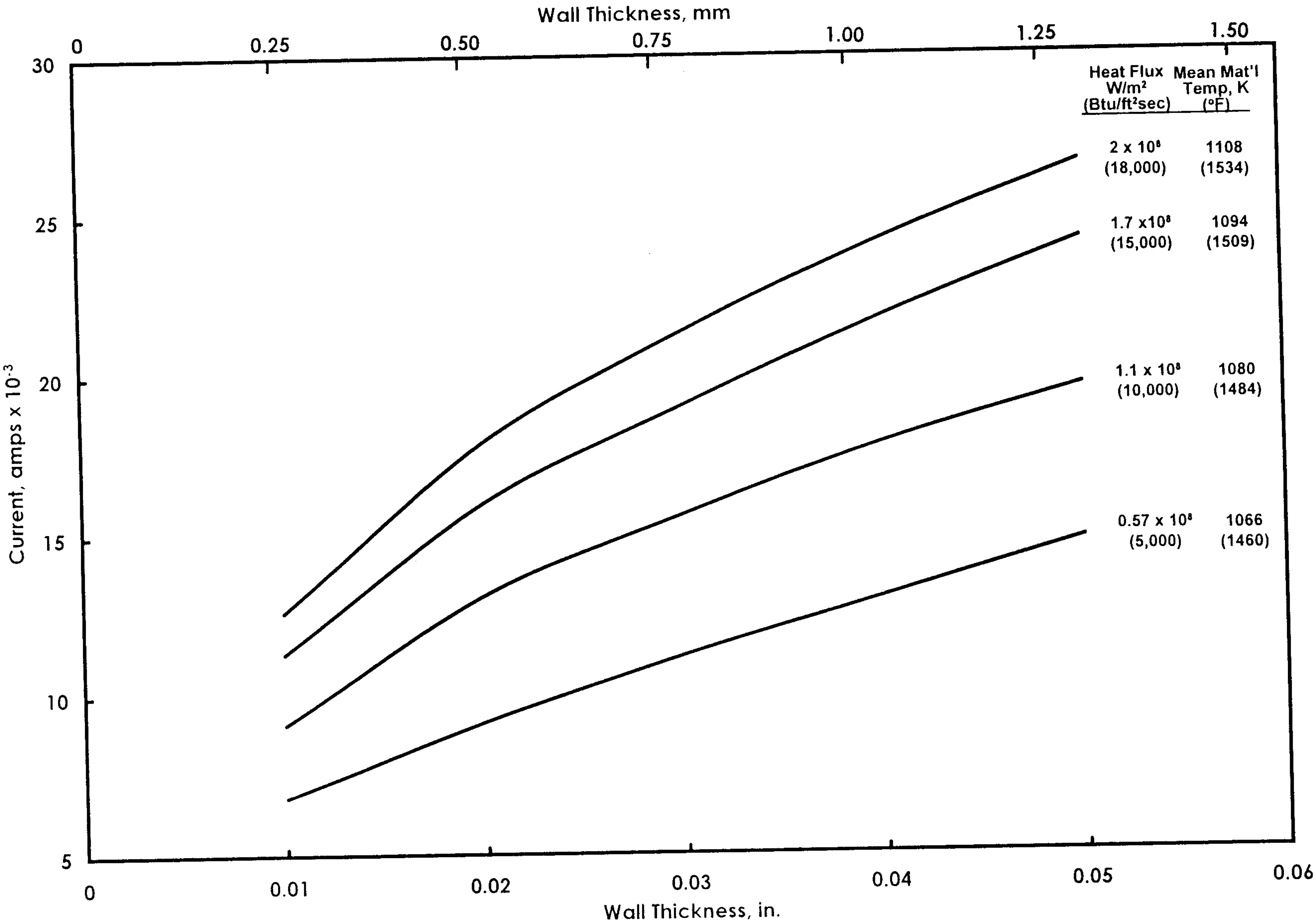

b. Outside Diameter of 0.75 in. (19.1 mm)

Figure 3. Continued

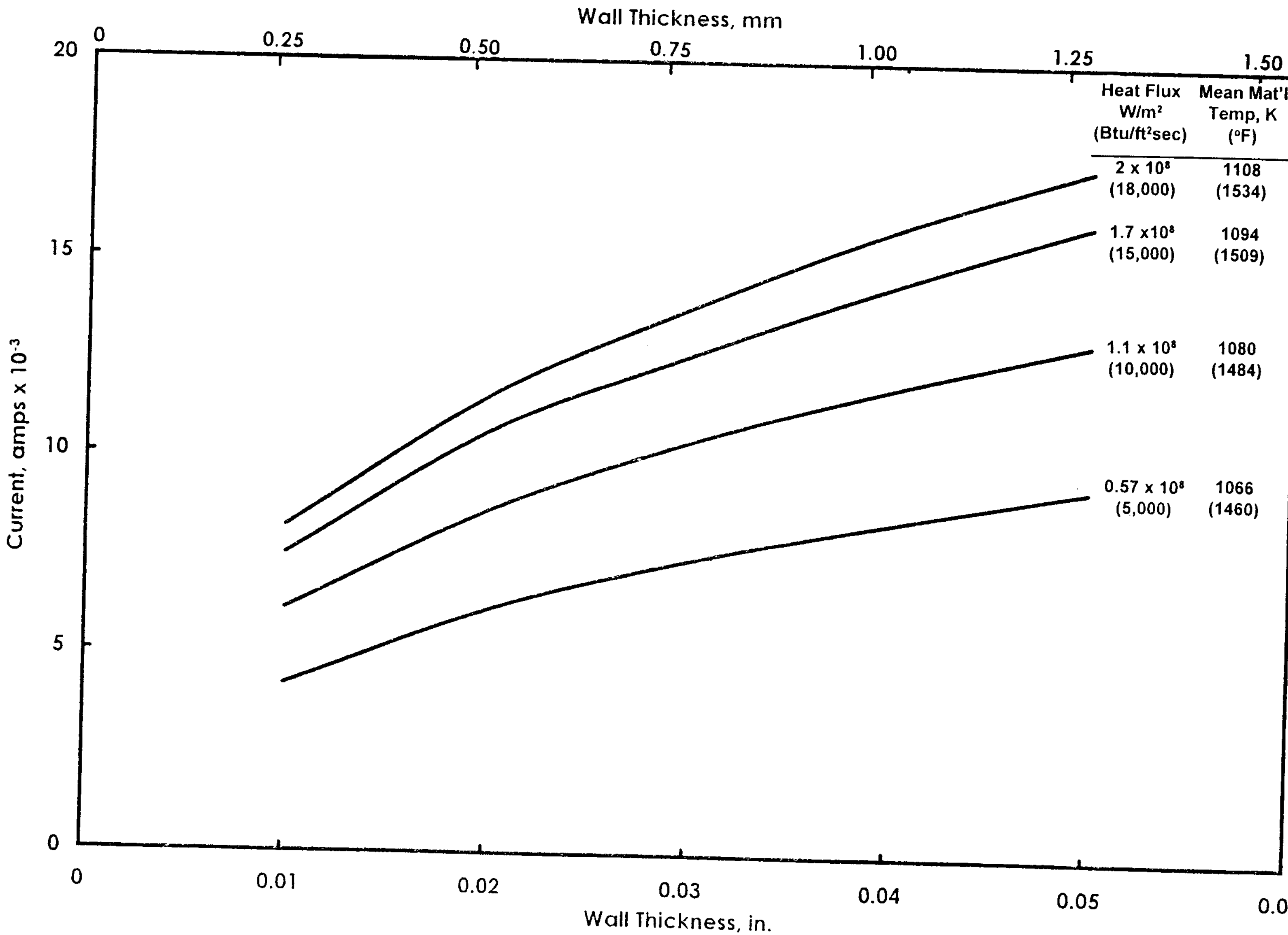

c. Outside Diameter of 0.5 in. (12.7 mm)

Figure 3. Concluded

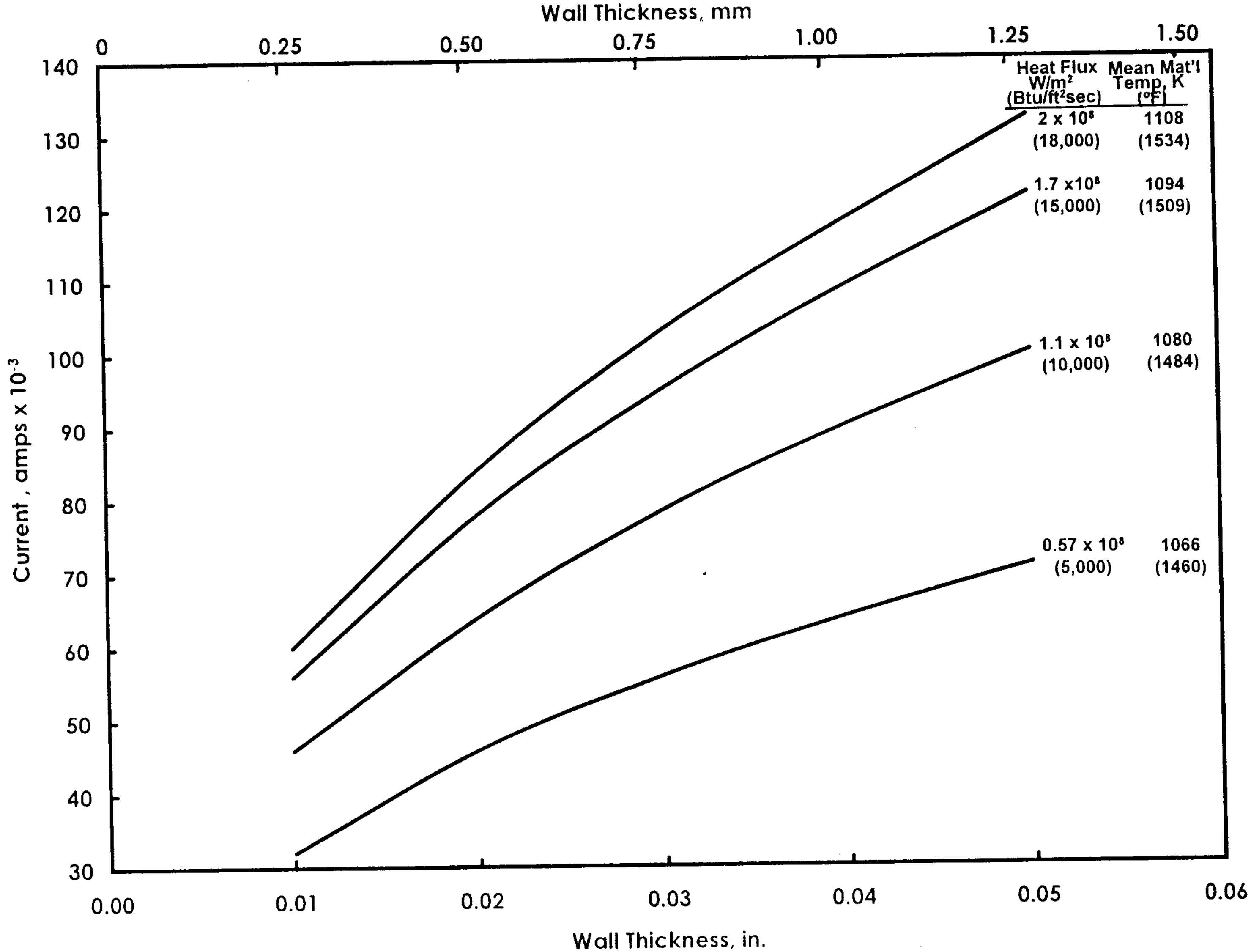

a. Outside Diameter of 1 in. (25.4 mm)

Figure 4. Power Supply Requirements for an Electrically-Heated Amzirc Tube

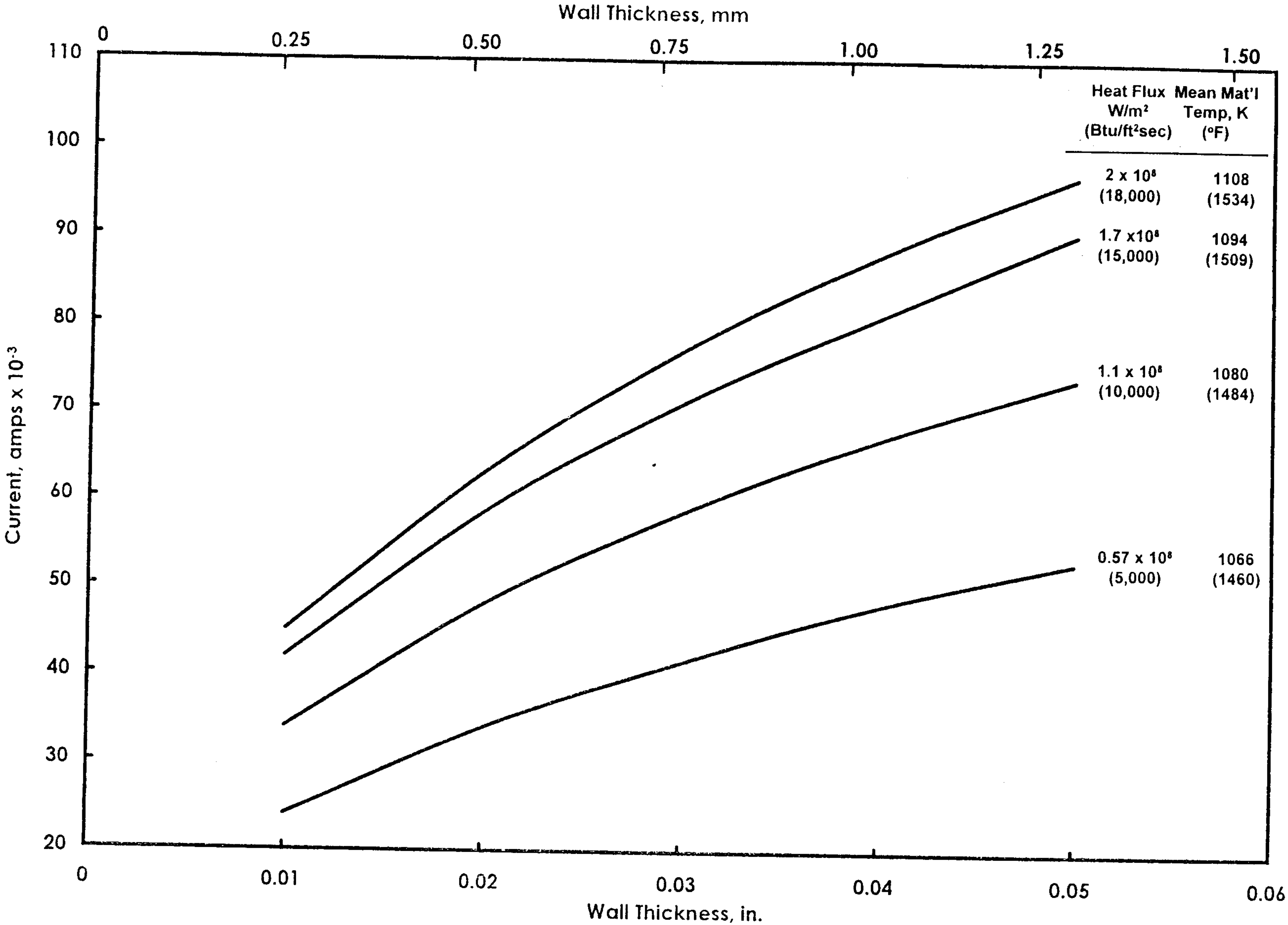

b. Outside Diameter of 0.75 in. (19.1 mm)
Figure 4. Continued

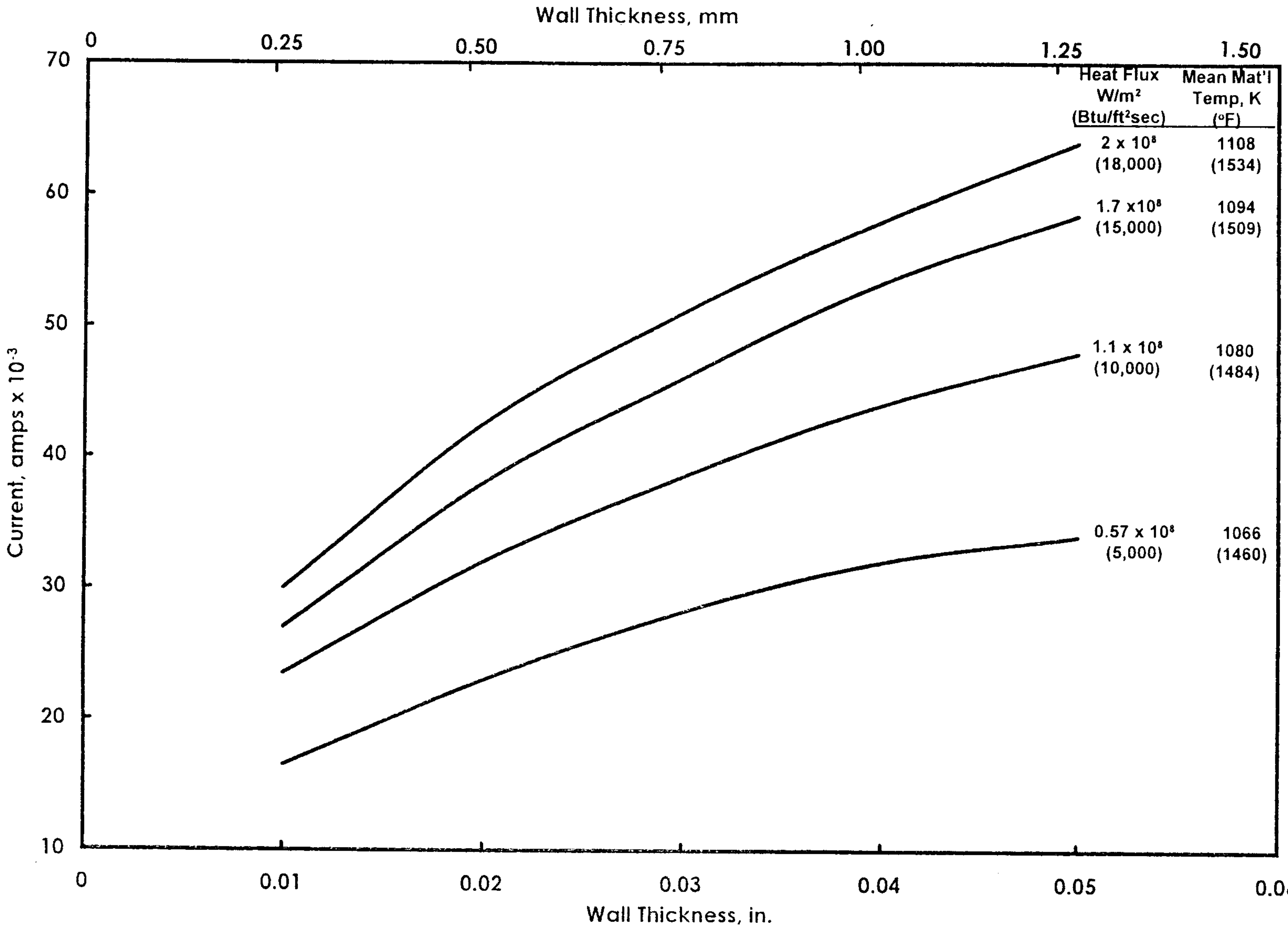

c. Outside Diameter of 0.5 in. (12.7 mm)

Figure 4. Concluded

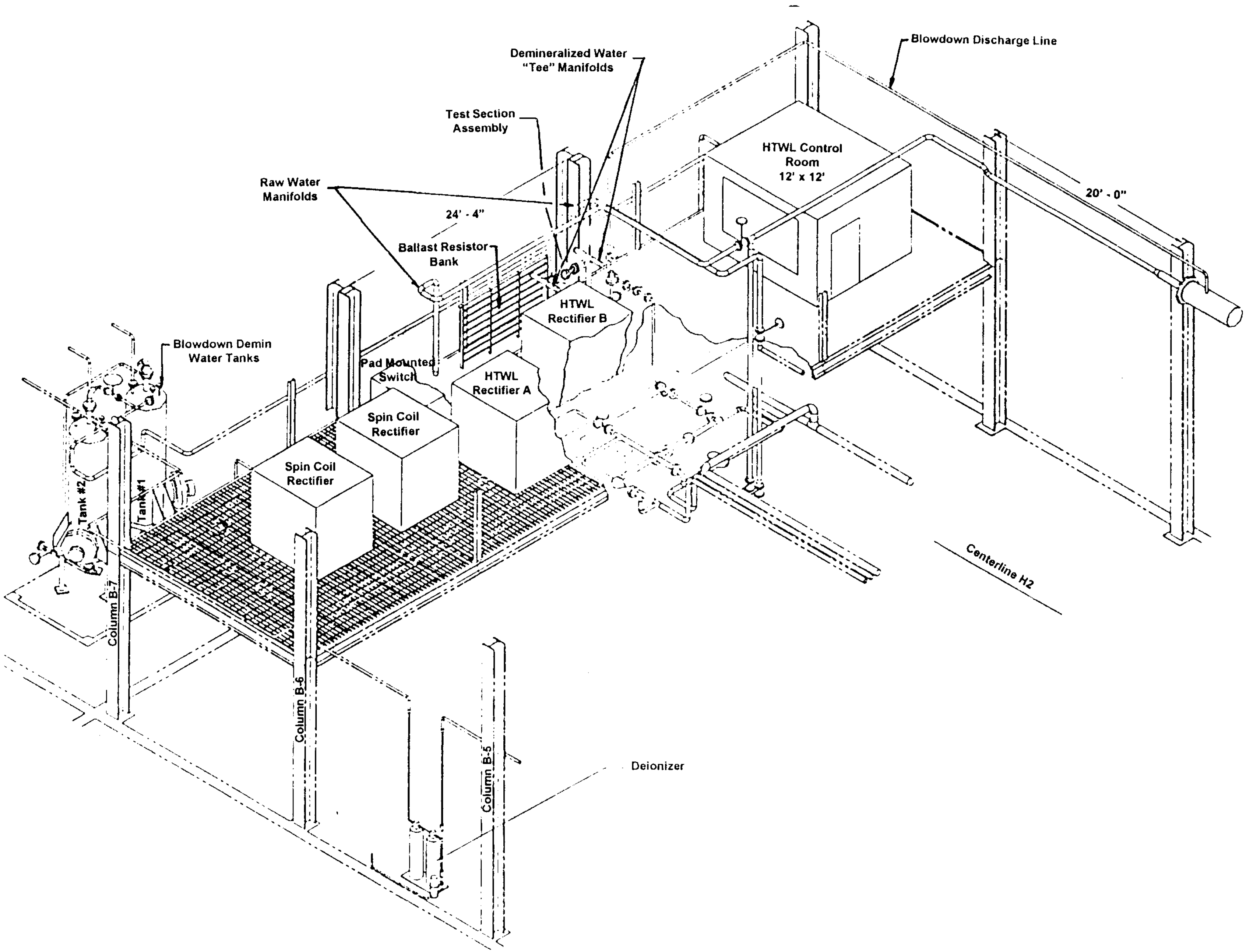

Figure 5. HTWL Equipment Layout

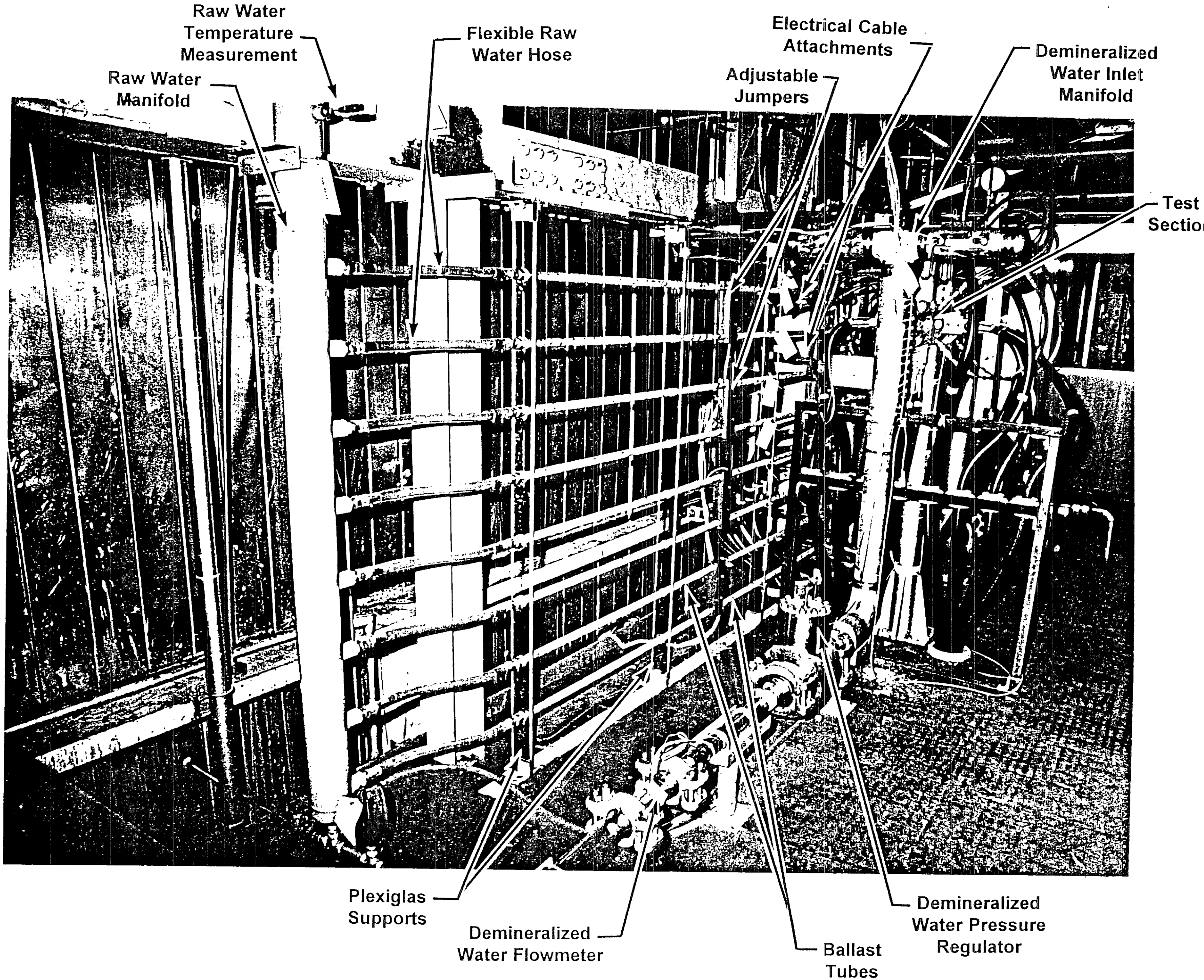

Figure 6. Ballast Resistor Bank and Water Flow System Details

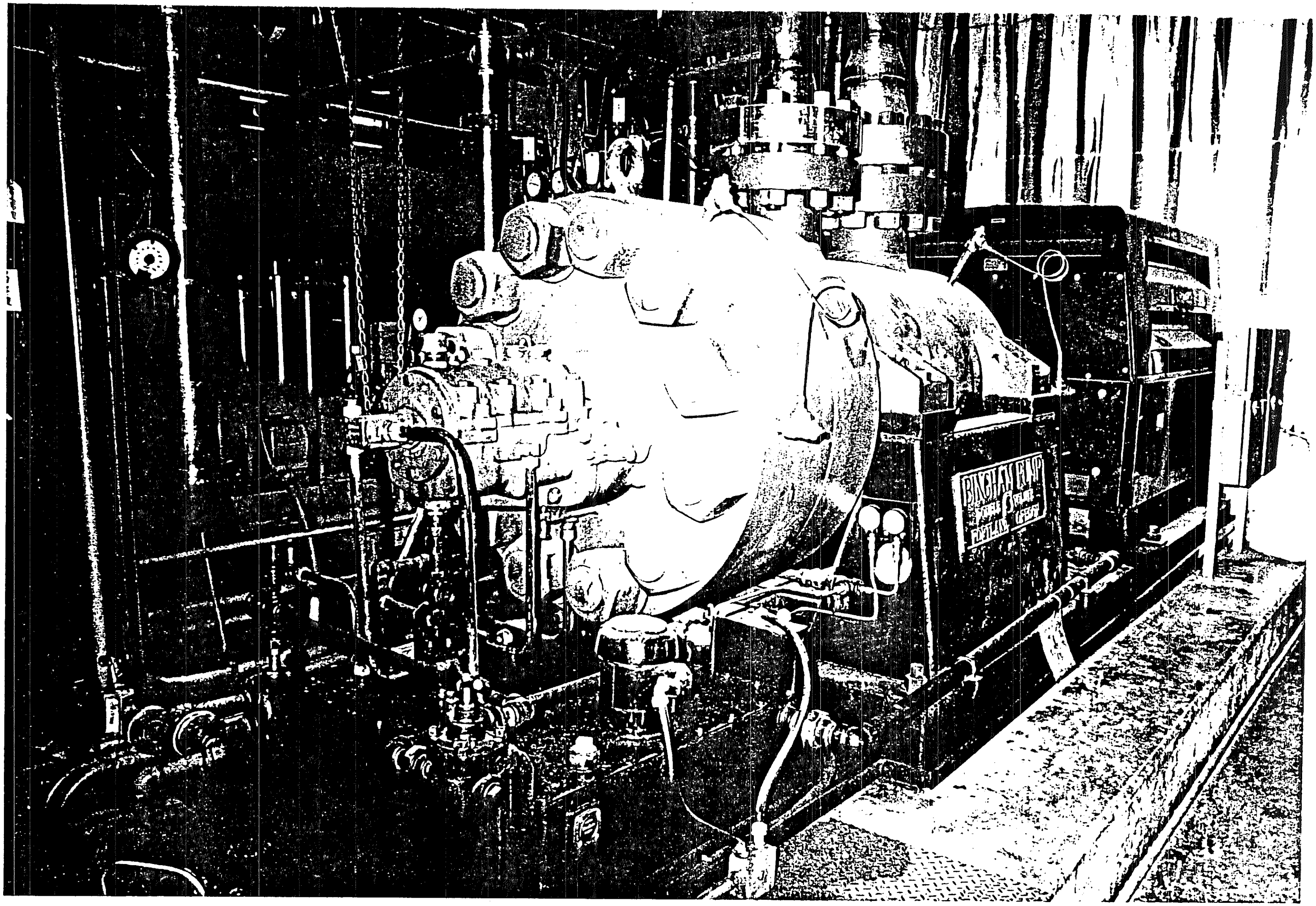

Figure 7. HTL High Pressure Demineralized Water Pump

a. Demineralized Water Tank Complex

Figure 8. Blowdown Circuit Equipment

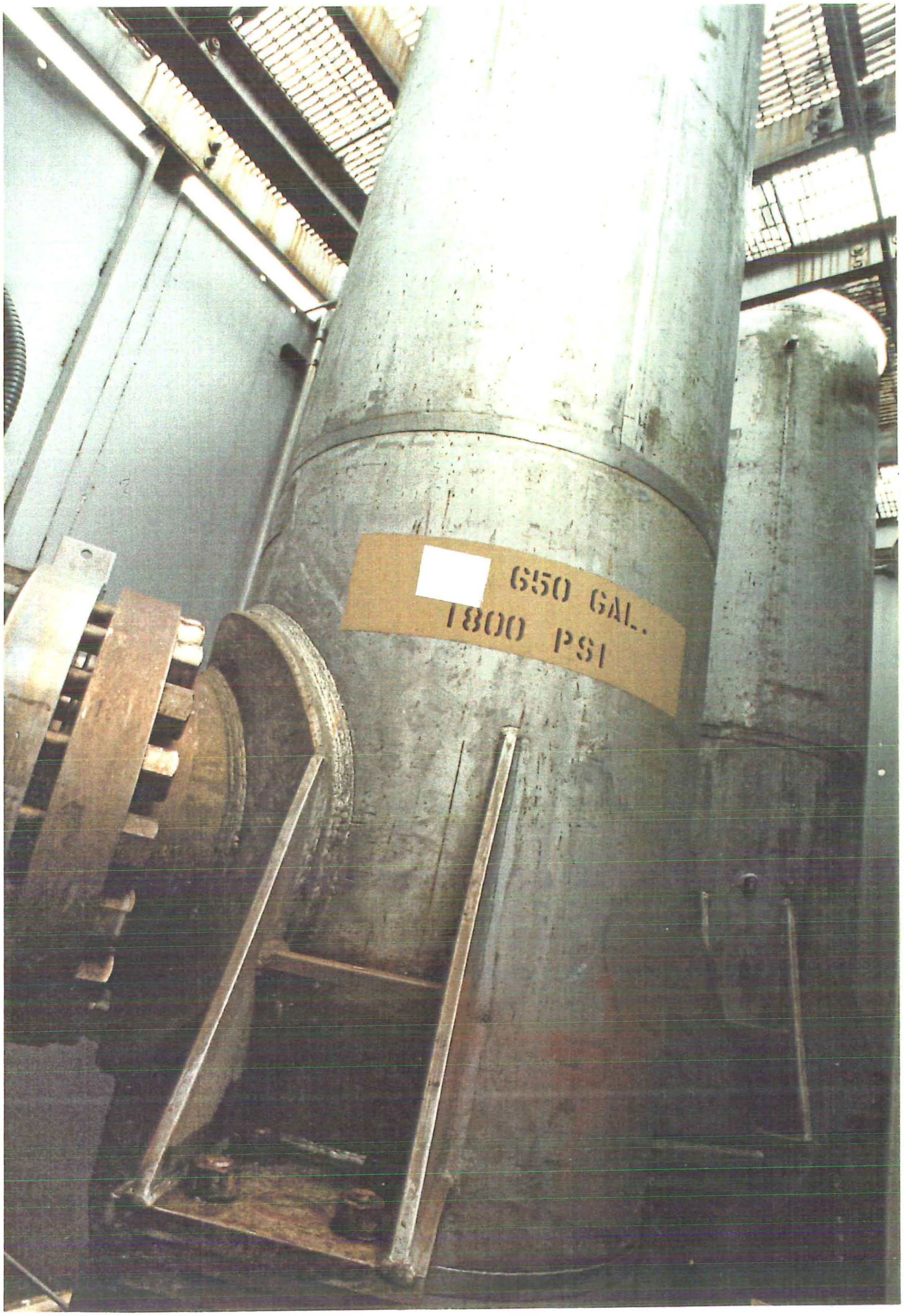

b. Demineralized Water Tanks
Figure 8. Continued

c. Gaseous Nitrogen Bottle Farm
Figure 8. Continued

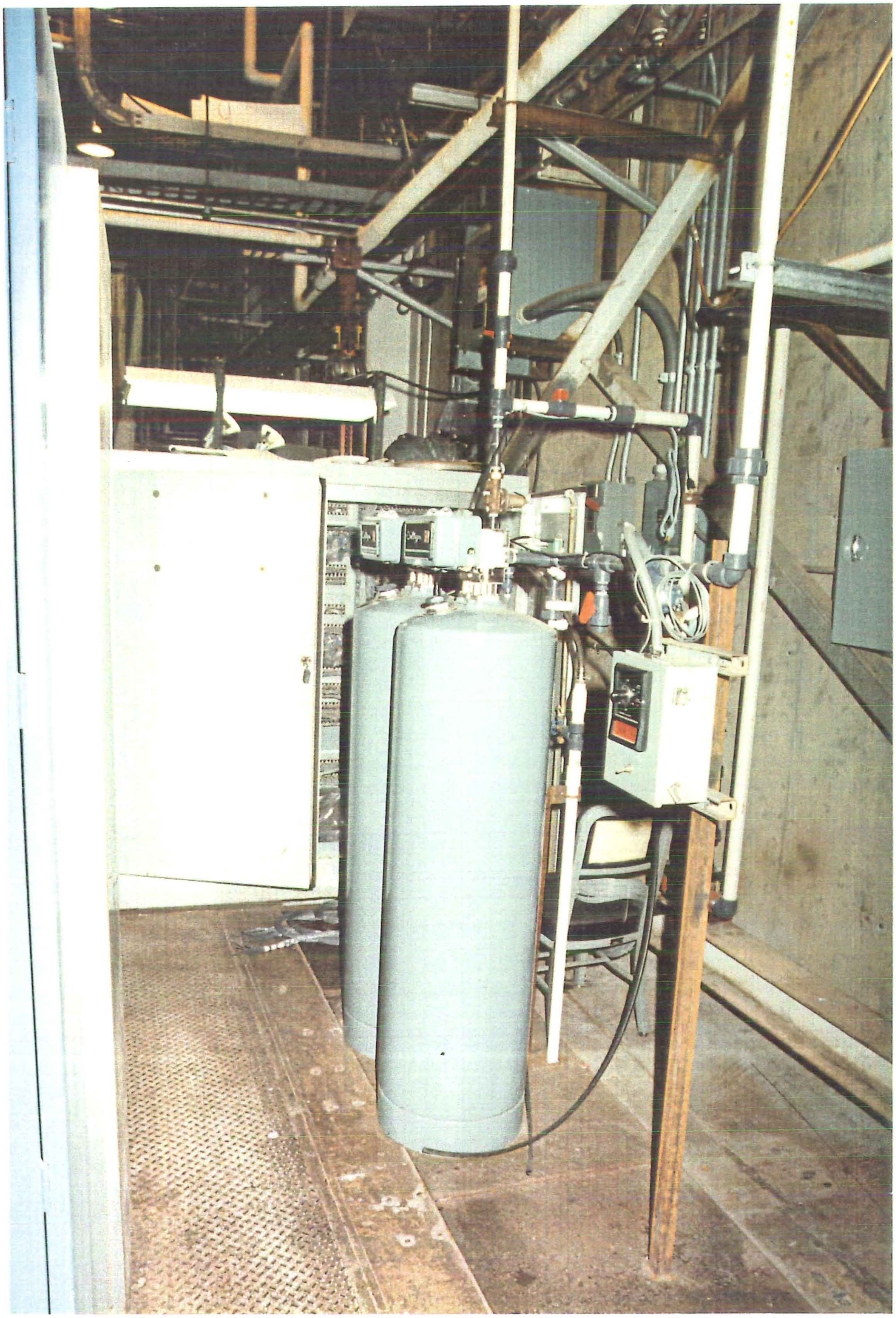

d. Blowdown Circuit Deionizer
Figure 8. Concluded

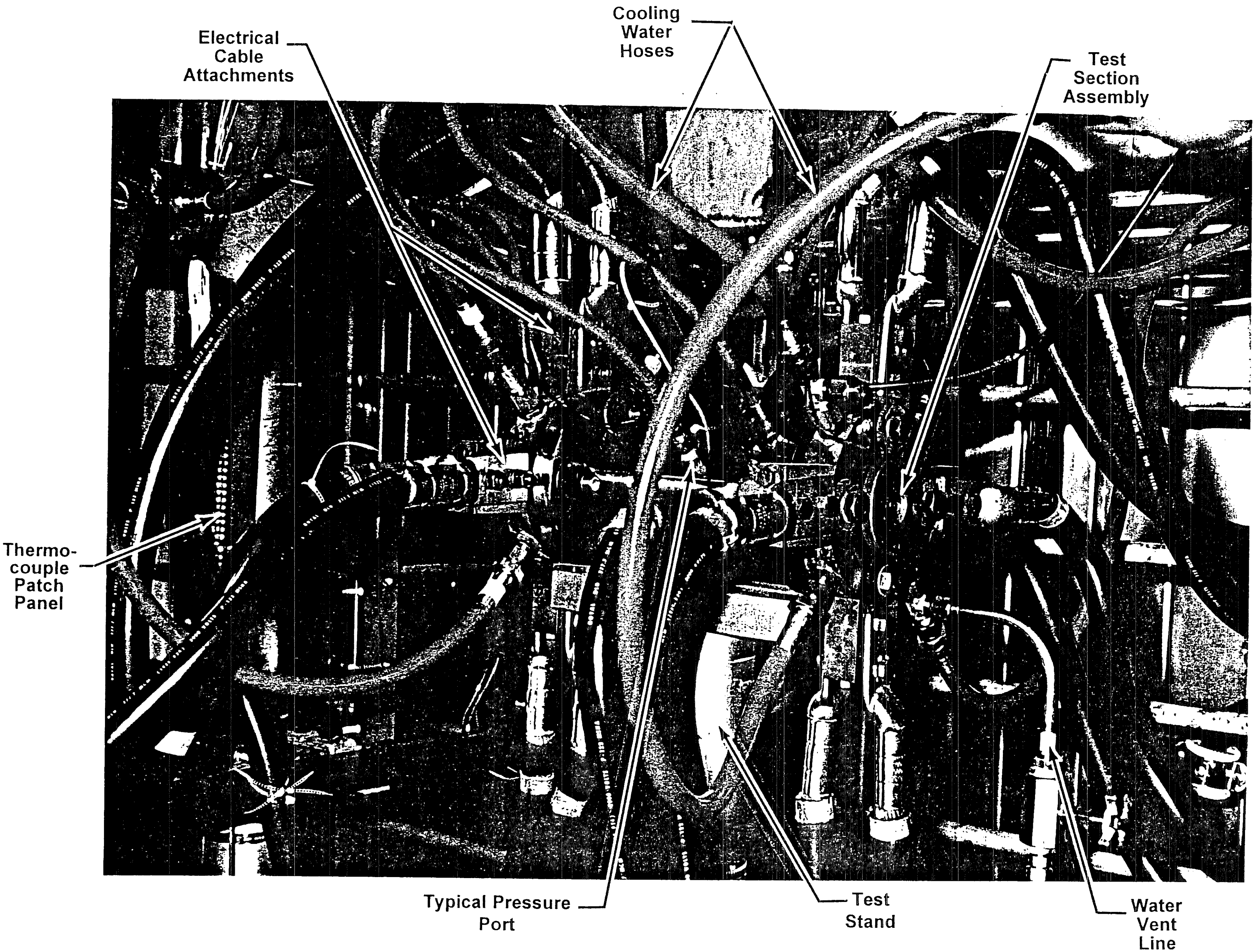

a. HTWL Test Section
Figure 9. HTWL Test Section Assembly

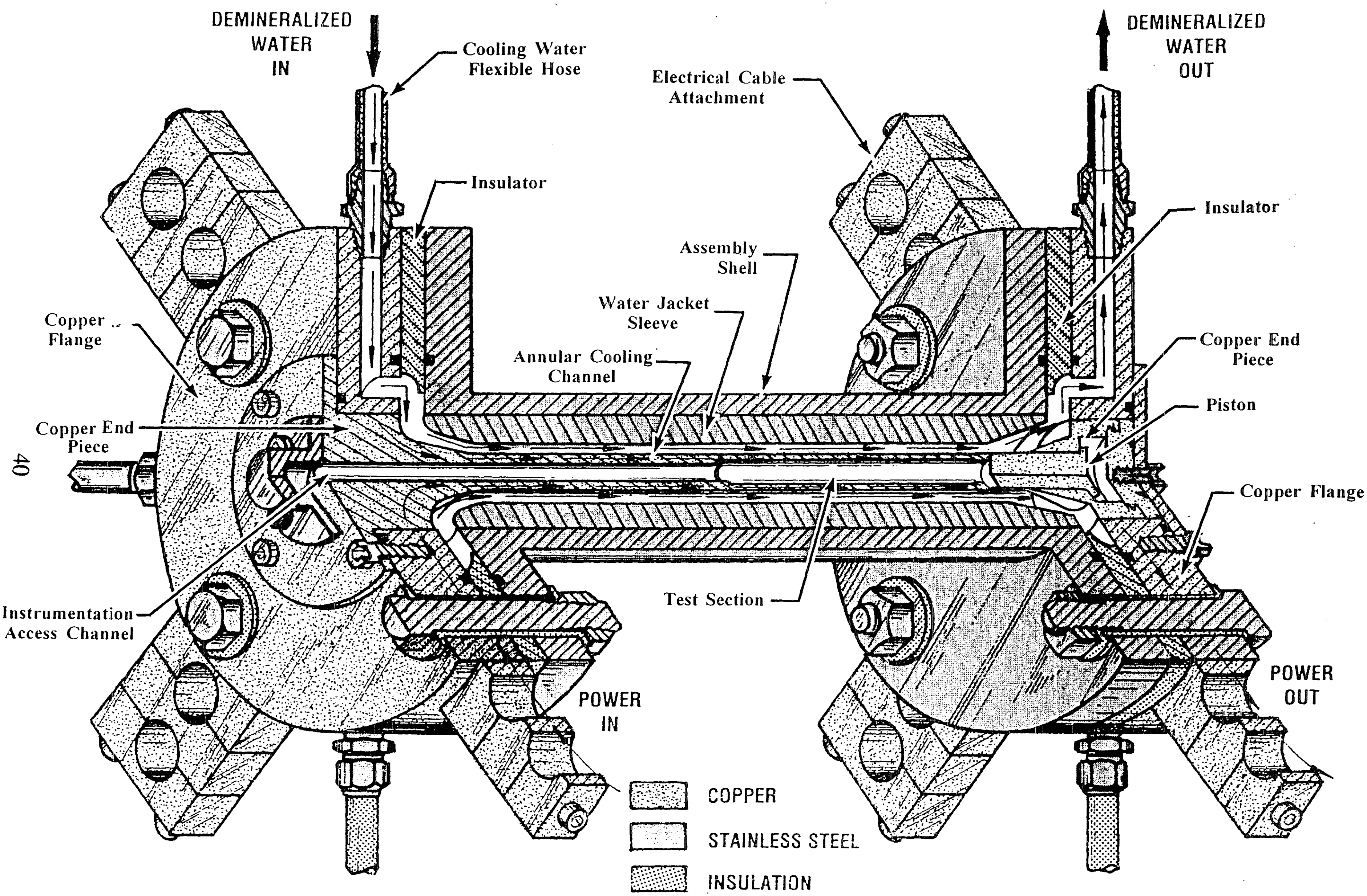

b. Cutaway of the HTWL Test Section Assembly
Figure 9. Concluded

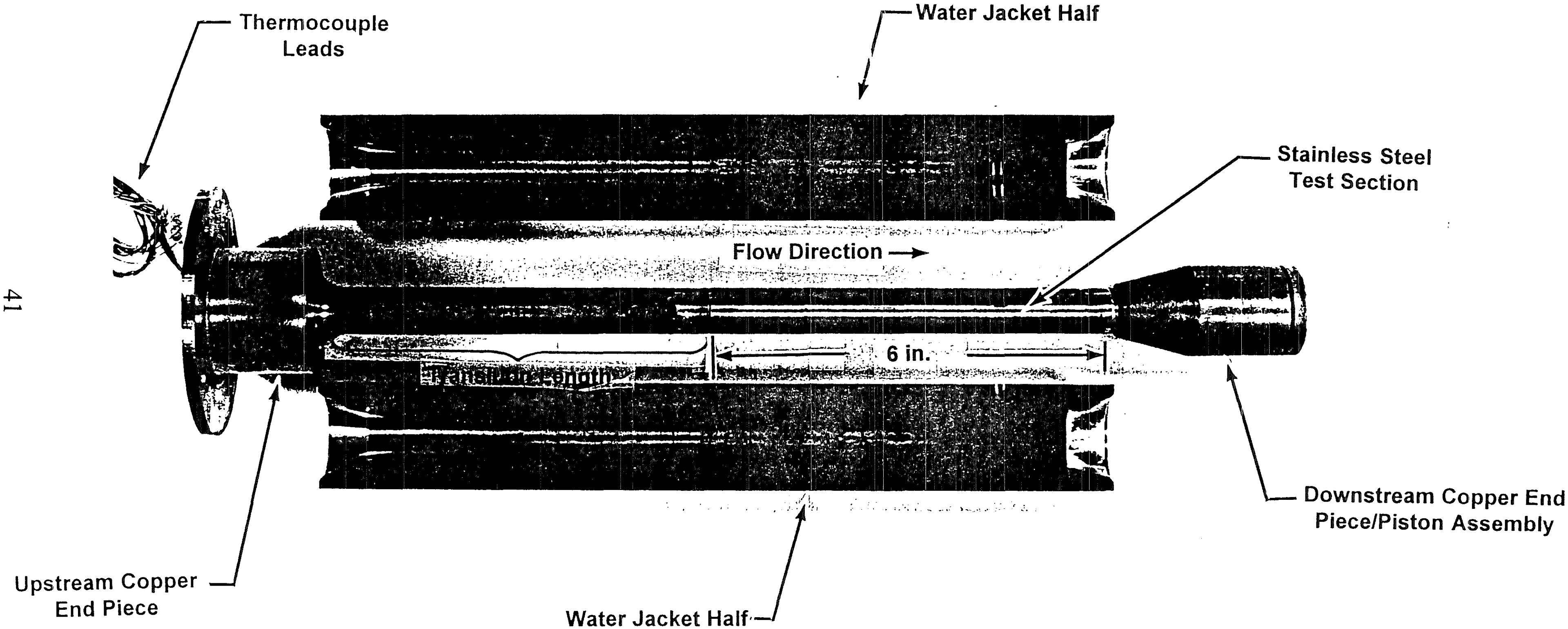

a. 19-mm Diam Stainless Steel Test Section and Water Jacket

Figure 10. HTWL Test Section

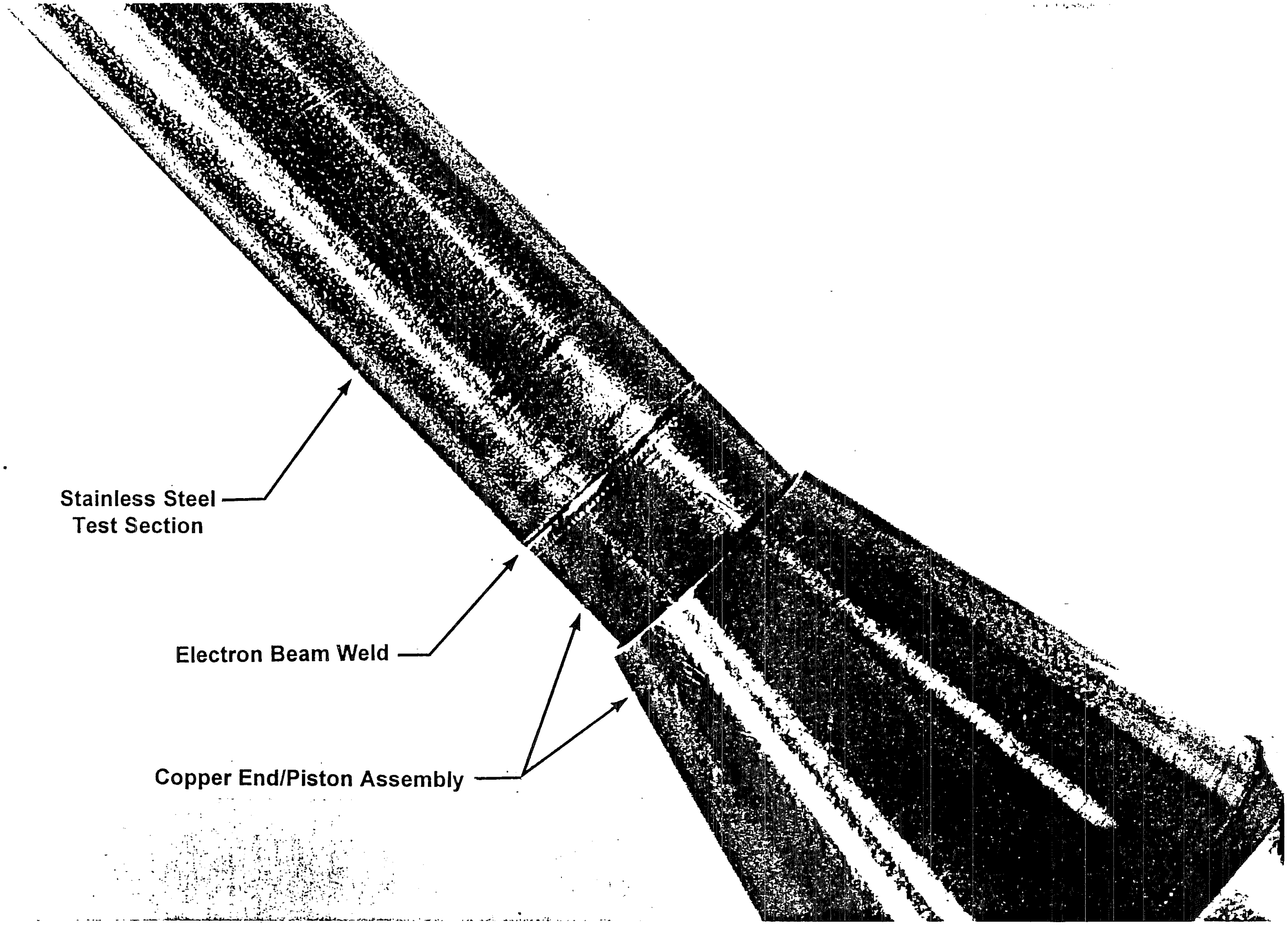

b. Closeup of Electron Beam Weld

Figure 10. Concluded

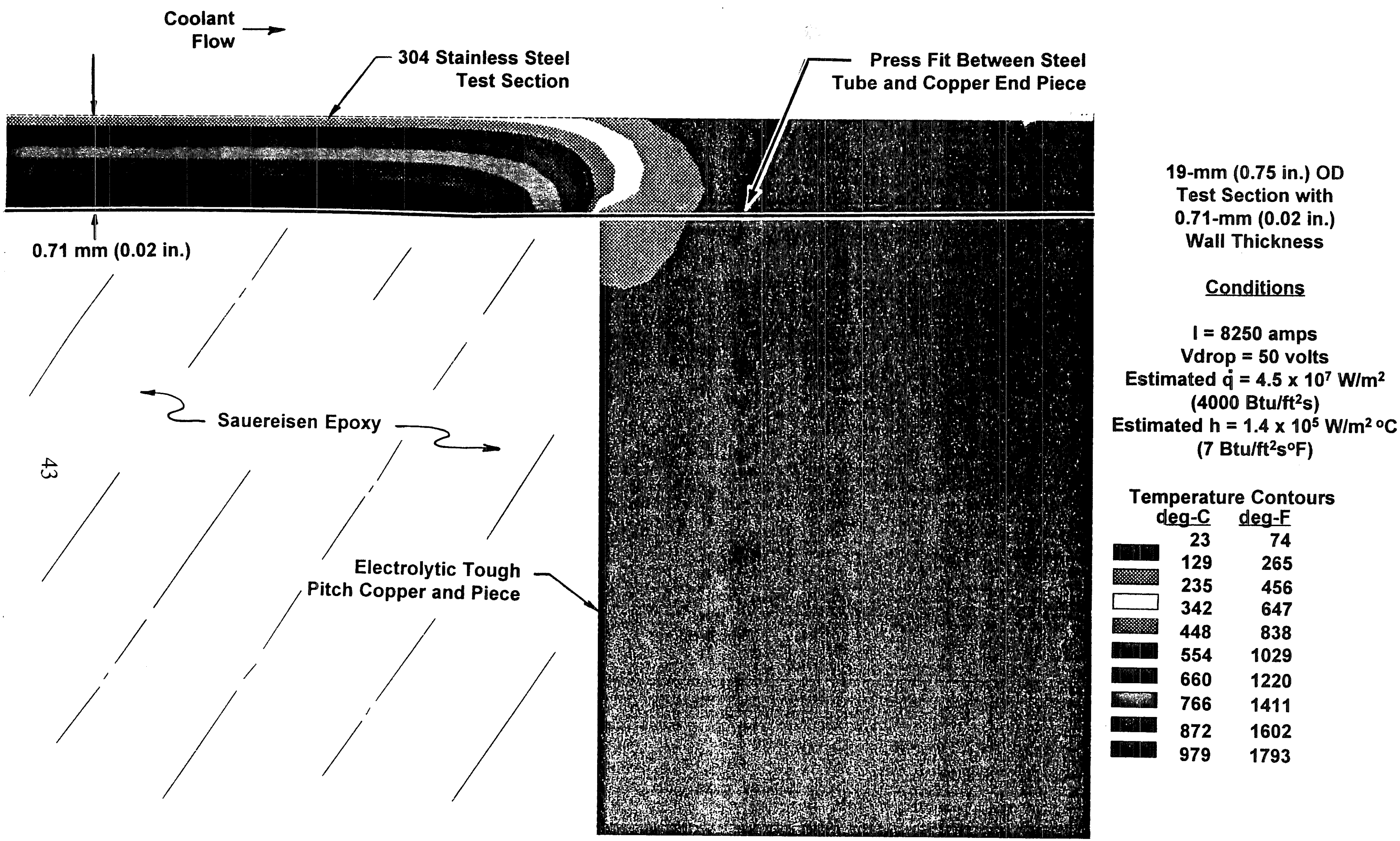

Figure 11. Theoretical Temperature Distribution of HTWL Test Section

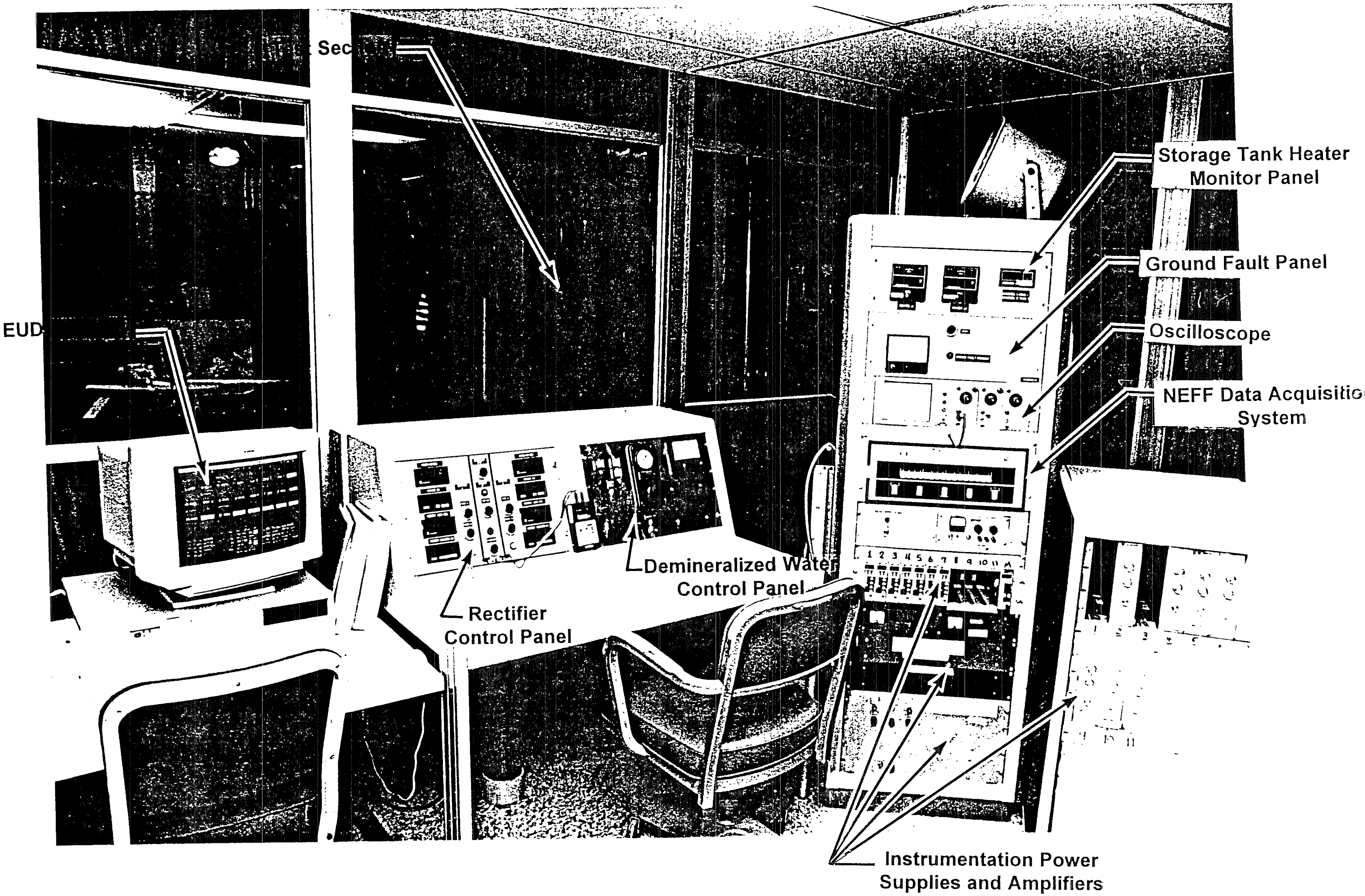

Figure 12. HTWL Control Room

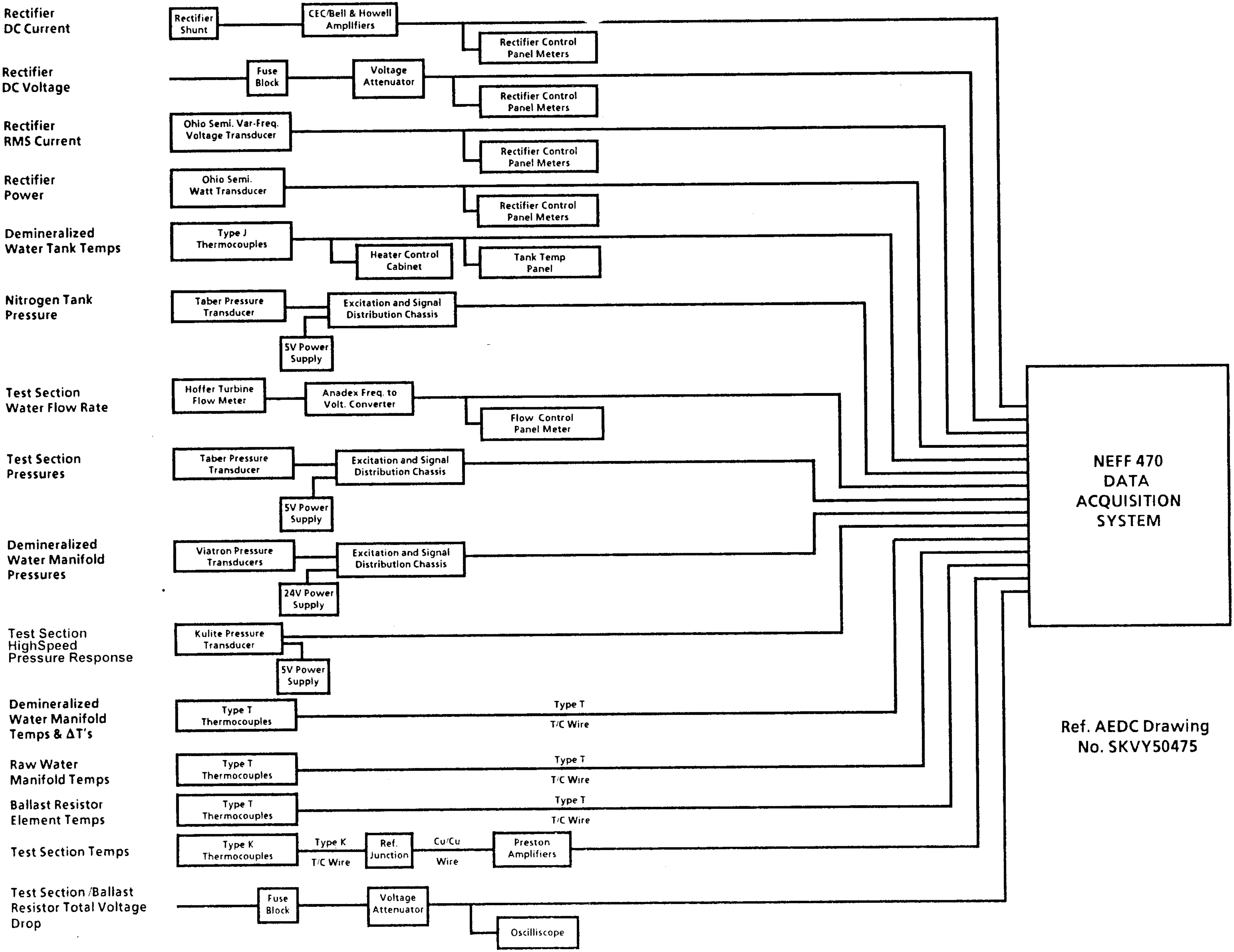
Rectifier DC Current
Rectifier Shunt
CEC/Bell & Howell Amplifiers
Rectifier Control Panel Meters
Rectifier DC Voltage
Fuse Block
Voltage Attenuator
Rectifier Control Panel Meters
Rectifier RMS Current
Ohio Semi. Var-Freq. Voltage Transducer
Rectifier Control Panel Meters
Rectifier Power
Ohio Semi. Watt Transducer
Rectifier Control Panel Meters
Demineralized Water Tank Temps
Type J Thermocouples
Heater Control Cabinet
Tank Temp Panel
Nitrogen Tank Pressure
Taber Pressure Transducer
Excitation and Signal Distribution Chassis
5V Power Supply
Test Section Water Flow Rate
Hoffer Turbine Flow Meter
Anadex Freq. to Volt. Converter
Flow Control Panel Meter
Test Section Pressures
Taber Pressure Transducer
Excitation and Signal Distribution Chassis
5V Power Supply
Demineralized Water Manifold Pressures
Viatron Pressure Transducers
Excitation and Signal Distribution Chassis
24V Power Supply
Test Section HighSpeed Pressure Response
Kulite Pressure Transducer
5V Power Supply
Demineralized Water Manifold Temps & ΔT's
Type T Thermocouples
Type T
T/C Wire
Raw Water Manifold Temps
Type T Thermocouples
Type T
T/C Wire
Ballast Resistor Element Temps
Type T Thermocouples
Type T
T/C Wire
Test Section Temps
Type K Thermocouples
Type K
T/C Wire
Ref. Junction
Cu/Cu
Wire
Preston Amplifiers
Test Section /Ballast Resistor Total Voltage Drop
Fuse Block
Voltage Attenuator
Oscilliscope
NEFF 470 DATA ACQUISITION SYSTEM
Ref. AEDC Drawing No. SKVY50475

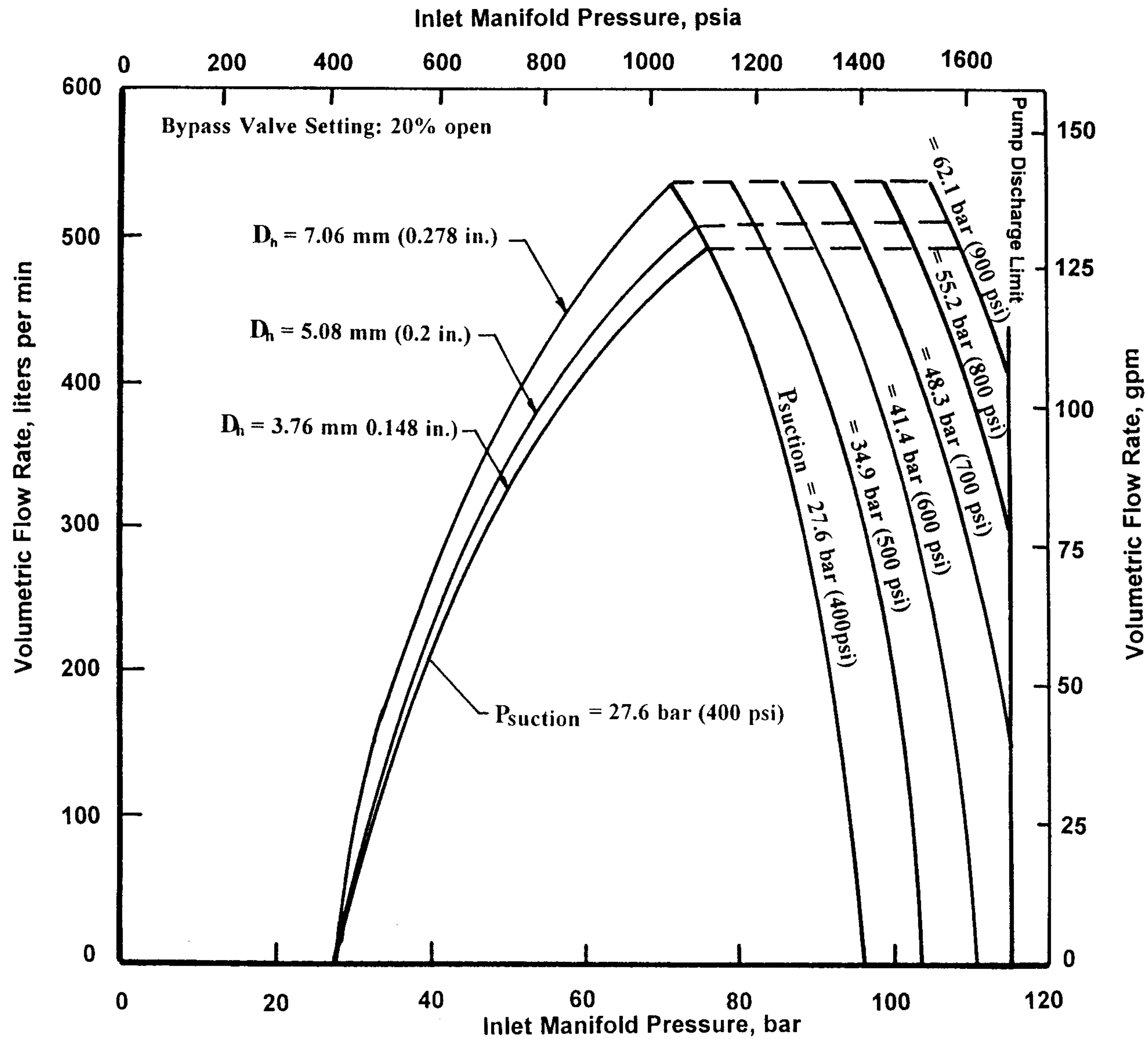

a. Inlet Manifold Conditions

Figure 14. HTWL Demineralized Water System Performance

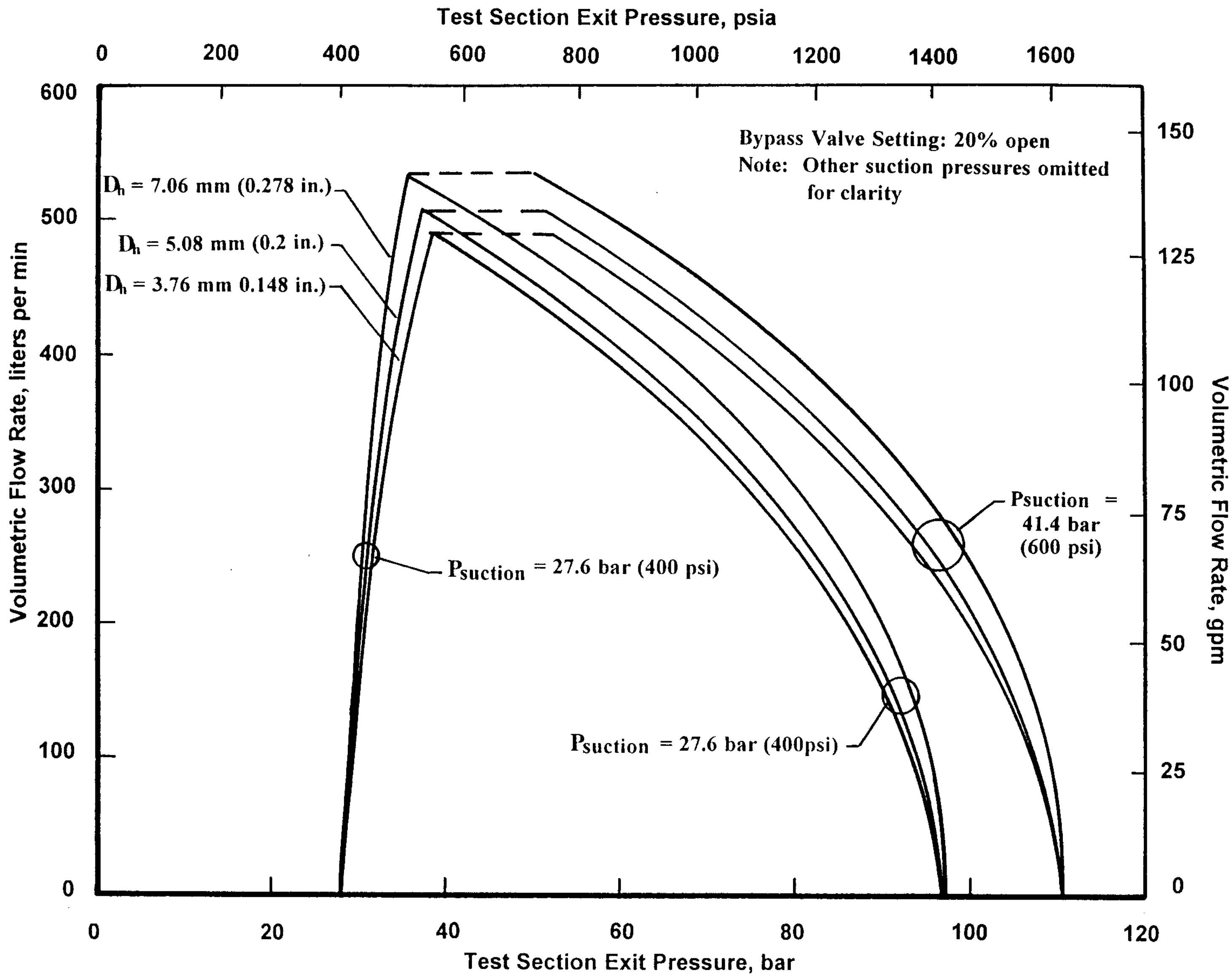

b. Test Section Exit Conditions

Figure 14. Concluded

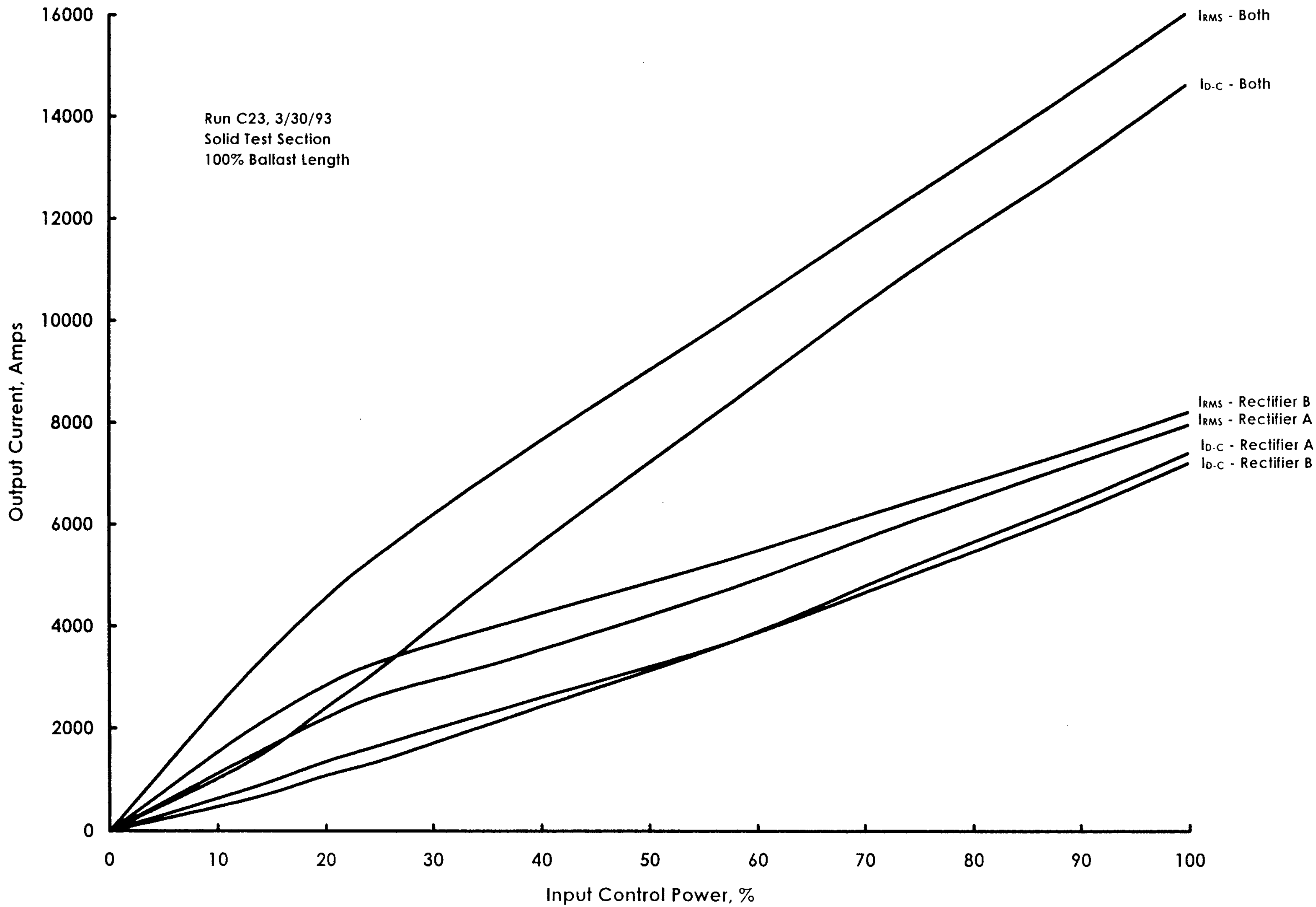

a. Current Characteristics
Figure 15. Rectifier Output Characteristics

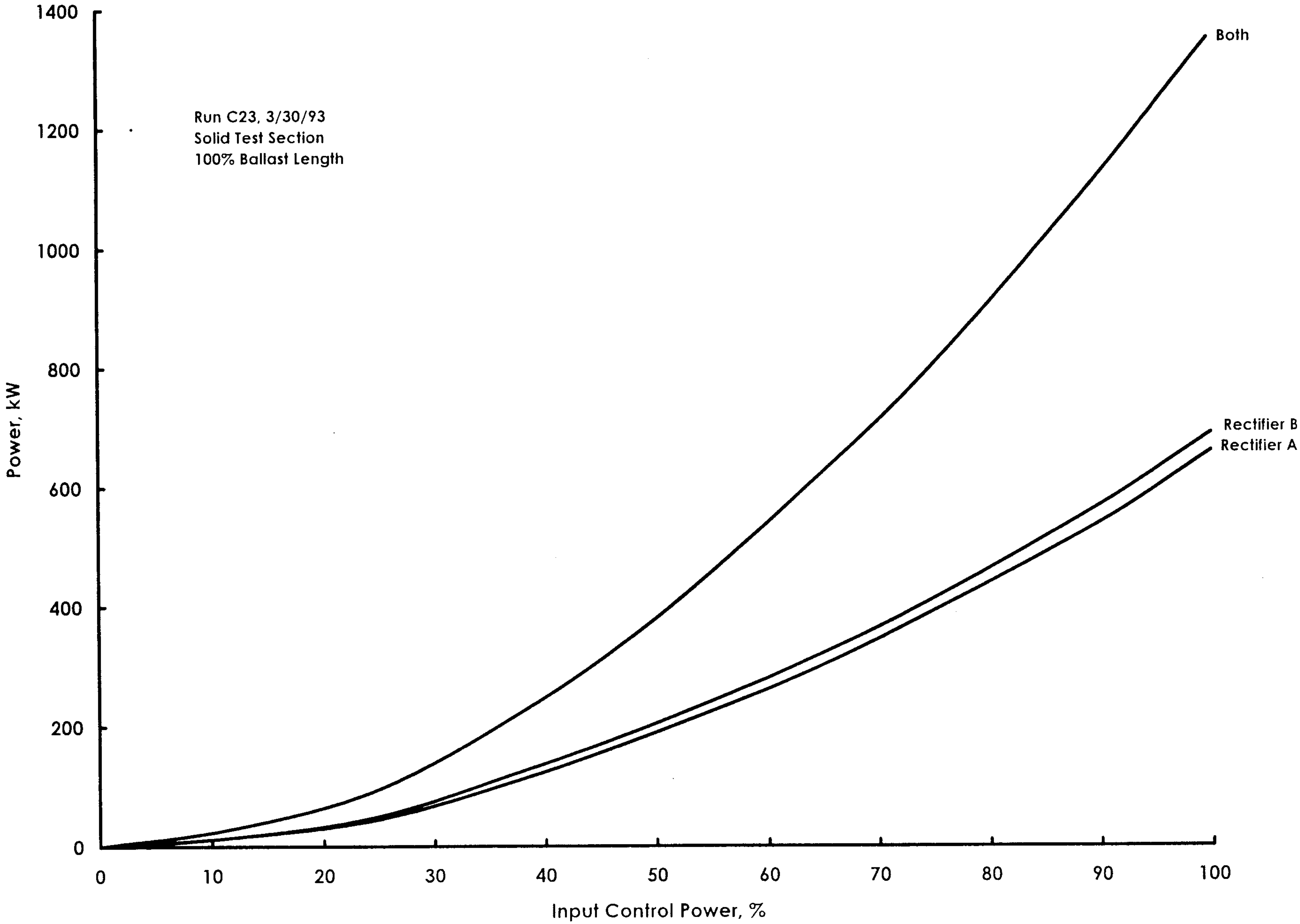

b. Power Based on I_{RMS}
Figure 15. Concluded

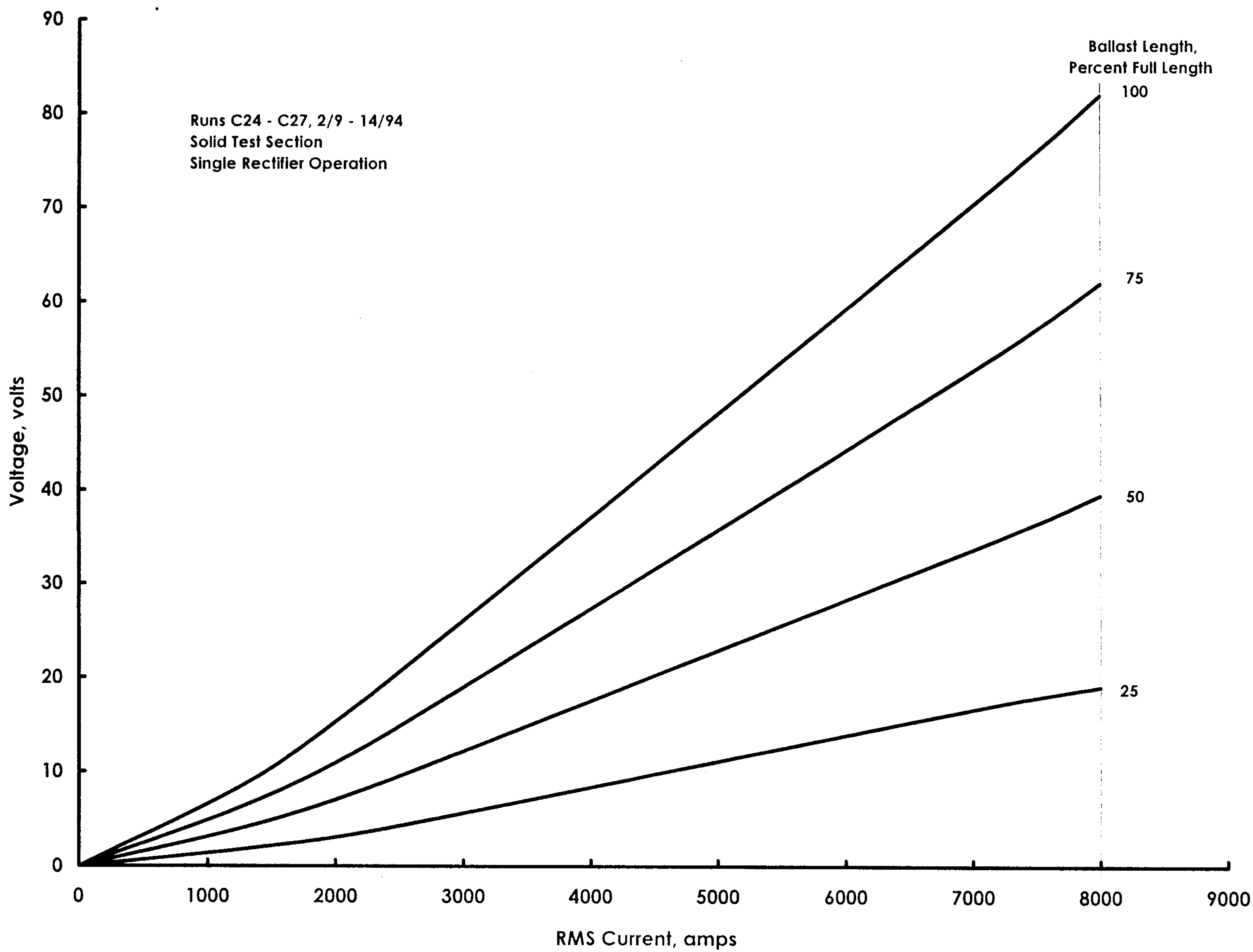

a. Voltage Drop
Figure 16. Ballast Resistor Characteristics

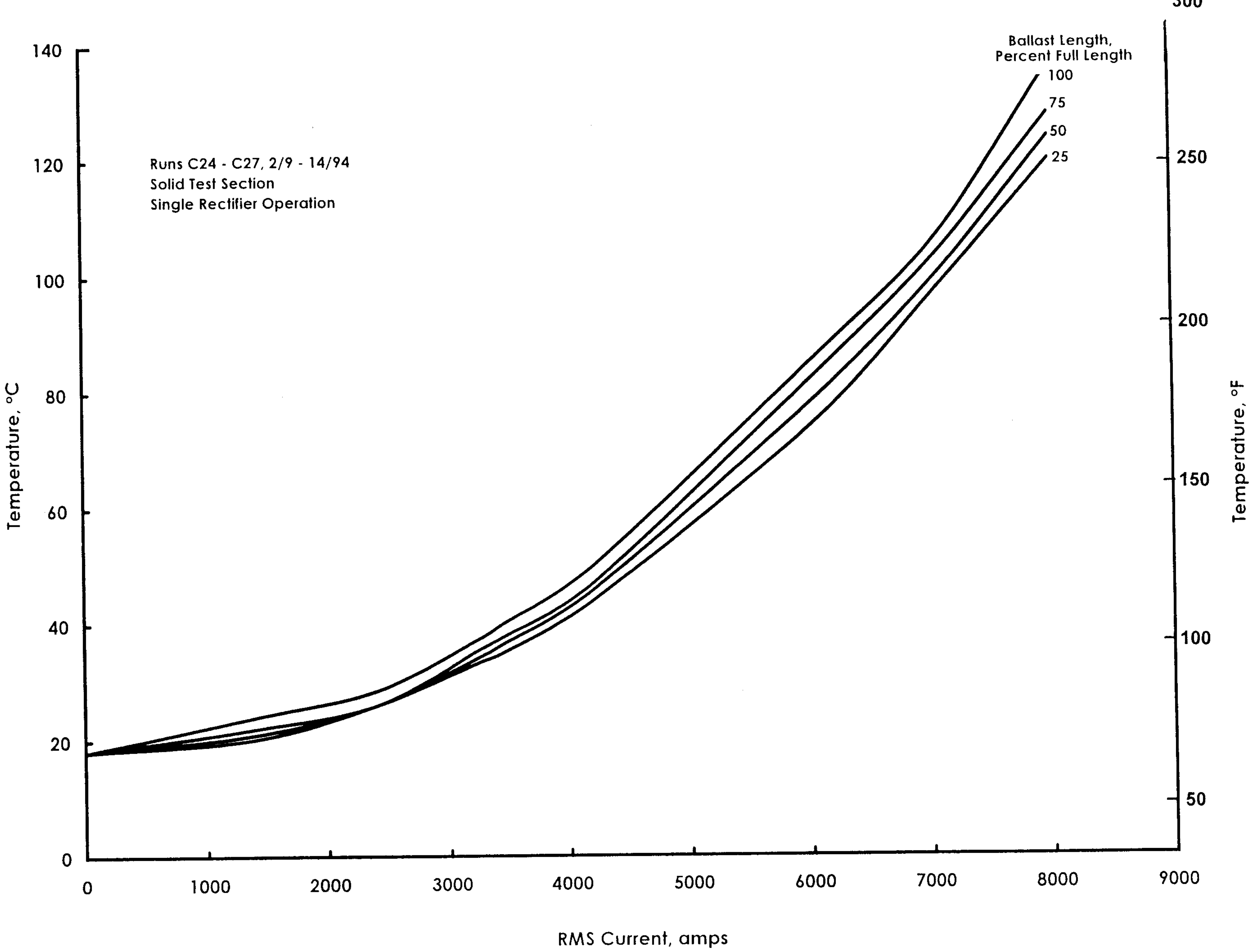

b. Highest Surface Temperature
Figure 16. Concluded

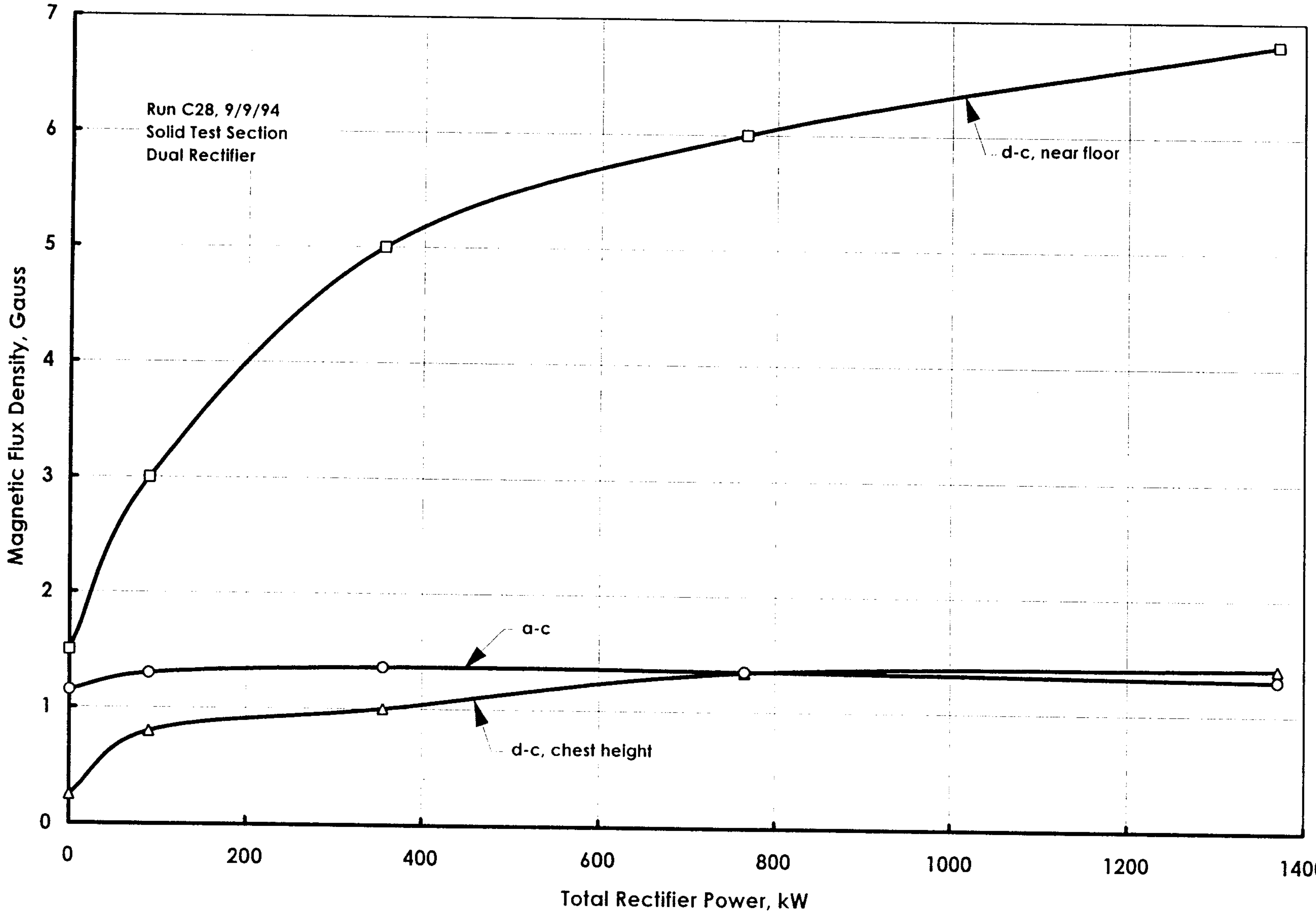

Figure 17. Magnetic Flux Density Measurements in HTWL Control Room

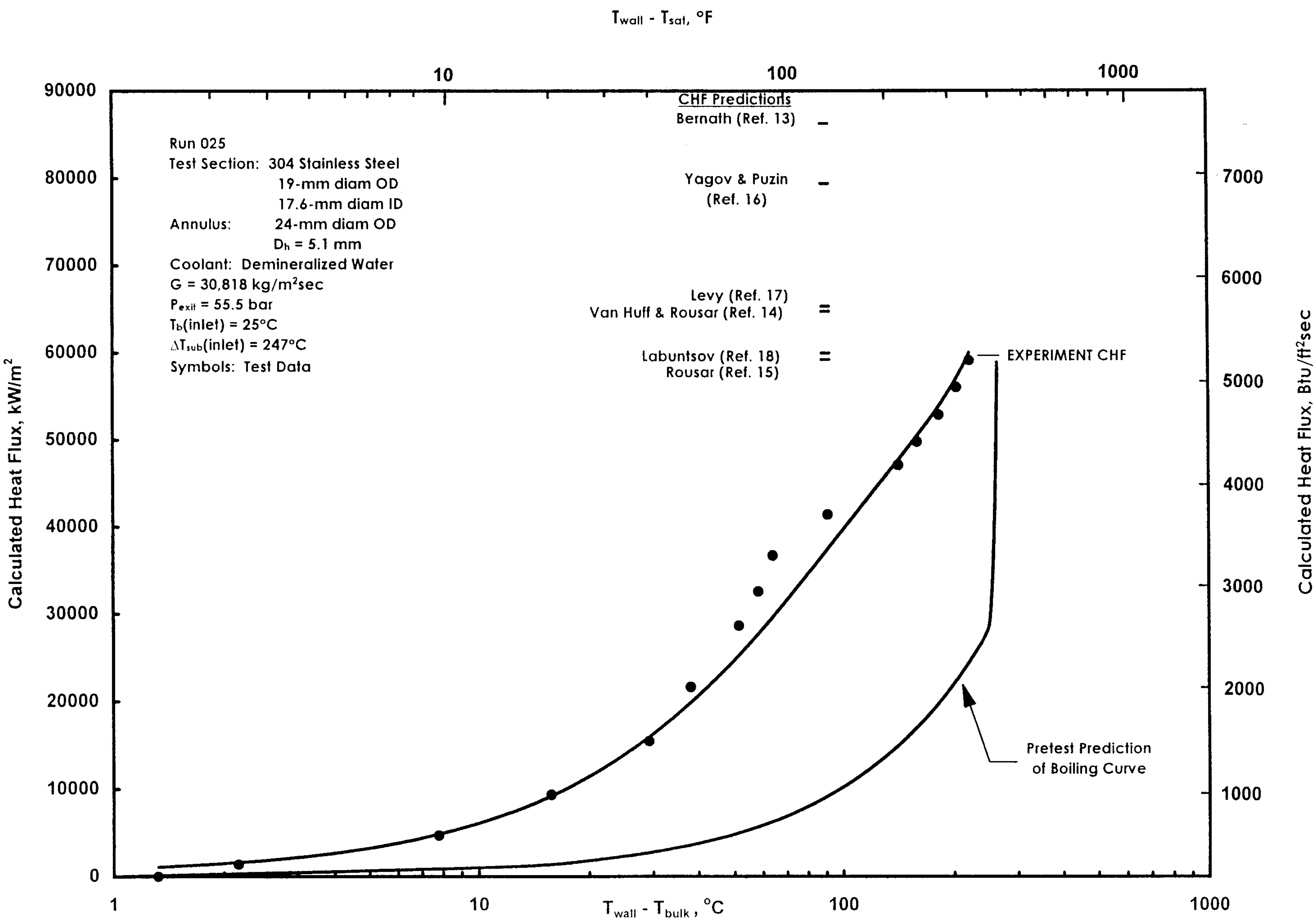

a. Boiling Curve at Burnout Location (Test Section Exit)

Figure 18. Typical HTWL Test Results

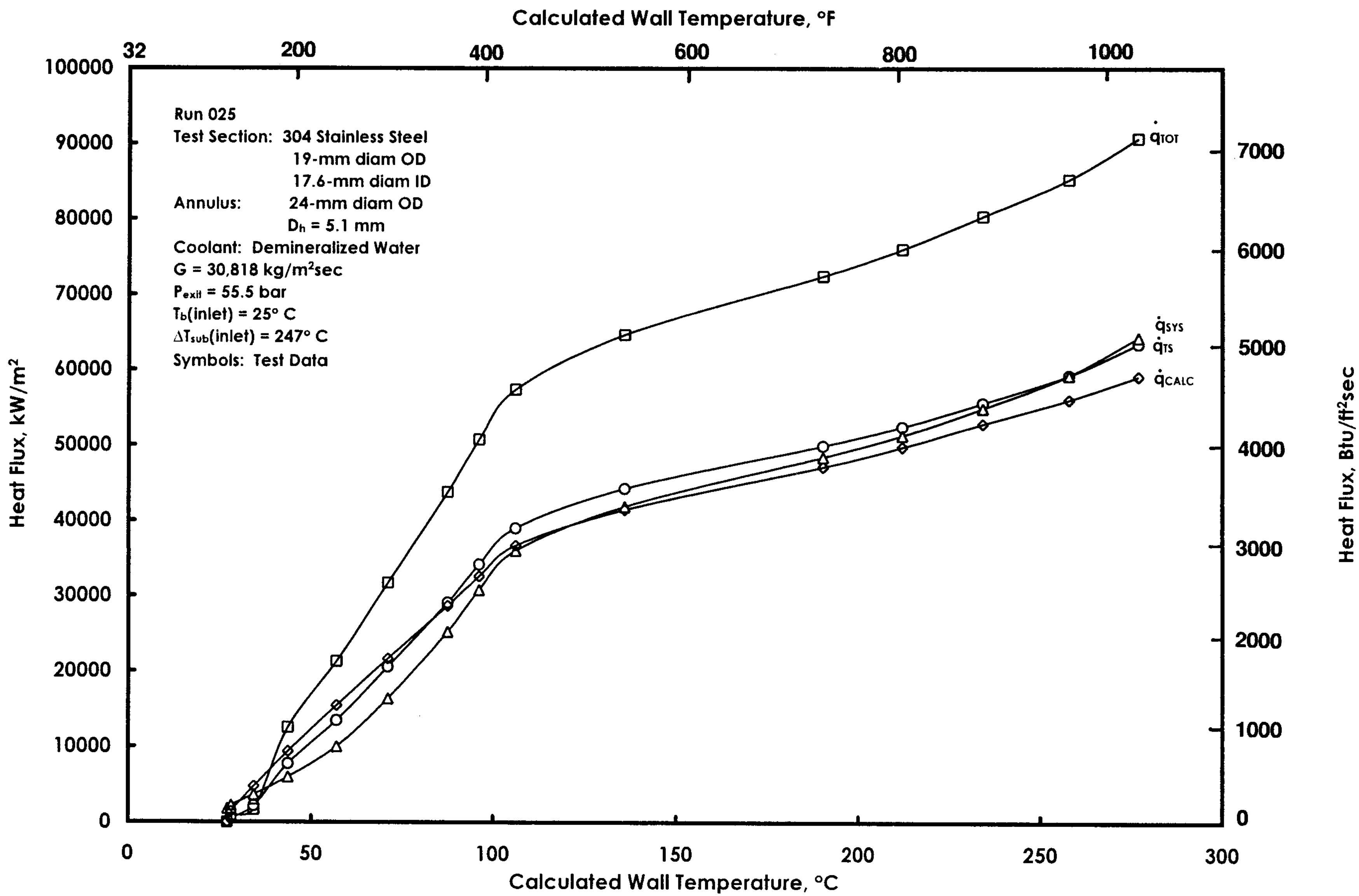

b. Comparison of Heat Flux Computation Methods

Figure 18. Continued

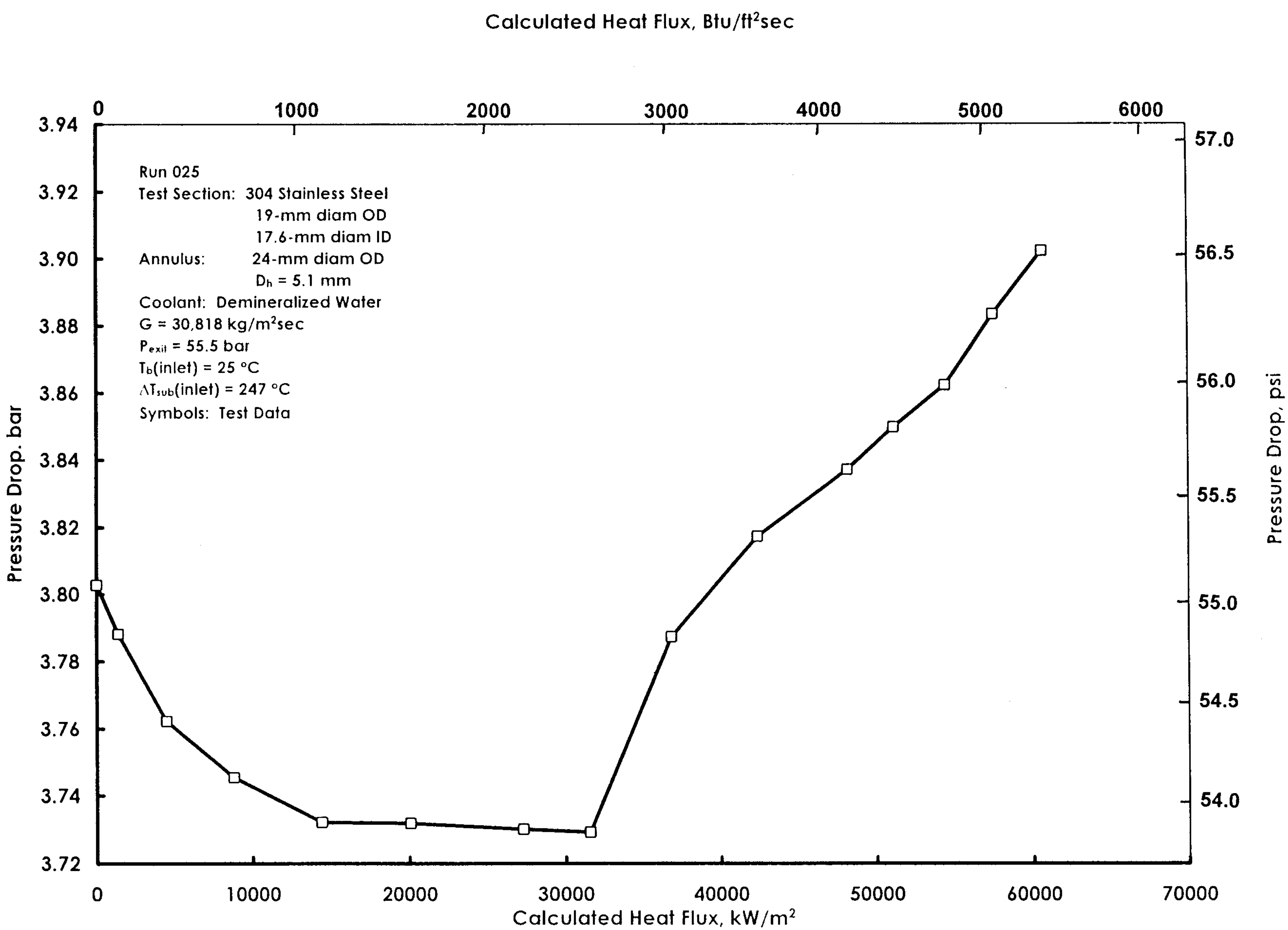

c. Pressure Drop Across Test Section
Figure 18. Continued

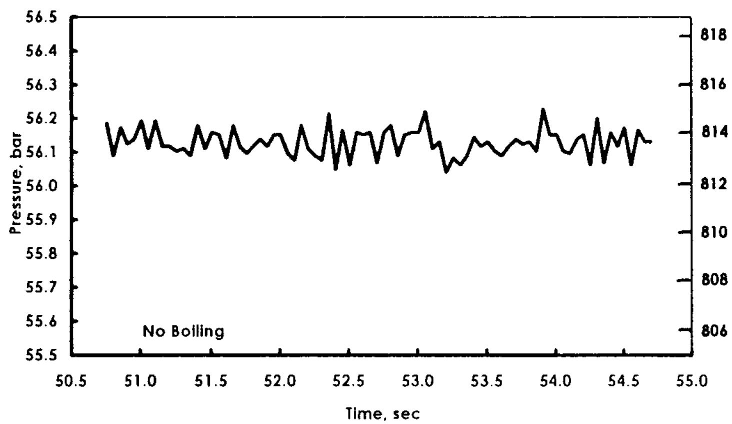

$\dot{q}_{calc}$ = 1338 kW/m² (118.1 Btu/ft²sec)

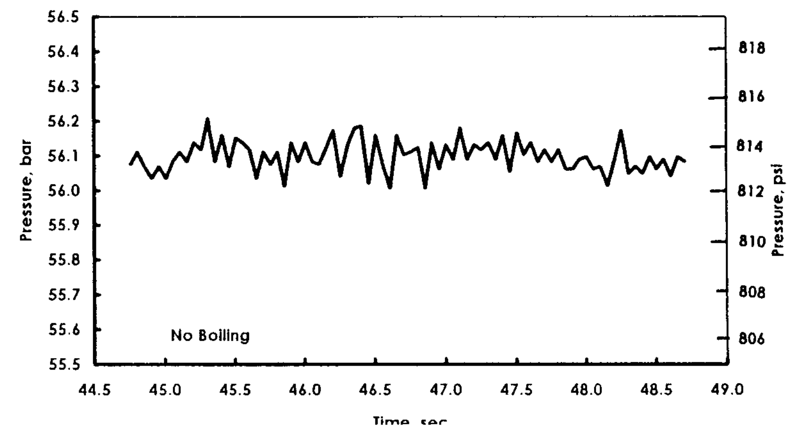

$\dot{q}_{calc}$ = 8786 kW/m² (775.6 Btu/ft²sec)

Note: Flow conditions given in Fig 18c.

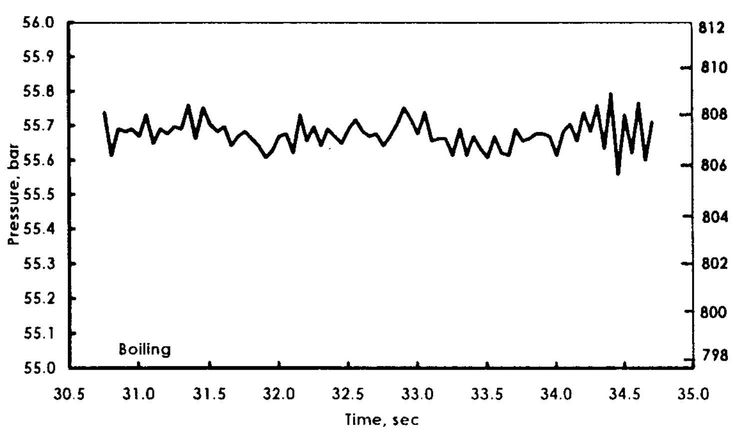

$\dot{q}_{calc}$ = 48173 kW/m² (4252 Btu/ft²sec)

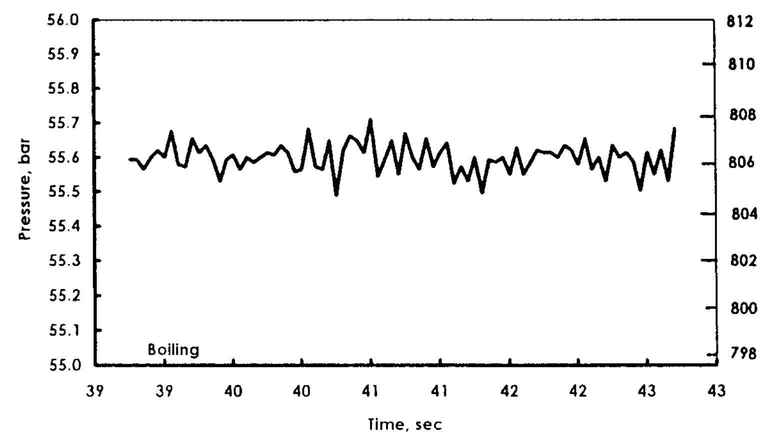

$\dot{q}_{calc}$ = 60651 kW/m² (5354 Btu/ft²sec)

d. Test Section High Speed Pressure Response
Figure 18. Concluded

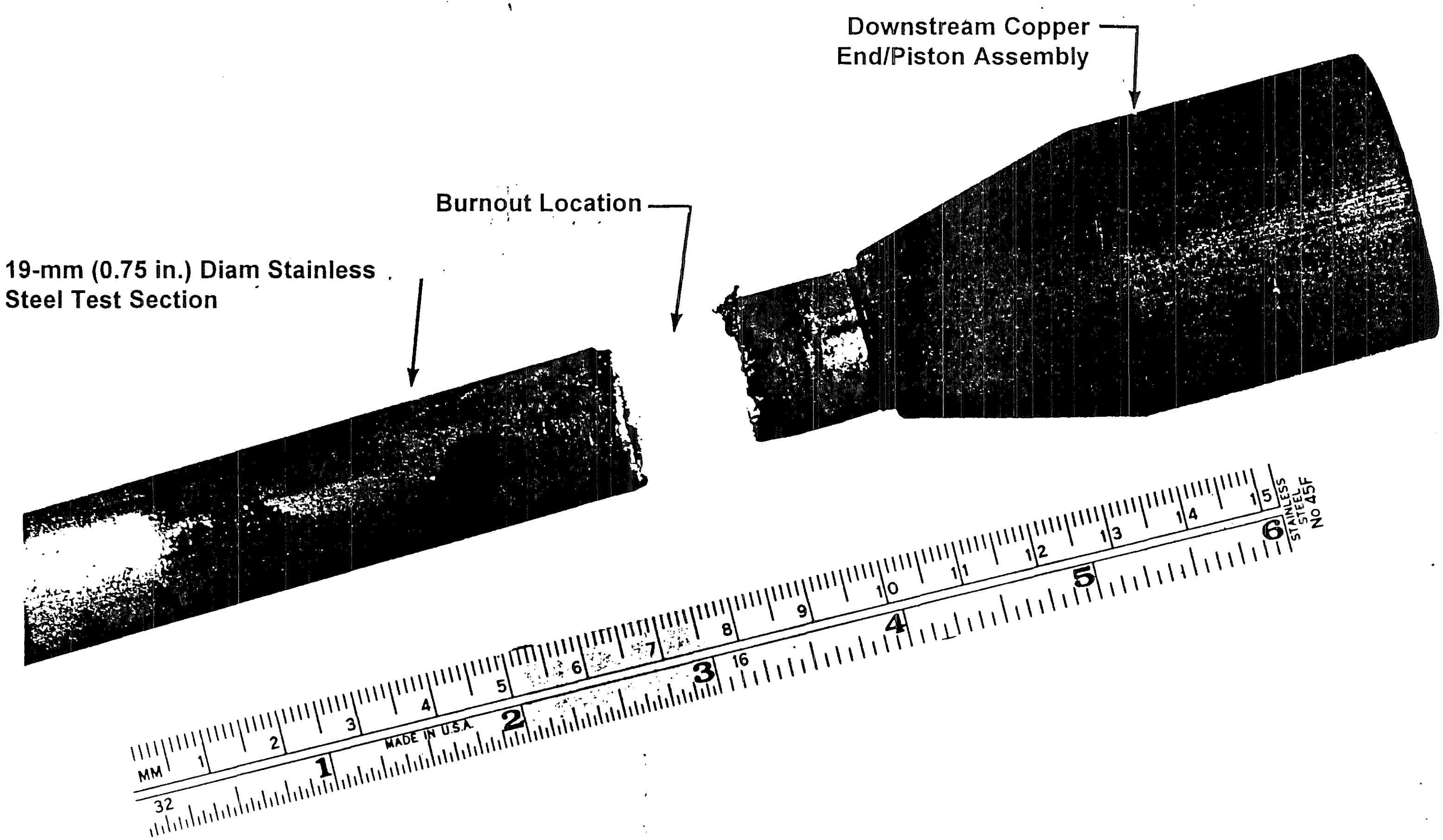

Figure 19. Posttest HTWL Test Section

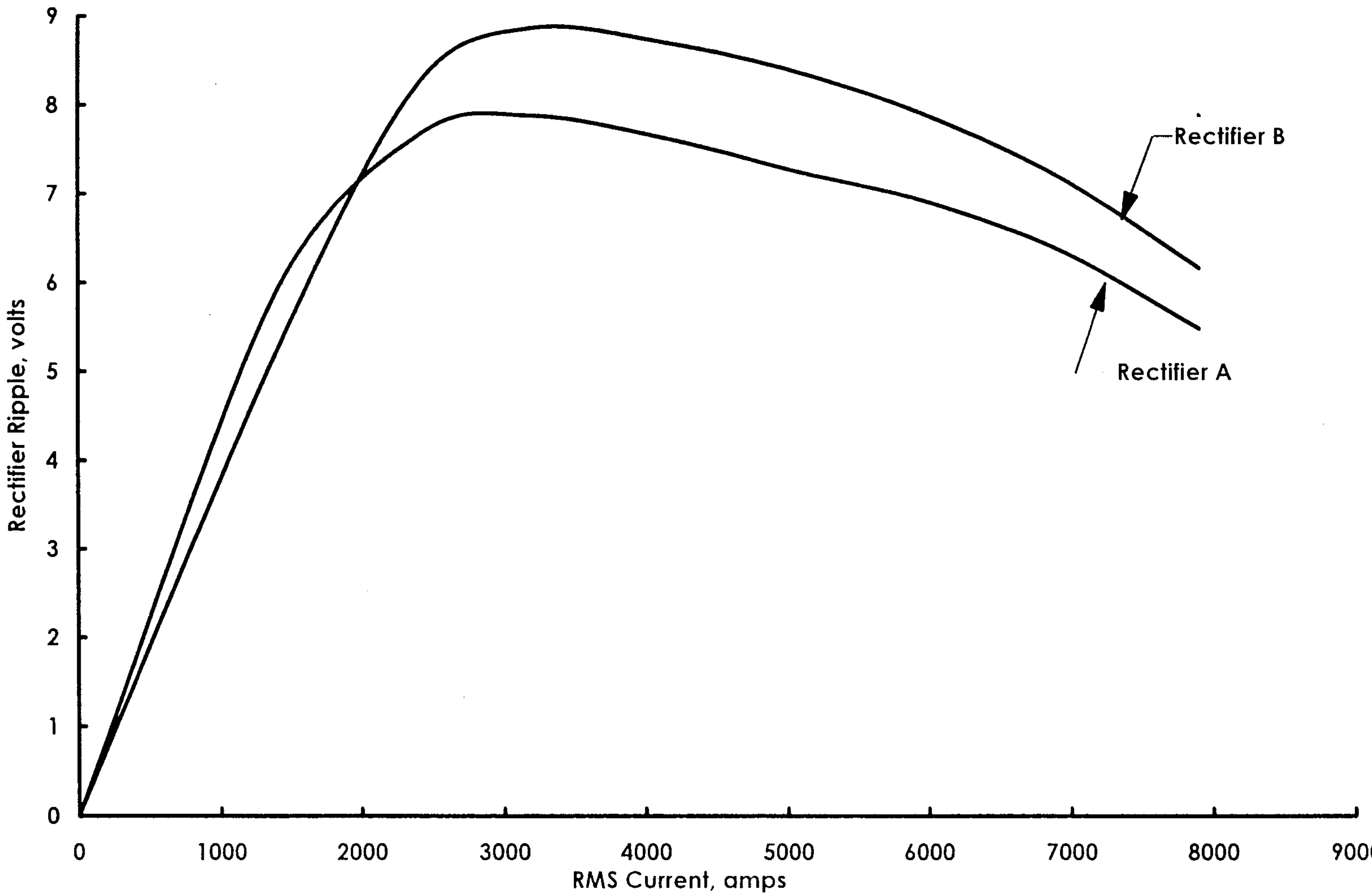

a. Ripple as a Function of rms Current
Figure 20. Rectifier Ripple Characteristics

Rectifier A

Rectifier B

I_{rms} = 1405 amps

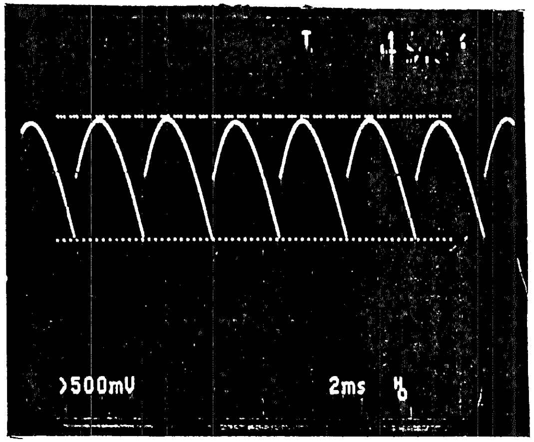

I_{rms} = 1790 amps

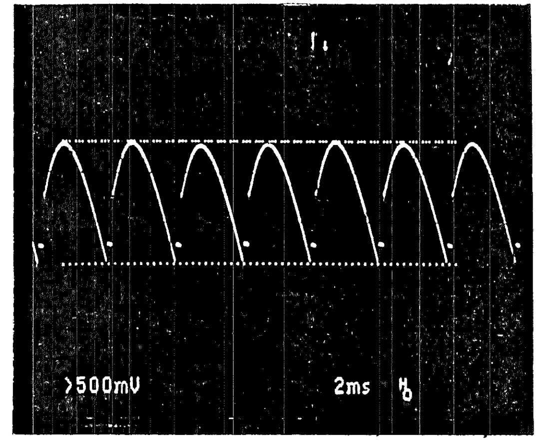

I_{rms} = 3247 amps

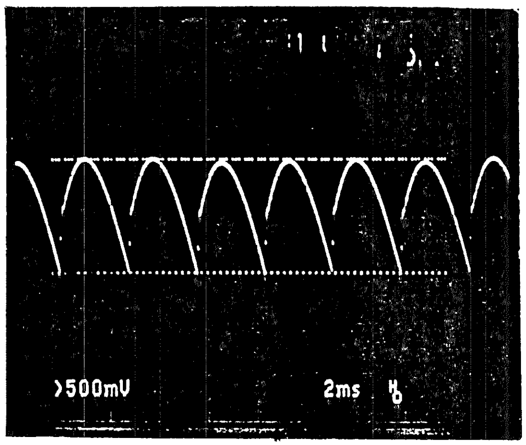

I_{rms} = 3114 amps

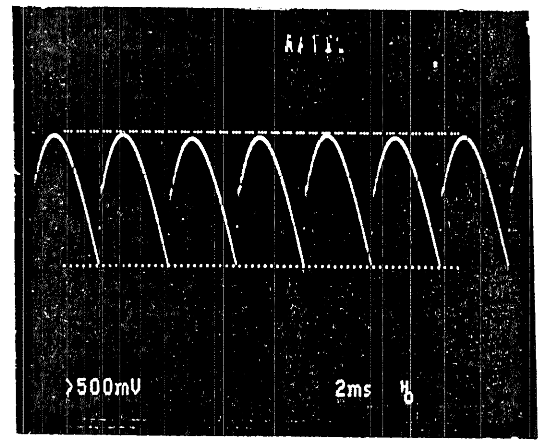

I_{rms} = 4125 amps

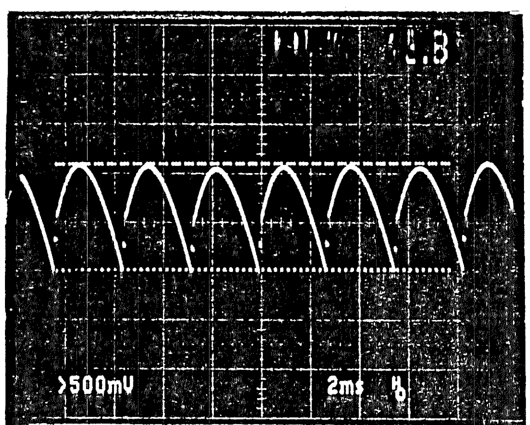

I_{rms} = 4023 amps

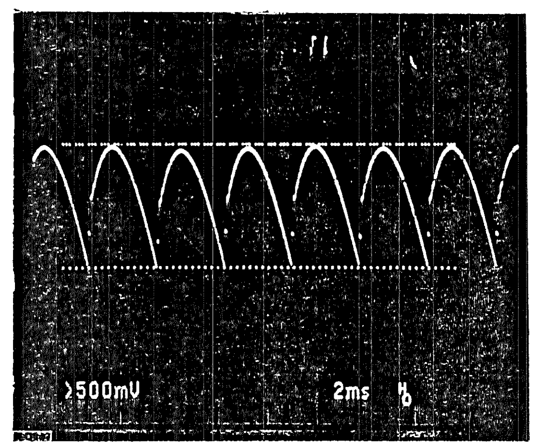

b. Rectifier Ripple Waveforms

Rectifier A

Rectifier B

I_{rms} = 5027 amps

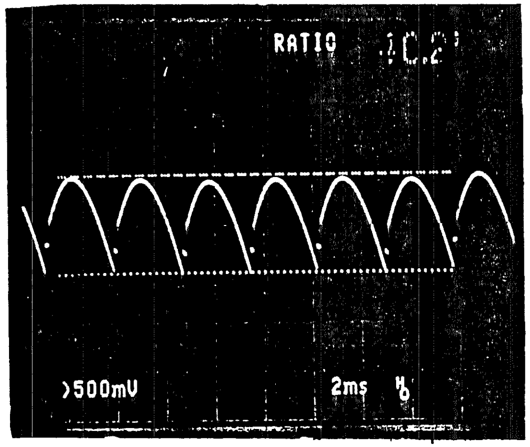

I_{rms} = 5370 amps

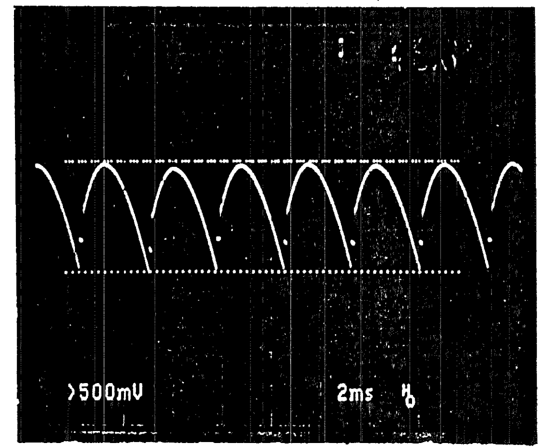

I_{rms} = 5945 amps

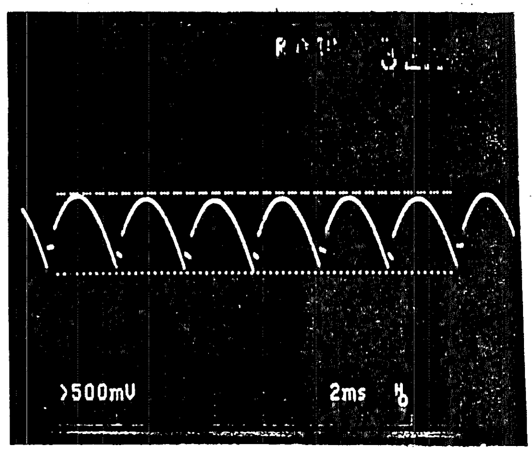

I_{rms} = 6127 amps

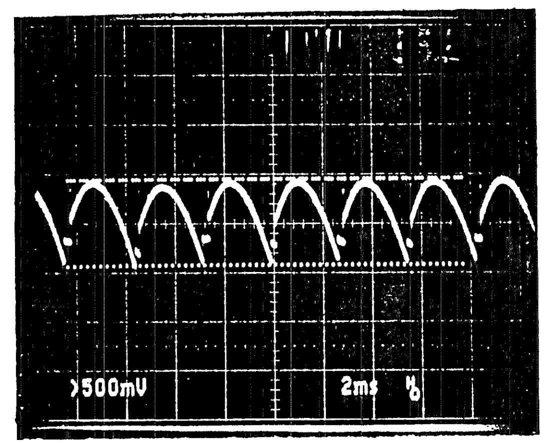

I_{rms} = 6880 amps

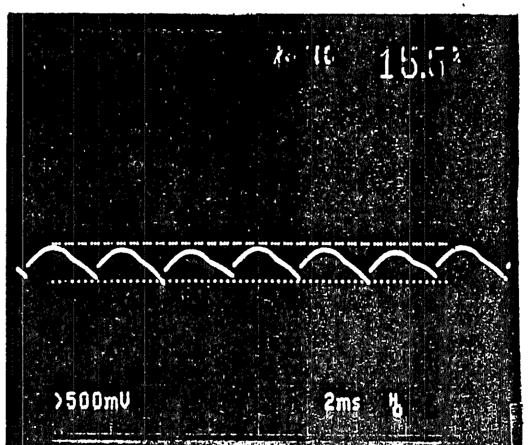

I_{rms} = 6938 amps

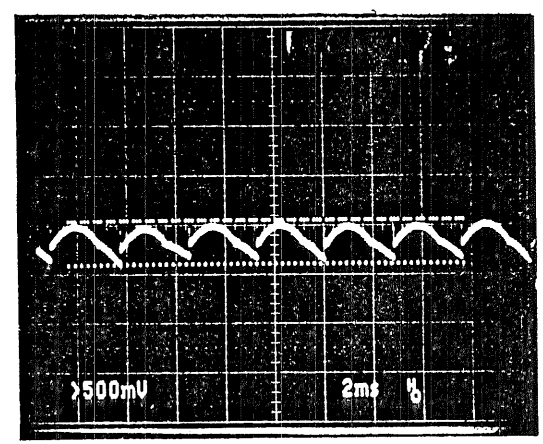

b. Concluded

Table 1. Estimated Uncertainties

a. Basic Measurements

Basic Measurement	Range	Precision Limit 2S*	Bias Limit B*	Uncertainty U_{RSS}*	Type of Measuring Device	Type of Recording Device	Method of Calibration
Manifold Pressure	13.8 - 138 bar 200 - 2000 psig	±0.06	±0.13	±0.14	Viatran Transducer	Neff Digital Data Acquisition System	In-place application of multiple pressure levels measured with a pressure measuring device calibrated in the Precision Measurement Equipment Lab
Test Section Pressure	13.8 - 138 bar (200 - 2000 psig)	±0.04	±0.17	±0.18	Teledyne Tabor Transducer	“	“
Test Section Pressure Drop	1 - 34.5 bar (15 - 500 psi)	±0.7	±0.37	±0.79	Statham Transducer	“	“
Test Section High Speed Pressure	13.8 - 138 bar (200 - 2000 psia)	±0.18	±0.1	±0.21	Kulite Transducer	“	“
Manifold Temperature	10 - 120° C) (50 - 250° F)	±2.4	±0.72	±2.5	Type T Thermocouple	Neff Digital Data Acquisition System with Internal Reference	Thermocouple verification of NBS conformity Voltage Substitution Calibration
Manifold Temperature Drop	0 - 110° C (32 - 230° F)	±1.15	±0.35	±1.2	“	“	“
Test Section Temperature	10 - 1400° C (50 - 2550° F)	±3.07	±1.3	±3.33	Type K Thermocouples	Neff D.D.A.S. with External Ice Point Ref. and Preston Amp/Filter	“
Coolant Flow Rate	0 - 850 lpm (0 - 225 gpm)	±1.3	±0.32	±1.34	Hoffer Flowmeter	Neff DDAS	NBS Conformity Rate Verification in the Precision Measurement Equipment Lab
Current-d-c	0 - 8,000 amps	±0.62	±1.9	±2.0	Rectifier Shunt	“	Manufacturer Calibration; In-place mv Substitution
Current-rms	0 - 10,000 amps	±1.0	±2.25	±2.46	Ohio Semitronics Voltage Transducer	“	“
Voltage - d-c	0 - 100 volts	±1.65	±0.71	±1.8	Rectifier Bus	“	“
Voltage-rms	0 - 100 volts	±2	±0.71	±2.1	Ohio Semitronics Voltage Transducer	“	“
Test Section Voltage Drop-d-c	0 - 100 volts	±1.65	±0.71	±1.8	Volt Meter	“	“
Rectifier Power-rms	5-1600 kW	±2	0^+	±2	Ohio Semitronics Watt Transducer	Digital Display Only	“
Magnetic Flux Density	d-c: 30 mG to 30G a-c: 50 to 99 Hz	±0.15 ±3.4	0^+	±0.15 ±3.4	F. W. Bell Gaussmeter	“	Unit Installed Standard
Test Section Roughness	0 - 10 μm (0 - 200 μin.)	±2.0	0^+	±2.0	Taylor-Hobson Roughness Machine	“	Manufacturer Calibration
Test Section Thickness	0.25 - 1 mm (0.01 - 0.04 in.)	±1.0	0^+	±1.0	Zeiss Coordinate Measurement Machine	“	“
Test Section Concentricity	25 - 38 mm (1 - 1.5 in.)	±0.1	0^+	±0.1	Dial Calipers	Manual	“
Material Electrical Resistivity	0 - 140 μohm-cm (0 - 4.5 μohm-ft)	±2.6	0^+	±2.6	Rubicon Standard Resistor/Voltage Measurement	“	Comparison to Standard Resistor and Reference Data

*Numerical values are in "% of reading".
+Assumed to be zero

Table 1. Concluded
b. Calculated Parameters

Parameter	Precision Limit, 2S % of Calculated Value	Bias Limit, B % of Calculated Value	Uncertainty, URSS % of Calculated Value
$\dot{q}_{TOT}$, E_{TOT}	± 2	± 0.71	± 2.1
$\dot{q}_{SYS}$, E_{SYS}	± 1.4	± 0.5	±1.49
$\dot{q}_{CALC}$, E_{CALC}	±3.2	± 0.71	± 3.3
$\dot{q}_{TS}$, E_{TS}	± 2	± 0.71	± 2.1
Coolant Velocity, Mass Velocity	±1.3	± 0.32	± 1.34
Calculated Wall Temperature	± 3.2	± 0.71	± 3.3
Test Section Voltage Drop-rms	± 2	± 0.71	± 2.1

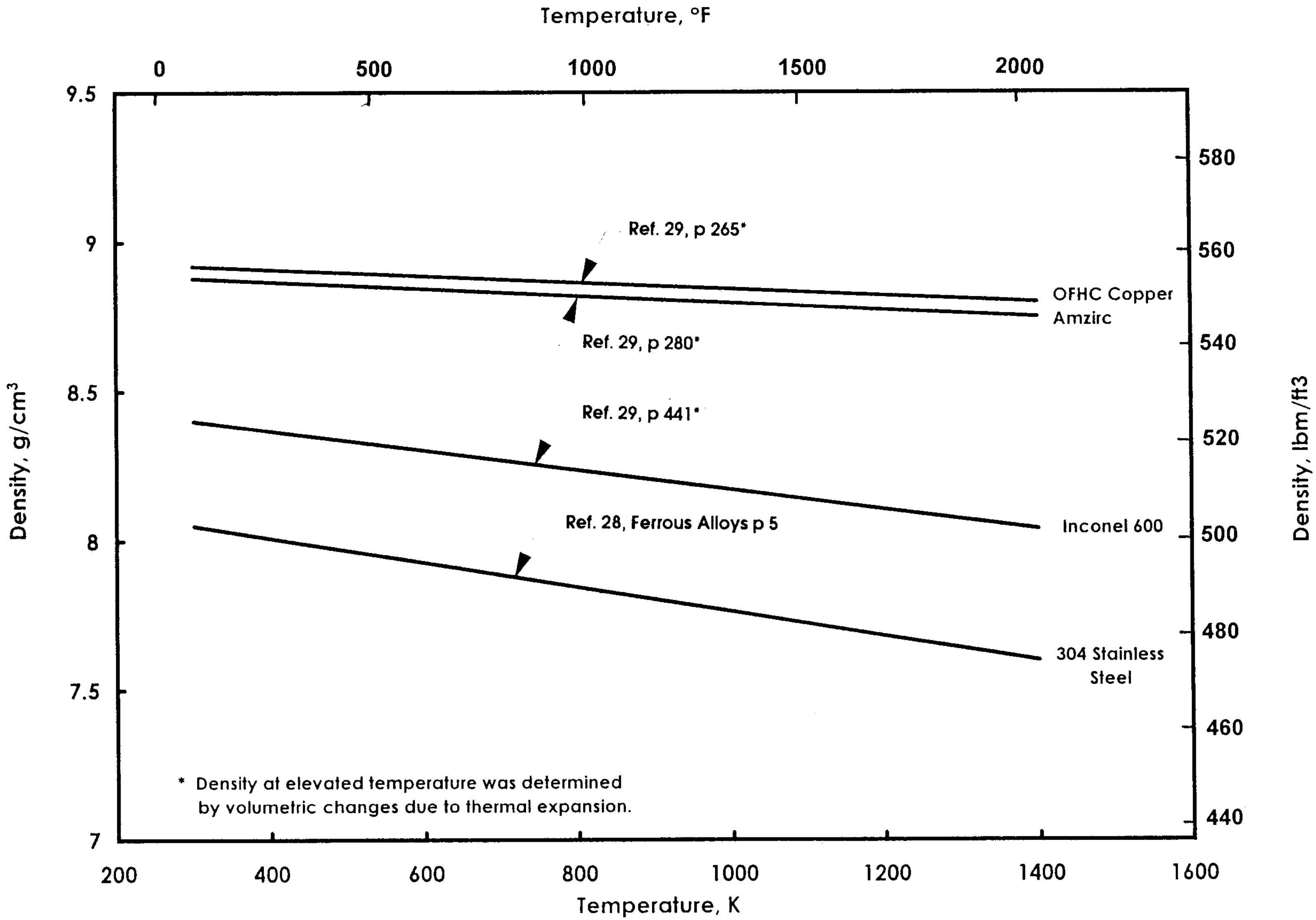

a. Density

Appendix 1. Test Section Material Properties

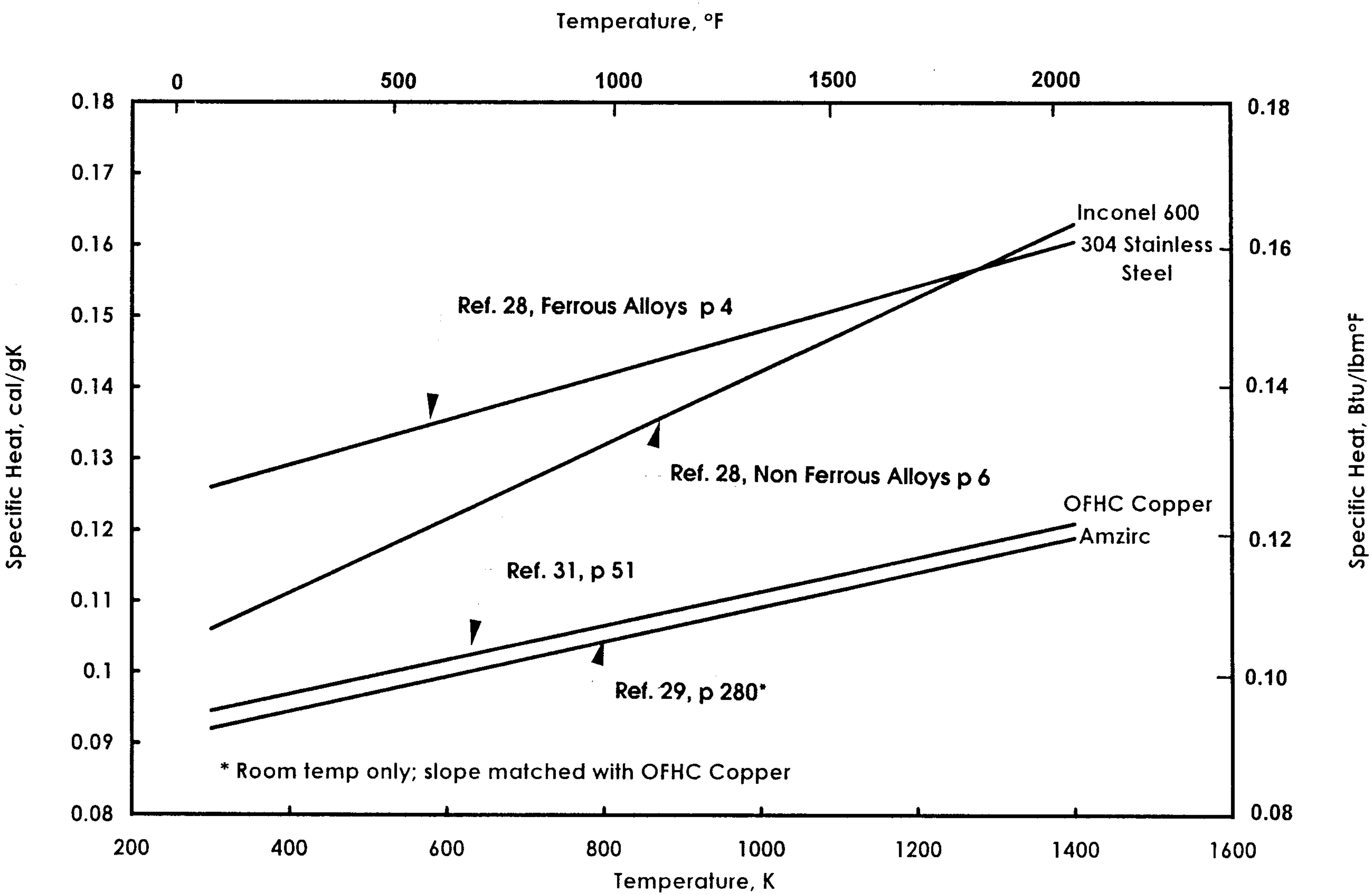

b. Specific Heat
Appendix 1. Continued

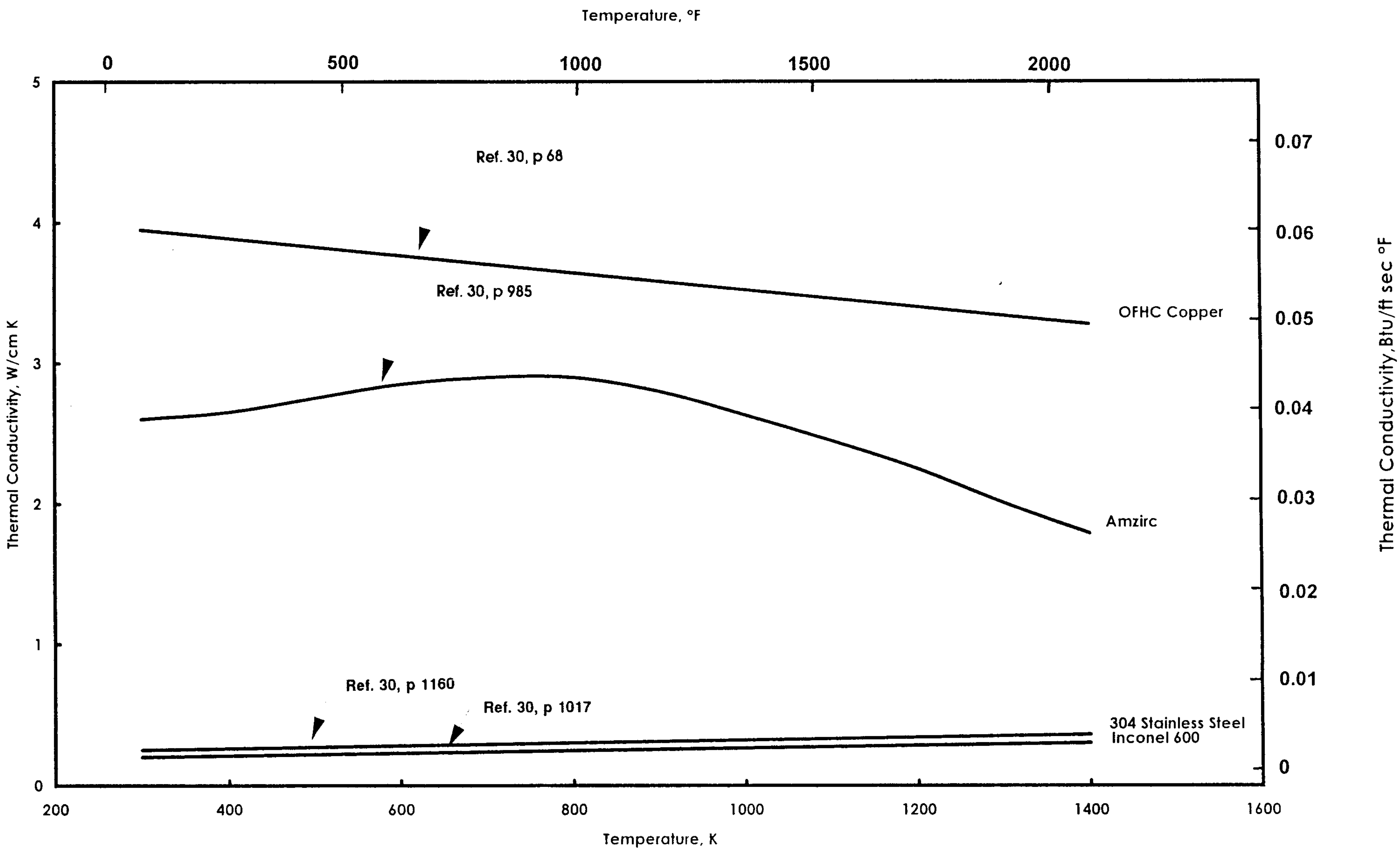

c. Thermal Conductivity
Appendix 1. Continued

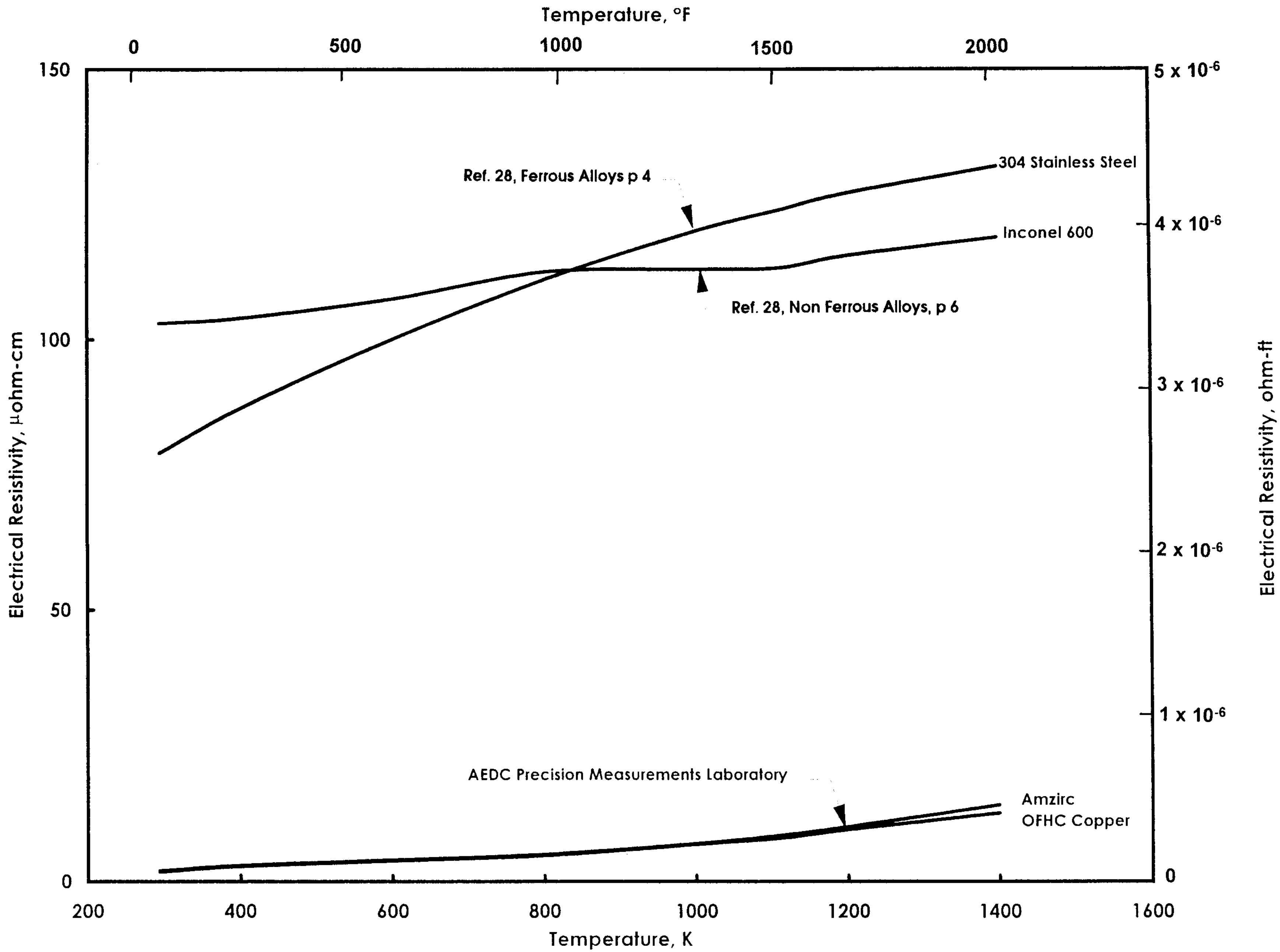

d. Electrical Resistivity
Appendix 1. Concluded

APPENDIX 2. Power Computation Procedure

Compute the surface area A_S and the cross-sectional area A_{CS} based on selected tube diameter, length, and wall thickness:

$$As = 2\pi rL = \pi d_o L$$

A_s in m^2

r, d_o, L in m

$$A_{CS} = \frac{1}{4}\pi\left(d_o^2 - d_i^2\right)$$

A_{cs} in m^2

$d_o, di,$ in m

Compute the energy required to reach the desired heat flux from:

$$E = \dot{q}\,A_s$$

$\dot{q}$ in kW/m^2

A_s in m^2

E in kW

Compute the resistance of the tubular test section:

$$R = \frac{\rho_e L}{Acs}$$

ρ_e in $ohm-m$

L in m

A_{cs} in m^2

R in ohm

Compute the current from:

$$I = \left(\frac{E}{R}\right)^{\frac{1}{2}}$$

E in W

R in ohm

I in $amps$

Compute voltage from:

$$V = \frac{E}{I}$$

E in W

I in $amps$

V in $volts$

APPENDIX 3. Data Reduction Equations and Program
a. Computational Approach

The primary calculations performed in the HTWLDR program include the energy balance/heat flux computations and the radial temperature distribution in the heated test section (for the wall/coolant interface temperature determination).

Energy/Heat Flux:

The total rectifier energy is calculated from:

$$E_{TOT} = I_{rms,TOT}\, V_{rms,avg}$$

where $I_{rms,TOT}$ is the sum of the rms current output for the two rectifiers and $V_{REC,avg}$ is the average voltage output of the rectifiers.

The corresponding heat flux is then:

$$\dot{q}_{TOT} = \frac{E_{TOT}}{A_s}$$

where A_S is the outside surface area of the test section.

A somewhat more accurate test section result may be obtained by using the measured voltage drop across the test section assembly rather than the rectifier voltage, thereby avoiding power cable, ballast resistor, and attachment losses:

$$E_{TS} = I_{rms,TOT}\, V_{TS,rms}$$

The corresponding heat flux is:

$$\dot{q}_{TS} = \frac{E_{TS}}{A_s}$$

The heat flux at the test section may also be determined by performing an energy balance on the coolant as it proceeds through the test section assembly. For an open system with no work and uniform, steady-state flow with negligible changes in kinetic and potential energy, the conservation of energy equation reduces to:

$$E_{SYS} = \dot{m}\left(h_{exit} - h_{inlet}\right)$$

where $\dot{m}$ is the mass flow of the coolant and the enthalpy change for an incompressible substance is given as:

$$h_{exit} - h_{inlet} = c_{avg}\left(T_{exit} - T_{inlet}\right) + \frac{1}{\rho}\left(P_{exit} - P_{inlet}\right)$$

where c_{avg} is the average specific heat of the coolant, ρ is the coolant density, and T and P are the temperature and pressure, respectively, at the inlet or exit of the test section. The contribution of the pressure drop on the enthalpy change is small compared to that of the temperature change, therefore:

$$h_{exit} - h_{inlet} \approx c_{avg}(T_{exit} - T_{inlet})$$

and

$$E_{SYS} = \dot{m} c_{avg}\ (T_{exit} - T_{inlet})$$

The heat flux from the test section then follows from:

$$\dot{q}_{SYS} = \frac{E_{SYS}}{A_S}$$

The fourth approach for determining heat flux at the test section requires the use of the test section voltage drop and the material electrical resistivity. Because the resistivity varies significantly with local temperature and the presence of a severe radial temperature gradient in the test section during heating, the heat flux based on electrical resistivity is determined as part of the test section temperature distribution computation presented in the following discussion.

Radial Temperature Distribution:

Because of the severe radial temperature gradient in the test section, the electrical resistivity will also vary in the radial direction and the internal heat generation will be radially nonuniform on a per volume basis. Therefore, a reasonable temperature distribution is not only important in estimating the outside wall temperature, but is necessary in determining the internal heat generation which, in turn, affects the temperature distribution.

Using the energy balance method and assuming no transverse heat conduction, a finite difference equation for a node at the center of an internal element of the test section tube may be obtained:

$$q_{i-1}\, A_{S,outer} + q_{i+1}\, A_{S,inner} + q_g Vol = 0 \qquad (1)$$

where, q_{i-1} is the heat flux into (or out of) the element at the outer face

$A_{S,outer}$ is the surface area of the outer face

q_{i+1} is the heat flux into (or out of) the element at the inner face

$A_{S,inner}$ is the surface area of the inner face

q_g is the internal heat generation
Vol is the element volume

The cylindrical geometry of the test section yields:

$$A_{S,outer} = \pi L\left(2R_i + dr\right)$$
$$A_{S,inner} = \pi L\left(2R_i - dr\right)$$
$$A_{CS} = 2\pi R_i\, dr$$
$$Vol = 2\pi R_i\, drL$$

where, L is the length of the test section tube
R_i is the radial distance to the node i
dr is the radial thickness of the element
A_{CS} is the element cross-sectional area

Invoking Fourier's law of heat conduction, the heat fluxes can be expressed as:

$$q_{i-1} = \left(\frac{k_{i-1} + k_i}{2}\right)\left[\frac{T_{i-1} - T_i}{dr}\right]$$

$$q_{i+1} = \left(\frac{k_{i+1} + k_i}{2}\right)\left[\frac{T_{i+1} - T_i}{dr}\right]$$

where k_{i+1}, k_{i-1}, and k_i are the material thermal conductivities at the inner face, outer face, and interior node, respectively. Similarly, T_{i+1}, T_{i-1}, and T_i are the respective temperatures. Substituting these equations into Eqn. (1) and rearranging, an equation for the temperature at the interior node, T_i, is obtained:

$$T_i = \left[\left(\frac{k_{i-1} + 2k_i + k_{i+1}}{2dr}\right) + \left(\frac{k_{i-1} - k_{i+1}}{4R_i}\right)\right]^{-1} \left\{\left[\left(\frac{k_{i-1} + k_i}{2dr}\right) + \left(\frac{k_{i-1} + k_i}{4R_i}\right)\right] T_{i-1} + \left[\left(\frac{k_{i+1} + k_i}{2dr}\right) - \left(\frac{k_{i+1} + k_i}{4R_i}\right)\right] T_{i+1} + q_g\, dr\right\} \quad (2)$$

The energy balance for the inner wall element is treated in a similar fashion but allowing for an adiabatic wall at the inner face:

$$q_{i-1} A_{s,outer} + \underbrace{q_{i+1} A_{s,inner}}_{=0} + q_g Vol = 0 \quad (3)$$

where,

$$A_{S,outer} = \pi L\left(2R_I + dr\right)$$
$$A_{CS} = \pi R_I\, dr$$
$$Vol = \pi R_I\, drL$$

and R_I is the test section inner diameter.

From Fourier's law:

$$q_{i-1} = \left(\frac{k_{i-1} + k_i}{2}\right)\left[\frac{T_{i-1} - T_I}{dr}\right]$$

Substituting into Eqn. (3) and solving for the inner wall temperature, T_I:

$$T_I = \left[\left(k_{i-1} + k_i\right)\left(\frac{R_I}{dr} + \frac{1}{2}\right)\right]^{-1}\left[\left(k_{i-1} + k_i\right)\left(\frac{R_I}{dr} + \frac{1}{2}\right)T_{i-1} + q_g\, dr\, R_I\right] \tag{4}$$

The energy balance on the outer wall element yields:

$$q_{i-1}\, A_{S,outer} + q_{i+1}\, A_{S,inner} + q_g Vol = 0 \tag{5}$$

where,

$$A_{S,outer} = 2\pi R_O L$$
$$A_{S,inner} = \pi L(2R_O - dr)$$
$$A_{CS} = \pi R_O\, dr$$
$$Vol = \pi R_O\, drL$$

and R_O is the test section outer diameter. From Fourier's law the inner face heat flux is:

$$q_{i+1} = \left(\frac{k_{i+1} + k_i}{2}\right)\left[\frac{T_{i+1} - T_O}{dr}\right]$$

where T_O is the outer wall temperature. From Newton's law of cooling the outer wall heat flux is given as:

$$q_{i-1} = h\left(T_b - T_O\right)$$

where h is the assumed convective heat transfer coefficient and T_b is the bulk coolant temperature. Substituting into Eqn. (5) and solving for the outer wall temperature, T_O:

$$T_O = \left[h + \left(\frac{k_{i+1} + k_i}{2dr}\right) - \left(\frac{k_{i+1} + k_i}{4Ro}\right)\right]^{-1} \left\{hT_b + \left(\frac{k_{i+1} + k_i}{2}\right)\left[\left(\frac{T_{i+1}}{dr}\right) - \left(\frac{T_{i+1}}{2Ro}\right)\right] + q_g\left(\frac{dr}{2}\right)\right\} \tag{6}$$

The heat generation q_g in Eqns. (2), (4), and (6) is given as:

$$q_g = \frac{E}{Vol}$$

However, the energy E can be written in the form of electrical measurements and geometry:

$$E = I^2 R = \frac{V^2}{R} = \frac{Acs\, V^2}{\rho_e L}$$

where,
E is the generated energy
I is the current
V is the voltage drop across the test section
R is the electrical resistance = $\frac{\rho_e L}{Acs}$
ρ_e is the material electrical resistivity

Therefore, $$q_g = \frac{Acs\, V^2}{\rho_e L Vol}$$

or simplifying,

$$q_g = \frac{V^2}{\rho_e L^2} \tag{7}$$

The radial temperature distribution can be solved with Gauss-Seidel iteration by using an initial estimate for the temperature distribution and heat transfer coefficient, and solving Eqns. (2), (4), and (6) for a refined temperature distribution solution. Substitution of this refined solution into the equations continues until a stable solution is achieved (a small residual between successive temperature calculations). The number of iterative cycles can be reduced by using relaxation of the form:

$$T_{new} = \beta\, T_{current} + (1 - \beta)T_{previous}$$

where, $T_{current}$ is the temperature computed from Eqns. (2), (4), and (6)
$T_{previous}$ is the temperature previously calculated and used in the equations to compute $T_{current}$
β is the relaxation factor ; for linear systems $1 < \beta < 2$

T_{new} is the new temperature to be used in the next iterative cycle

The heat rates from each elemental heat generation may be summed for all elements when temperature convergence is achieved, and the total heat flux from the test section, $\dot{q}_{CALC}$, is calculated using the overall test section geometry. The corresponding calculated energy is:

$$E_{CALC} = \dot{q}_{CALC} \, A_S$$

Since the inner wall temperature is measured at several stations along the test section length, a direct comparison between the measured value and the calculated inner wall temperature can be made. Some difference between the two temperatures is expected because the convective heat transfer coefficient on the outer surface of the test section that is used in the computations is only an estimate. This heat transfer coefficient can be adjusted within the data reduction program to provide a match between the measured and calculated values of the inner wall temperature.

In addition to the heat rates from each elemental heat generation, the current flow through each element may be summed to obtain the total current flow through the test section. Because the measured voltage drop across the test section has some uncertainty associated with a-c ripple and losses in slip fit joints within the test section assembly, the voltage drop used in the heat generation calculation, Eqn. (7), may be adjusted within the program such that the calculated current and measured rms current match. Such voltage drop corrections are typically small.

The selection of the number of elements in the finite difference scheme is important such that continuity is maintained, i.e., the resistance to conduction within the test section is much less than the resistance to convection across the coolant boundary layer. The thickness, dr, of the elements is selected such that the Biot number, Bi, remains less than 0.1:

$$B_i = \frac{h}{k}\left(\frac{dr}{2}\right) < 0.1$$

where h is the largest heat transfer coefficient expected, and k is the lowest test section material thermal conductivity expected.

For comparison purposes, a simplistic solution of the integrated cylindrical 1-D heat transfer equation can be used to compute a test section outer wall temperature. Assuming steady-state conditions, constant material properties, uniform heat generation, and no transverse heat conduction, the heat equation reduces to:

$$\frac{1}{r}\frac{d}{dr}\left(r\frac{dT}{dr}\right) + \frac{q_g}{k} = 0$$

For the HTWL test section the appropriate boundary conditions are:

1) $T\left(R_I\right) = T_I$ measured with a thermocouple

2) $\left.\dfrac{dT}{dr}\right|_{R_I} = 0$ assumed adiabatic inner wall

Integrating the above heat equation and invoking the boundary conditions, the temperature as a function of radial position, r, is:

$$T\left(r\right) = T_I + \frac{q_g}{4k}\left(R_I^2 - r^2\right) - \frac{q_g}{2k} R_I^2 \ln \frac{R_I}{r}$$

and solving for the outer wall temperature:

$$T_O = T_I + \frac{q_g}{4k}\left(R_I^2 - R_O^2\right) - \frac{q_g}{2k} R_I^2 \ln \frac{R_I}{R_O} \tag{8}$$

Because of the severe temperature gradients expected and, hence, the nonuniform material properties and heat generation per unit volume in the radial direction, Eqn. (8) is expected to have a significant error.

APPENDIX 3. Continued

b. Program Listing

```
C
C      PROGRAM HTWLDR
C
C        This program performs the required data reduction for the
C        raw data acquired in the HTWL experiment.  It computes the
C        steady-state temperature distribution in a tube with internal
C        heat generation (resistance heating), temperature dependent
C        material properties, and a convective boundary condition on
C        the outside surface / adiabatic wall on the inside.  A finite
C        difference scheme employing Gauss-Seidel iteration with
C        relaxation is used to reach a steady-state solution.  The
C        initial estimate for the heat-transfer coefficient on the out-
C        side wall and the test section voltage drop can be adjusted to
C        force a match of the computed inside wall temperature and
C        current with the actual measured values. Suspected bad
C        thermocouple measurements may be bypassed when the heat-
C        transfer coefficient adjustment is performed and the calculated
C        heat flux is matched to the heat flux from the coolant
C        temperature rise to get a reasonable wall temperature.  Coolant
C        conditions and energy balances are also computed.  For
C        comparison purposes, a simplistic solution of the integrated
C        1D heat transfer equation (cylindrical) is used to compute an
C        outside surface temperature.  The 1D solution assumes constant
C        material properties, uniform heat generation, and no transverse
C        heat conduction.
C
C
C         INPUTS
C
C        RUN            Run number
C        IMT,IDY,IYR    Run month,day,year
C        IHR,IMN,ISC    Run time in hr,min,sec
C        UNITS          Output units:  1 - SI    2 - English
C        BOL            Burnout location: 0 - none     1 - upstream
C                                                      2 - downstream
C        NPR            Print increment for radial distribution, SEC/10
C        NX             Number of thermocouple axial locations
C        NP             Number of power settings (excluding 0 setting)
C        NR             Number of rectifiers operating:  1 - single
C                                                        2 - both
C        IMAT           Material type:  1 - 304 SS       2 - OFHC Copper
C                                       3 - Amzirc       4 - Inconel 600
C        IDIST          0 = bypass    1 = Print radial temp distribution
C        SEC            Number of radial elements (real): 200. (for Biot
C                           No. < 0.1)
C        NOR            Number of radial nodes (integer): 201 (SEC+1)
C        BETA           Relaxation factor in temp distribution calc: 1.6
C        EPS            Error on temp for residual check: 0.001
C        ERV            Error on current for voltage correction: 10.
C        ERRT           Error on temp for h correction: 5.
C        ERQ            Error on heat flux for Twall calc (if all TC's
C                           are bad for a given power setting): 100.
C        IHCORR         0 = bypass    1 = corrects h estimate for tc match
C        IICORR         0 = bypass    1 = corrects voltage for curr match
C        D1,D2,D3       Tube ID, OD, and annulus ID, in.
C        LTUBE          Tube length, in.
C        RWATER         Water resistivity, microS/cm
C        FLLP           Flow loop,  0 = closed, 1 = open
C        PMANIN         Inlet manifold pressure, psig
C        TMANIN         Inlet manifold temperature, deg-F
```

```
C        WF            Water flow rate, gpm
C        PMANOUT       Outlet manifold pressure, psig
C        PTS1-4        Test section pressure - locations 1-4, psig
C        DPTS          Delta-P across test section, psi
C        TMANOUT       Outlet manifold temperature, deg-F
C        DTMAN1,2      Location 1 & 2 Delta-T on manifolds, millivolts
C        IREC1,2       #1 and #2 rectifier current, amps
C        IRMS1,2       #1 and #2 rectifier rms current, amps
C        VREC1,2       #1 and #2 rectifier voltage, volts
C        DVTS          Total voltage drop across test section, volts
C        ETOT1,2       Total power from rectifier #1 and #2, watts
C        H             Outside wall heat-transfer coefficient (estimate),
C                       Btu/sq-ft hr deg-F
C        XLOC1-NX      Axial locations along test section for the
C                      following, in.
C        TTS1-NX       Thermocouple output along test section, deg-F
C        TCBAD1-NX     Suspected bad thermocouple reading indicator,
C                       used to bypass h correction when IHCORR = 1:
C                       0 = ok     1 = bad reading
C
C
C
C         OUTPUT
C
C        PMAN-IN       Inlet manifold pressure, bar or psia
C        TMAN-IN       Inlet manifold temperature, deg-C or deg-F
C        G             Coolant mass velocity, kg/m^2 s or lbm/ft^2 s
C        VEL           Coolant velocity, m/s or ft/s
C        R(WATER)      Water resistivity, microS/cm
C        QDOT-TS       Heat flux calculated using rms current and test
C                       section voltage drop, kW/m^2 or Btu/ft^2 s
C        QDOT-SYS      Heat flux calculated using coolant mass flow,
C                       specific heat, and temperature rise across test
C                       section, kW/m^2 or Btu/ft^2 s
C        QDOT-TOT      Heat flux calculated using rms current and
C                       rectifier voltage, kW/m^2 or Btu/ft^2 s
C        QDOT-CALC     Heat flux calculated using material resisitivity
C                       (computed in finite difference calculation of
C                       temperature distribution), kW/m^2 or Btu/ft^2 s
C        TWALL         Test section outside wall temperature (computed
C                       in finite difference calculation of temperature
C                       distribution), deg-C or deg-F
C        TW1D          Test section outside wall temperature (computed
C                       from integrated 1D cylindrical heat transfer
C                       equation), deg-C or deg-F
C        TBULK         Local bulk coolant temperature computed from
C                       linear fit of inlet and outlet manifold
C                       temperatures, deg-C or deg-F
C        TSAT          Coolant saturation temperature, deg-C or deg-F
C        DTSAT         Difference between coolant saturation temperature
C                       and bulk temperature, deg-C or deg-F
C        DTSUB         Difference between test section wall temperature
C                       and coolant saturation temperature, deg-C or
C                       deg-F
C        E-TS          Energy calculated using rms current and test
C                       section voltage drop, kW
C        E-SYS         Energy calculated using coolant mass flow,
C                       specific heat, and temperature rise across test
C                       section, kW
C        E-TOT         Energy calculated using rms current and
C                       rectifier voltage, kW
C        E-CALC        Energy calculated using material resisitivity
C                       (computed in finite difference calculation of
C                       temperature distribution), kW
```

```
C        IREC-TOT      Total rectifier d-c current, amps
C        IRMS-TOT      Total rectifier rms current,amps
C        VREC-TOT      Average rectifier d-c voltage, volts
C        VRMS-TOT      Average rectifier rms voltage, volts
C        DVTS-DC       Total d-c voltage drop across test section, volts
C        DVTS-RMS      Total rms voltage drop across test section, volts
C        PTS1-4        Test section pressure - locations 1-4, bar or psia
C        DPTS          Delta-P across test section, bar or psi
C        PMAN-OUT      Outlet manifold pressure, bar or psia
C        TMAN-OUT      Outlet manifold temperature, deg-C or deg-F
C        DTMAN         Average delta-T across manifolds, deg-C or deg-F
C        QGEN TOT      Heat generation calculated using local voltage
C                       and material resistivity, kW/m^3 or Btu/ft^3 s
C        CURR TOT      Calculated total current using local voltage
C                       and material resistivity, amps
C        VOLT CORR     Corrected local voltage in test section to match
C                       computed inside wall temperature with measured
C                       inside wall temperature, volts
C        H CORR        Corrected heat transfer coefficient on outside of
C                       test section to match computed current with
C                       measured current,kW/m^2 deg-C or Btu/ft^2 s deg-F
C        H ESTIMATE    Estimated outside wall heat-transfer coefficient,
C                       kW/m^2 deg-C or Btu/ft^2 s deg-F
C        RADIUS        Distance from centerline of test section to
C                       calculated local temperature/heat flux position
C                       (temperature distribution calculation), mm or in.
C        T1-5          Calculated local temperature (temperature
C                       distribution calculation), deg-C or deg-F
C        QDOT          Calculated local heat flux (temperature
C                       distribution calculation), kW/m^2 or Btu/ft^2 s
C        QGEN          Calculated local heat generation (temperature
C                       distribution calculation), kW/m^3 or Btu/ft^3 s
C        RESIDUAL      Calculated temperature residual in Gauss-Seidel
C                       iteration (temperature distribution calculation),
C                       deg-C or deg-F
C        NP            Power setting number
C        STATION       Axial station number along test section
C
C
      IMPLICIT REAL*8(A-H,M-Z)
      COMMON I,J,K
      DIMENSION PMANOUT(0:20),PTS1(0:20),PTS2(0:20),PTS3(0:20),
     $          PTS4(0:20),DPTS(0:20),IREC1(0:20),IREC2(0:20),
     $          IREC(0:20),IRMS1(0:20),IRMS2(0:20),IRMS(0:20),
     $          VREC1(0:20),VREC2(0:20),VREC(0:20),DVTS(0:20),
     $          ETOT1(0:20),ETOT2(0:20),ETOT(0:20),TMANOUT(0:20),
     $          DTMAN1(0:20),DTMAN2(0:20),DTMAN(0:20),ETS(0:20),
     $          ECALC(10,0:20),QCALC(10,0:20),QTOT(0:20),
     $          QTS(0:20),ESYS(0:20),QSYS(0:20),XLOC(10),
     $          TTS(10,0:20),TSAT(10,0:20),TBULK(10,0:20),
     $          TWALL(10,0:20),PLOCAL(10,0:20),HG(0:20),TWIN(10,0:20),
     $          T(10,0:20,0:300),XLOCMM(10),RADMM(300),VRMS1(0:20),
     $          TW(10,0:20,0:300),DTSAT(10,0:20),H(0:20),VRMS2(0:20),
     $          DTSUB(10,0:20),QGTOT(10,0:20),CURTOT(10,0:20),
     $          RADI(10,0:20,300),RESID(10,0:20,0:300),VRMS(0:20),
     $          QDOT(10,0:20,300),QGEN(10,0:20,300),DVTSRMS(0:20),
     $          RESTOT(10,0:20),TCBAD(10,0:20),HC(10,0:20),
     $          KMT(10,0:20,0:300),TW1D(10,0:20),PTS1SI(0:20),
     $          TDBAD(10,0:20),VCBAD(10,0:20),HCBAD(10,0:20),
     $          QTSE(0:20),QSYSE(0:20),QTOTE(0:20),DPTSSI(0:20),
     $          QCALCE(10,0:20),TWALLF(10,0:20),PTS2SI(0:20),
     $          TW1DF(10,0:20),TBULKF(10,0:20),TSATF(10,0:20),
     $          DTSATF(10,0:20),DTSUBF(10,0:20),TMANOUTF(0:20),
     $          DTMANF(0:20),PTS3SI(0:20),PTS4SI(0:20),HGSI(0:20),
```

```
     $             PMANOUTS(0:20),QDTOTE(10,0:20),QGTOTE(10,0:20),
     $             HCSI(10,0:20),RADIN(300),TWF(10,0:20,0:300),
     $             QDOTE(10,0:20,300),QGENE(10,0:20,300),TW1DI(10,0:20),
     $             VOLTC(10,0:20),RESIDF(10,0:20,0:300),KMTAVG(10,0:20),
     $             QDTOT(10,0:20),TTSF(10,0:20),QGT(10,0:20)
      REAL*8 KMT,LTUBE,LTUBEIN,LTUBEMM,IREC1,IREC2,IREC,IRMS1,IRMS2,
     $       IRMS,KMTAVG
C       INTEGER*2 IHOUR,IMINUTE,ISECOND,IHUN,IYEAR,IMONTH,IDAY
      INTEGER*2 IHOUR,IMINUTE,ISECOND,IYEAR,IMONTH,IDAY
      INTEGER NX,NP,NR,FLLP,RUN,NOR,N,TDBAD,VCBAD,HCBAD,CHK,BOL,TCBAD,
     $          TCBD,NPR,UNITS
C
C         TIME & DATE ON PC USING GETTIM & GETDAT
C       CALL GETTIM(IHOUR,IMINUTE,ISECOND,IHUN)
C       CALL GETDAT(IYEAR,IMONTH,IDAY)
C
C         TIME & DATE ON WORKSTATION (UNIX) USING date
      CALL SYSTEM('date "+%m %d 19%y %H %M %S" > DTTMP')
      OPEN(99,FILE='DTTMP')
      READ(99,999)IMONTH,IDAY,IYEAR,IHOUR,IMINUTE,ISECOND
      CLOSE(99)
C
C        OPEN PROGRESS FILE
C
      OPEN(98,FILE='DRPROG')
C
C        INPUT STATEMENTS
C
      READ(*,*)RUN,IHR,IMN,ISC,IMT,IDY,IYR,UNITS,BOL,NPR
      WRITE(98,5)RUN
      CLOSE(98)
      WRITE(*,*)
      WRITE(*,5)RUN
      WRITE(*,*)
      WRITE(*,*)RUN,IHR,IMN,ISC,IMT,IDY,IYR,UNITS,BOL,NPR
      READ(*,*)NX,NP,NR,IMAT,IDIST,SEC,NOR,BETA,EPS,ERV,IHCORR,IICORR,
     $           ERRT,ERQ
      WRITE(*,*)NX,NP,NR,IMAT,IDIST,SEC,NOR,BETA,EPS,ERV,IHCORR,IICORR,
     $            ERRT,ERQ
      READ(*,*)D1,D2,D3,LTUBE,RWATER,FLLP,PMANIN,TMANIN,WF
      WRITE(*,*)D1,D2,D3,LTUBE,RWATER,FLLP,PMANIN,TMANIN,WF
C        CONVERT TMANIN FROM DEGF TO DEGC
      TMANIN = (5./9.) * (TMANIN - 32.)
      DO 10 J=0,NP
      READ(*,*)PMANOUT(J),PTS1(J),PTS2(J),PTS3(J),PTS4(J),DPTS(J),
     $           TMANOUT(J),DTMAN1(J),DTMAN2(J),IREC1(J),IREC2(J),
     $           IRMS1(J),IRMS2(J),VREC1(J),VREC2(J),DVTS(J),ETOT1(J),
     $           ETOT2(J),H(J)
      WRITE(*,*)PMANOUT(J),PTS1(J),PTS2(J),PTS3(J),PTS4(J),DPTS(J),
     $           TMANOUT(J),DTMAN1(J),DTMAN2(J),IREC1(J),IREC2(J),
     $           IRMS1(J),IRMS2(J),VREC1(J),VREC2(J),DVTS(J),ETOT1(J),
     $           ETOT2(J),H(J)
      HG(J) = H(J)
C        CONVERT DTMAN FROM MILLIVOLTS TO DEGC
      DTMAN1(J) = 0.0089 + 25.2736 * DTMAN1(J) - 0.2844 *
     $              (DTMAN1(J)**2.)
      DTMAN2(J) = 0.0089 + 25.2736 * DTMAN2(J) - 0.2844 *
     $              (DTMAN2(J)**2.)
C        CONVERT TMANOUT FROM DEGF TO DEGC
      TMANOUT(J) = (5./9.) * (TMANOUT(J) - 32.)
 10   CONTINUE
      DO 25 J=0,NP
      DO 20 I=1,NX
      READ(*,*)XLOC(I),TTS(I,J),TCBAD(I,J)
```

```
      WRITE(*,*)XLOC(I),TTS(I,J),TCBAD(I,J)
C       CONVERT TTS FROM DEGF TO DEGC
      TTS(I,J) = (5./9.) * (TTS(I,J) - 32.)
      IF(TTS(I,J).GT.0.0)GO TO 15
      TTS(I,J) = 0.0
 15   CONTINUE
      XLOCMM(I) = XLOC(I) * 25.4
C       INITIALIZE CONVERGENCE CHECKS
      TDBAD(I,J)=0
      VCBAD(I,J)=0
      HCBAD(I,J)=0
 20   CONTINUE
 25   CONTINUE
C
C       CONDITIONS
C
C       CONVERT LENGTHS FROM IN. TO METERS
      PI = 3.14159
      D1IN = D1
      D2IN = D2
      D3IN = D3
      LTUBEIN = LTUBE
      D1 = 0.0254 * D1
      D2 = 0.0254 * D2
      D3 = 0.0254 * D3
      LTUBE = 0.0254 * LTUBE
      D1MM = D1 * 1000.
      D2MM = D2 * 1000.
      D3MM = D3 * 1000.
      LTUBEMM = LTUBE * 1000.
C
      PMANIN = PMANIN + 14.7
      CALL WATPROP(TMANIN,RHOW,CPW)
      WFSI = ((WF * 0.003785)/60.) * RHOW
      AANN = (PI/4.0) * ((D3**2) - (D2**2))
      VEL = WFSI/(RHOW * AANN)
      G = RHOW * VEL
C
C       PRINT HEADER
C
      WRITE(*,490)
      WRITE(*,*)
      WRITE(*,500)IMONTH,IDAY,IYEAR
      WRITE(*,510)IHOUR,IMINUTE,ISECOND
      WRITE(*,520)IMT,IDY,IYR
      WRITE(*,530)IHR,IMN,ISC
      WRITE(*,*)
      WRITE(*,*)
      WRITE(*,540)
      WRITE(*,*)
      WRITE(*,550)
      WRITE(*,*)
      WRITE(*,560)
      IF(UNITS.EQ.1)GO TO 26
      WRITE(*,571)
      GO TO 27
 26   CONTINUE
      WRITE(*,570)
 27   CONTINUE
      IF(IMAT.GT.1)GO TO 40
      IF(FLLP.GT.0)GO TO 30
      IF(UNITS.EQ.1)GO TO 28
      WRITE(*,580)RUN,D1IN,D2IN,D2IN,D3IN,LTUBEIN
      GO TO 29
```

```
28      CONTINUE
        WRITE(*,580)RUN,D1MM,D2MM,D2MM,D3MM,LTUBEMM
29      CONTINUE
        GO TO 100
30      CONTINUE
        IF(UNITS.EQ.1)GO TO 31
        WRITE(*,590)RUN,D1IN,D2IN,D2IN,D3IN,LTUBEIN
        GO TO 32
31      CONTINUE
        WRITE(*,590)RUN,D1MM,D2MM,D2MM,D3MM,LTUBEMM
32      CONTINUE
        GO TO 100
40      CONTINUE
        IF(IMAT.GT.2)GO TO 60
        IF(FLLP.GT.0)GO TO 50
        IF(UNITS.EQ.1)GO TO 41
        WRITE(*,600)RUN,D1IN,D2IN,D2IN,D3IN,LTUBEIN
        GO TO 42
41      CONTINUE
        WRITE(*,600)RUN,D1MM,D2MM,D2MM,D3MM,LTUBEMM
42      CONTINUE
        GO TO 100
50      CONTINUE
        IF(UNITS.EQ.1)GO TO 51
        WRITE(*,610)RUN,D1IN,D2IN,D2IN,D3IN,LTUBEIN
        GO TO 52
51      CONTINUE
        WRITE(*,610)RUN,D1MM,D2MM,D2MM,D3MM,LTUBEMM
52      CONTINUE
        GO TO 100
60      CONTINUE
        IF(IMAT.GT..3)GO TO 80
        IF(FLLP.GT.0)GO TO 70
        IF(UNITS.EQ.1)GO TO 61
        WRITE(*,620)RUN,D1IN,D2IN,D2IN,D3IN,LTUBEIN
        GO TO 62
61      CONTINUE
        WRITE(*,620)RUN,D1MM,D2MM,D2MM,D3MM,LTUBEMM
62      CONTINUE
        GO TO 100
70      CONTINUE
        IF(UNITS.EQ.1)GO TO 71
        WRITE(*,630)RUN,D1IN,D2IN,D2IN,D3IN,LTUBEIN
        GO TO 72
71      CONTINUE
        WRITE(*,630)RUN,D1MM,D2MM,D2MM,D3MM,LTUBEMM
72      CONTINUE
        GO TO 100
80      CONTINUE
        IF(FLLP.GT.0)GO TO 90
        IF(UNITS.EQ.1)GO TO 81
        WRITE(*,640)RUN,D1IN,D2IN,D2IN,D3IN,LTUBEIN
        GO TO 82
81      CONTINUE
        WRITE(*,640)RUN,D1MM,D2MM,D2MM,D3MM,LTUBEMM
82      CONTINUE
        GO TO 100
90      CONTINUE
        IF(UNITS.EQ.1)GO TO 91
        WRITE(*,650)RUN,D1IN,D2IN,D2IN,D3IN,LTUBEIN
        GO TO 92
91      CONTINUE
        WRITE(*,650)RUN,D1MM,D2MM,D2MM,D3MM,LTUBEMM
92      CONTINUE
```

```
 100    CONTINUE
        WRITE(*,*)
        WRITE(*,660)
        WRITE(*,*)
        WRITE(*,670)
        IF(UNITS.EQ.1)GO TO 101
        WRITE(*,681)
        TMANINF=(TMANIN*(9./5.))+32.
        WFLB=WFSI*2.205
        GENG=G*0.2048
        VELENG=VEL*3.281
        WRITE(*,690)PMANIN,TMANINF,WF,WFLB,GENG,VELENG,RWATER
        GO TO 102
 101    CONTINUE
        WRITE(*,680)
        PMANINSI=PMANIN/14.5
        WFL=WF*3.785
        WRITE(*,690)PMANINSI,TMANIN,WFL,WFSI,G,VEL,RWATER
 102    CONTINUE
        WRITE(*,*)
        IF(UNITS.EQ.1)GO TO 106
        WRITE(*,701)XLOC(1)
        GO TO 107
 106    CONTINUE
        WRITE(*,700)XLOCMM(1)
 107    CONTINUE
        WRITE(*,*)
        WRITE(*,710)
        IF(UNITS.EQ.1)GO TO 108
        WRITE(*,721)
        GO TO 109
 108    CONTINUE
        WRITE(*,720)
 109    CONTINUE
C
C         CALCULATE HEAT FLUX AND ENERGY BALANCE
C
        DO 120 J=0,NP
        CHK = 0
        AS = PI * D2 * LTUBE
        ACS = (PI/4.0) * ((D2**2) - (D1**2))
        IF(VREC1(J).GT.10.)GO TO 325
        VRMS1(J) = VREC1(J)
 325    CONTINUE
        IF(VREC2(J).GT.10.)GO TO 326
        VRMS2(J) = VREC2(J)
        GO TO 327
 326    CONTINUE
        VRMS1(J) = (IRMS1(J)/IREC1(J)) * VREC1(J)
        VRMS2(J) = (IRMS2(J)/IREC2(J)) * VREC2(J)
 327    CONTINUE
        IF(NR.EQ.2) GO TO 103
        IREC(J) = DMAX1(IREC1(J),IREC2(J))
        IRMS(J) = DMAX1(IRMS1(J),IRMS2(J))
        VREC(J) = DMAX1(VREC1(J),VREC2(J))
        VRMS(J) = DMAX1(VRMS1(J),VRMS2(J))
        ETOT(J) = IRMS(J) * VRMS(J) / 1000.
        IF(DVTS(J).GT.10.) GO TO 328
        DVTSRMS(J) = DVTS(J)
        GO TO 104
 328    CONTINUE
        DVTSRMS(J) = (IRMS(J)/IREC(J)) * DVTS(J)
        GO TO 104
 103    CONTINUE
```

```
      IRMS(J) = IRMS1(J) + IRMS2(J)
      ETOT(J) = IRMS(J) * ((VRMS1(J) + VRMS2(J)) / 2.) / 1000.
      IF(DVTS(J).GT.10.) GO TO 330
      DVTSRMS(J) = DVTS(J)
      GO TO 104
 330  CONTINUE
      DVTSRMS(J) = (((IRMS1(J)/IREC1(J)) + (IRMS2(J)/IREC2(J))) / 2.) *
     $             DVTS(J)
 104  CONTINUE
      QTOT(J) = ETOT(J) / AS
      ETS(J) = IRMS(J) * DVTSRMS(J) / 1000.
      QTS(J) = ETS(J) / AS
      DTMAN(J) = (DTMAN1(J) + DTMAN2(J)) / 2.0
      ESYS(J) = WFSI * CPW * DTMAN(J) / 1000.
      QSYS(J) = ESYS(J) / AS
      QSYSE(J) = QSYS(J)*0.08827
      LLLL = 0
C
C       TEMPERATURE CALCULATION
C
      DO 115 I=1,NX
      DISPORT = 4.75
      PLOCAL(I,J) = (-1.0 * DPTS(J) / DISPORT) * XLOC(I) + PTS2(J)
      PL = PLOCAL(I,J)
      CALL SAT(PL,TEMPS)
      TSAT(I,J) = TEMPS
      TBULK(I,J) = (DTMAN(J)/DISPORT) * XLOC(I) + TMANIN
      R1 = D1 / 2.
      R2 = D2 / 2.
      DRAD = (R2 - R1) / SEC
      TINIT=TTS(I,J)
      TEXP=TTS(I,J)
      TCBD=TCBAD(I,J)
      IF(J.GT.0)GO TO 299
      TINIP=TTS(I,J)
 299  CONTINUE
      IF(TINIT.GT.0.)GO TO 320
      TCN=5.
      IF(TTS(1,J).GT.0.)GO TO 300
      TCN=TCN-1.
 300  CONTINUE
      IF(TTS(2,J).GT.0.)GO TO 301
      TCN=TCN-1.
 301  CONTINUE
      IF(TTS(3,J).GT.0.)GO TO 302
      TCN=TCN-1.
 302  CONTINUE
      IF(TTS(4,J).GT.0.)GO TO 303
      TCN=TCN-1.
 303  CONTINUE
      IF(TTS(5,J).GT.0.)GO TO 304
      TCN=TCN-1.
 304  CONTINUE
      IF(TCN.GT.0.)GO TO 310
      TINIT=TINIP
      TCBD=1
      LLLL=1
      GO TO 320
 310  CONTINUE
      TINIT=(TTS(1,J)+TTS(2,J)+TTS(3,J)+TTS(4,J)+TTS(5,J))/TCN
      TWIN(I,J)=TINIT
      TEXP=TINIT
      TCBD=0
 320  CONTINUE
```

```
      TINIP=TINIT
      IF(IICORR.EQ.0)GO TO 110
      IF(CHK.EQ.0)GO TO 110
      VINIT=VOLTC(I-1,J)
      GO TO 111
 110  CONTINUE
      VINIT=DVTSRMS(J)
 111  CONTINUE
      TBLK=TBULK(I,J)
      CURRMS=IRMS(J)
      CALL WALL2D(NOR,IMAT,CURRMS,TINIT,DRAD,R1,R2,LTUBE,TBLK,H,VINIT,
     $            BETA,EPS,ERV,ERRT,ERQ,LLLL,QSYSE,TEXP,TCBD,IICORR,
     $            IHCORR,T,QDOT,QGEN,RADI,RESID,N,QDTOT,QGTOT,CURTOT,
     $            RESTOT,VOLTC,HC,KMT,TDBAD,VCBAD,HCBAD)
      OPEN(98,FILE='DRPROG')
      WRITE(98,6)J,I
      CLOSE(98)
      CHK = 1
      DO 105 K=1,NOR
      TW(I,J,K) = T(I,J,K)
 105  CONTINUE
C       CONVERT KMAT FROM BTU/HR-FT-F TO KW/M-C
      KMT(I,J,1) = (KMT(I,J,1)*0.2931*1.8)/(1000.*0.3048)
      KMT(I,J,NOR) = (KMT(I,J,NOR)*0.2931*1.8)/(1000.*0.3048)
      KMTAVG(I,J) = (KMT(I,J,1) + KMT(I,J,NOR)) / 2.
C       CALCULATE 1D HT TRANS WALL TEMP
      QGT(I,J) = QGTOT(I,J)
C      TVOL = PI * LTUBE * (R2**2. - R1**2.)
C      QGT(I,J) = ESYS(J)/TVOL
      TW1DI(I,J) = TTS(I,J)
      IF(TTS(I,J).GT.0.0)GO TO 135
      IF(TCN.EQ.0)GO TO 129
      TW1DI(I,J) = TWIN(I,J)
      GO TO 135
 129  CONTINUE
      TW1DI(I,J) = TW(I,J,NOR)
 135  CONTINUE
      TW1D(I,J) = TW1DI(I,J) + ((QGT(I,J) / (4. * KMTAVG(I,J))) *
     $            ((R1**2.) - (R2**2.))) - ((QGT(I,J) / (2. *
     $            KMTAVG(I,J))) * (R1**2.) * DLOG(R1/R2))
      QCALC(I,J) = QDTOT(I,J)
      ECALC(I,J) = QCALC(I,J) * AS
      TWALL(I,J) = T(I,J,1)
      DTSUB(I,J) = TSAT(I,J) - TBULK(I,J)
      DTSAT(I,J) = TWALL(I,J) - TSAT(I,J)
 115  CONTINUE
C
C       MISCELLANEOUS CALCULATIONS
C
      IF(NR.EQ.1) GOTO 118
      VREC(J) = (VREC1(J) + VREC2(J)) / 2.
      VRMS(J) = (VRMS1(J) + VRMS2(J)) / 2.
      IREC(J) = IREC1(J) + IREC2(J)
      IRMS(J) = IRMS1(J) + IRMS2(J)
 118  CONTINUE
 120  CONTINUE
C
C     PRINT RESULTS
C
      DO 130 J=0,NP
      IF(UNITS.EQ.1)GO TO 121
      QTSE(J)=QTS(J)*0.08827
      QSYSE(J)=QSYS(J)*0.08827
      QTOTE(J)=QTOT(J)*0.08827
```

```
      DO 119 I=1,NX
      QCALCE(I,J)=QCALC(I,J)*0.08827
      TWALLF(I,J)=(TWALL(I,J)*(9./5.))+32.
      TW1DF(I,J)=(TW1D(I,J)*(9./5.))+32.
      IF(TW1D(I,J).GT.0.0)GO TO 128
      TW1DF(I,J) = 0.0
 128  CONTINUE
      TBULKF(I,J)=(TBULK(I,J)*(9./5.))+32.
      TSATF(I,J)=(TSAT(I,J)*(9./5.))+32.
      DTSATF(I,J)=DTSAT(I,J)*1.8
      DTSUBF(I,J)=DTSUB(I,J)*1.8
 119  CONTINUE
      WRITE(*,730)J,QTSE(J),QSYSE(J),QTOTE(J),QCALCE(1,J),TWALLF(1,J),
     $              TW1DF(1,J),TBULKF(1,J),TSATF(1,J),DTSATF(1,J),
     $              DTSUBF(1,J)
      GO TO 122
 121  CONTINUE
      WRITE(*,730)J,QTS(J),QSYS(J),QTOT(J),QCALC(1,J),TWALL(1,J),
     $              TW1D(1,J),TBULK(1,J),TSAT(1,J),DTSAT(1,J),DTSUB(1,J)
 122  CONTINUE
 130  CONTINUE
      IF(BOL.NE.1)GO TO 123
      WRITE(*,*)
      WRITE(*,735)
 123  CONTINUE
      WRITE(*,490)
      WRITE(*,*)
      WRITE(*,500)IMONTH,IDAY,IYEAR
      WRITE(*,510)IHOUR,IMINUTE,ISECOND
      WRITE(*,520)IMT,IDY,IYR
      WRITE(*,530)IHR,IMN,ISC
      WRITE(*,*)
      WRITE(*,*)
      WRITE(*,540)
      WRITE(*,*)
      WRITE(*,740)
      WRITE(*,*)
      IF(UNITS.EQ.1)GO TO 131
      WRITE(*,701)XLOC(2)
      GO TO 132
 131  CONTINUE
      WRITE(*,700)XLOCMM(2)
 132  CONTINUE
      WRITE(*,*)
      WRITE(*,710)
      IF(UNITS.EQ.1)GO TO 145
      WRITE(*,721)
      GO TO 146
 145  CONTINUE
      WRITE(*,720)
 146  CONTINUE
      DO 140 J=0,NP
      IF(UNITS.EQ.1)GO TO 133
      WRITE(*,730)J,QTSE(J),QSYSE(J),QTOTE(J),QCALCE(2,J),TWALLF(2,J),
     $              TW1DF(2,J),TBULKF(2,J),TSATF(2,J),DTSATF(2,J),
     $              DTSUBF(2,J)
      GO TO 134
 133  CONTINUE
      WRITE(*,730)J,QTS(J),QSYS(J),QTOT(J),QCALC(2,J),TWALL(2,J),
     $              TW1D(2,J),TBULK(2,J),TSAT(2,J),DTSAT(2,J),DTSUB(2,J)
 134  CONTINUE
 140  CONTINUE
      WRITE(*,490)
      WRITE(*,*)
```

```
      WRITE(*,500)IMONTH,IDAY,IYEAR
      WRITE(*,510)IHOUR,IMINUTE,ISECOND
      WRITE(*,520)IMT,IDY,IYR
      WRITE(*,530)IHR,IMN,ISC
      WRITE(*,*)
      WRITE(*,*)
      WRITE(*,540)
      WRITE(*,*)
      WRITE(*,760)
      WRITE(*,*)
      IF(UNITS.EQ.1)GO TO 141
      WRITE(*,701)XLOC(3)
      GO TO 142
141   CONTINUE
      WRITE(*,700)XLOCMM(3)
142   CONTINUE
      WRITE(*,*)
      WRITE(*,710)
      IF(UNITS.EQ.1)GO TO 147
      WRITE(*,721)
      GO TO 148
147   CONTINUE
      WRITE(*,720)
148   CONTINUE
      DO 150 J=0,NP
      IF(UNITS.EQ.1)GO TO 143
      WRITE(*,730)J,QTSE(J),QSYSE(J),QTOTE(J),QCALCE(3,J),TWALLF(3,J),
     $            TW1DF(3,J),TBULKF(3,J),TSATF(3,J),DTSATF(3,J),
     $            DTSUBF(3,J)
      GO TO 144
143   CONTINUE
      WRITE(*,730)J,QTS(J),QSYS(J),QTOT(J),QCALC(3,J),TWALL(3,J),
     $            TW1D(3,J),TBULK(3,J),TSAT(3,J),DTSAT(3,J),DTSUB(3,J)
144   CONTINUE
150   CONTINUE
      WRITE(*,490)
      WRITE(*,*)
      WRITE(*,500)IMONTH,IDAY,IYEAR
      WRITE(*,510)IHOUR,IMINUTE,ISECOND
      WRITE(*,520)IMT,IDY,IYR
      WRITE(*,530)IHR,IMN,ISC
      WRITE(*,*)
      WRITE(*,*)
      WRITE(*,540)
      WRITE(*,*)
      WRITE(*,780)
      WRITE(*,*)
      IF(UNITS.EQ.1)GO TO 151
      WRITE(*,701)XLOC(4)
      GO TO 152
151   CONTINUE
      WRITE(*,700)XLOCMM(4)
152   CONTINUE
      WRITE(*,*)
      WRITE(*,710)
      IF(UNITS.EQ.1)GO TO 149
      WRITE(*,721)
      GO TO 166
149   CONTINUE
      WRITE(*,720)
166   CONTINUE
      DO 154 J=0,NP
      IF(UNITS.EQ.1)GO TO 153
      WRITE(*,730)J,QTSE(J),QSYSE(J),QTOTE(J),QCALCE(4,J),TWALLF(4,J),
```

```
     $                TW1DF(4,J),TBULKF(4,J),TSATF(4,J),DTSATF(4,J),
     $                DTSUBF(4,J)
      GO TO 155
153   CONTINUE
      WRITE(*,730)J,QTS(J),QSYS(J),QTOT(J),QCALC(4,J),TWALL(4,J),
     $                TW1D(4,J),TBULK(4,J),TSAT(4,J),DTSAT(4,J),DTSUB(4,J)
155   CONTINUE
154   CONTINUE
      WRITE(*,490)
      WRITE(*,*)
      WRITE(*,500)IMONTH,IDAY,IYEAR
      WRITE(*,510)IHOUR,IMINUTE,ISECOND
      WRITE(*,520)IMT,IDY,IYR
      WRITE(*,530)IHR,IMN,ISC
      WRITE(*,*)
      WRITE(*,*)
      WRITE(*,540)
      WRITE(*,*)
      WRITE(*,820)
      WRITE(*,*)
      IF(UNITS.EQ.1)GO TO 157
      WRITE(*,701)XLOC(5)
      GO TO 158
157   CONTINUE
      WRITE(*,700)XLOCMM(5)
158   CONTINUE
      WRITE(*,*)
      WRITE(*,710)
      IF(UNITS.EQ.1)GO TO 167
      WRITE(*,721)
      GO TO 168
167   CONTINUE
      WRITE(*,720)
168   CONTINUE
      DO 156 J=0,NP
      IF(UNITS.EQ.1)GO TO 159
      WRITE(*,730)J,QTSE(J),QSYSE(J),QTOTE(J),QCALCE(5,J),TWALLF(5,J),
     $                TW1DF(5,J),TBULKF(5,J),TSATF(5,J),DTSATF(5,J),
     $                DTSUBF(5,J)
      GO TO 161
159   CONTINUE
      WRITE(*,730)J,QTS(J),QSYS(J),QTOT(J),QCALC(5,J),TWALL(5,J),
     $                TW1D(5,J),TBULK(5,J),TSAT(5,J),DTSAT(5,J),DTSUB(5,J)
161   CONTINUE
156   CONTINUE
      IF(BOL.EQ.1)GO TO 172
      WRITE(*,*)
      IF(BOL.EQ.2)GO TO 171
      WRITE(*,736)
      GO TO 172
171   CONTINUE
      WRITE(*,737)
172   CONTINUE
      WRITE(*,490)
      WRITE(*,*)
      WRITE(*,500)IMONTH,IDAY,IYEAR
      WRITE(*,510)IHOUR,IMINUTE,ISECOND
      WRITE(*,520)IMT,IDY,IYR
      WRITE(*,530)IHR,IMN,ISC
      WRITE(*,*)
      WRITE(*,*)
      WRITE(*,540)
      WRITE(*,*)
      WRITE(*,860)
```

```
      WRITE(*,*)
      WRITE(*,790)
      WRITE(*,800)
      DO 160 J=0,NP
      WRITE(*,810)J,ETS(J),ESYS(J),ETOT(J),ECALC(5,J),IREC(J),IRMS(J),
     $            VREC(J),VRMS(J),DVTS(J),DVTSRMS(J)
160   CONTINUE
      WRITE(*,490)
      WRITE(*,*)
      WRITE(*,500)IMONTH,IDAY,IYEAR
      WRITE(*,510)IHOUR,IMINUTE,ISECOND
      WRITE(*,520)IMT,IDY,IYR
      WRITE(*,530)IHR,IMN,ISC
      WRITE(*,*)
      WRITE(*,*)
      WRITE(*,540)
      WRITE(*,*)
      WRITE(*,940)
      WRITE(*,*)
      WRITE(*,830)
      IF(UNITS.EQ.1)GO TO 162
      WRITE(*,841)
      GO TO 163
162   CONTINUE
      WRITE(*,840)
163   CONTINUE
      DO 170 J=0,NP
      PTS1(J) = PTS1(J) + 14.7
      PTS2(J) = PTS2(J) + 14.7
      PTS3(J) = PTS3(J) + 14.7
      PTS4(J) = PTS4(J) + 14.7
      PMANOUT(J) = PMANOUT(J) + 14.7
      IF(UNITS.EQ.1)GO TO 164
      TMANOUTF(J)=(TMANOUT(J)*(9./5.))+32.
      DTMANF(J)=DTMAN(J)*1.8
      WRITE(*,850)J,PTS1(J),PTS2(J),PTS3(J),PTS4(J),DPTS(J),
     $            PMANOUT(J),TMANOUTF(J),DTMANF(J)
      GO TO 165
164   CONTINUE
      PTS1SI(J) = PTS1(J) / 14.5
      PTS2SI(J) = PTS2(J) / 14.5
      PTS3SI(J) = PTS3(J) / 14.5
      PTS4SI(J) = PTS4(J) / 14.5
      PMANOUTS(J) = PMANOUT(J) / 14.5
      DPTSSI(J) = DPTS(J) / 14.5
      WRITE(*,850)J,PTS1SI(J),PTS2SI(J),PTS3SI(J),PTS4SI(J),DPTSSI(J),
     $            PMANOUTS(J),TMANOUT(J),DTMAN(J)
165   CONTINUE
170   CONTINUE
180   CONTINUE
      IF(IDIST.EQ.0)GO TO 210
      WRITE(*,490)
      DO 200 J=0,NP
      WRITE(*,*)
      WRITE(*,*)
      WRITE(*,*)
      DRADMM = DRAD * 1000.
      WRITE(*,900)J
      WRITE(*,*)
      DO 181 I=1,NX
      HC(I,J)=HC(I,J)/3600.
181   CONTINUE
      IF(UNITS.EQ.1) GO TO 187
      DO 186 I=1,NX
```

```
      QDTOTE(I,J)=QDTOT(I,J)*0.08827
      QGTOTE(I,J)=QGTOT(I,J)*0.08827
 186  CONTINUE
      WRITE(*,891)QDTOTE(1,J),QGTOTE(1,J),CURTOT(1,J),VOLTC(1,J),
     $       HC(1,J)
      WRITE(*,892)QDTOTE(2,J),QGTOTE(2,J),CURTOT(2,J),VOLTC(2,J),
     $       HC(2,J)
      WRITE(*,893)QDTOTE(3,J),QGTOTE(3,J),CURTOT(3,J),VOLTC(3,J),
     $       HC(3,J)
      WRITE(*,894)QDTOTE(4,J),QGTOTE(4,J),CURTOT(4,J),VOLTC(4,J),
     $       HC(4,J)
      WRITE(*,895)QDTOTE(5,J),QGTOTE(5,J),CURTOT(5,J),VOLTC(5,J),
     $       HC(5,J)
      GO TO 189
 187  CONTINUE
      DO 188 I=1,NX
      HCSI(I,J)=HC(I,J)*(1.8/0.08827)
 188  CONTINUE
      WRITE(*,901)QDTOT(1,J),QGTOT(1,J),CURTOT(1,J),VOLTC(1,J),
     $       HCSI(1,J)
      WRITE(*,902)QDTOT(2,J),QGTOT(2,J),CURTOT(2,J),VOLTC(2,J),
     $       HCSI(2,J)
      WRITE(*,903)QDTOT(3,J),QGTOT(3,J),CURTOT(3,J),VOLTC(3,J),
     $       HCSI(3,J)
      WRITE(*,904)QDTOT(4,J),QGTOT(4,J),CURTOT(4,J),VOLTC(4,J),
     $       HCSI(4,J)
      WRITE(*,905)QDTOT(5,J),QGTOT(5,J),CURTOT(5,J),VOLTC(5,J),
     $       HCSI(5,J)
 189  CONTINUE
      WRITE(*,*)
      HG(J)=HG(J)/3600.
      IF(UNITS.EQ.1)GO TO 193
      DO 207 I=1,NX
      TTSF(I,J)=(TTS(I,J)*(9./5.))+32.
      IF(TTSF(I,J).GT.40.)GO TO 206
      TTSF(I,J)=0.0
 206  CONTINUE
 207  CONTINUE
      WRITE(*,896)IRMS(J),DVTSRMS(J),HG(J)
      WRITE(*,*)
      WRITE(*,907)TTSF(1,J),TTSF(2,J),TTSF(3,J),TTSF(4,J),TTSF(5,J)
      GO TO 194
 193  CONTINUE
      HGSI(J)=HG(J)*(1.8/0.08827)
      WRITE(*,906)IRMS(J),DVTSRMS(J),HGSI(J)
      WRITE(*,*)
      DO 215 I=1,NX
      IF(TTS(I,J).GT.1.)GO TO 214
      TTS(I,J)=0.0
 214  CONTINUE
 215  CONTINUE
      WRITE(*,908)TTS(1,J),TTS(2,J),TTS(3,J),TTS(4,J),TTS(5,J)
 194  CONTINUE
      WRITE(*,*)
      WRITE(*,909)
      WRITE(*,*)
      WRITE(*,910)
      IF(UNITS.EQ.1)GO TO 198
      WRITE(*,922)
      DO 195 K=1,NOR,NPR
      DO 201 I=1,NX
      TWF(I,J,K)=(TW(I,J,K)*(9./5.))+32.
      QDOTE(I,J,K)=QDOT(I,J,K)*0.08827
      QGENE(I,J,K)=QGEN(I,J,K)*(0.08827/3.281)
```

```
      RESIDF(I,J,K)=RESID(I,J,K)*1.8
201   CONTINUE
      RADIN(K) = RADI(1,J,K) * 39.37
      WRITE(*,930)RADIN(K),TWF(1,J,K),QDOTE(1,J,K),QGENE(1,J,K),
     $            RESIDF(1,J,K),TWF(2,J,K),QDOTE(2,J,K),QGENE(2,J,K),
     $            RESIDF(2,J,K)
195   CONTINUE
      WRITE(*,*)
      WRITE(*,911)
      WRITE(*,922)
      DO 196 K=1,NOR,NPR
      WRITE(*,930)RADIN(K),TWF(3,J,K),QDOTE(3,J,K),QGENE(3,J,K),
     $            RESIDF(3,J,K),TWF(4,J,K),QDOTE(4,J,K),QGENE(4,J,K),
     $            RESIDF(4,J,K)
196   CONTINUE
      WRITE(*,*)
      WRITE(*,912)
      WRITE(*,923)
      DO 197 K=1,NOR,NPR
      WRITE(*,930)RADIN(K),TWF(5,J,K),QDOTE(5,J,K),QGENE(5,J,K),
     $            RESIDF(5,J,K)
197   CONTINUE
      GO TO 199
198   CONTINUE
      WRITE(*,920)
      DO 190 K=1,NOR,NPR
      RADMM(K) = RADI(1,J,K) * 1000.
      WRITE(*,930)RADMM(K),TW(1,J,K),QDOT(1,J,K),QGEN(1,J,K),
     $            RESID(1,J,K),TW(2,J,K),QDOT(2,J,K),QGEN(2,J,K),
     $            RESID(2,J,K)
190   CONTINUE
      WRITE(*,*)
      WRITE(*,911)
      WRITE(*,920)
      DO 191 K=1,NOR,NPR
      WRITE(*,930)RADMM(K),TW(3,J,K),QDOT(3,J,K),QGEN(3,J,K),
     $            RESID(3,J,K),TW(4,J,K),QDOT(4,J,K),QGEN(4,J,K),
     $            RESID(4,J,K)
191   CONTINUE
      WRITE(*,*)
      WRITE(*,912)
      WRITE(*,921)
      DO 192 K=1,NOR,NPR
      WRITE(*,930)RADMM(K),TW(5,J,K),QDOT(5,J,K),QGEN(5,J,K),
     $            RESID(5,J,K)
192   CONTINUE
199   CONTINUE
      WRITE(*,490)
200   CONTINUE
210   CONTINUE
      WRITE(*,*)
      WRITE(*,*)
      WRITE(*,970)
      WRITE(*,*)
      WRITE(*,971)
      DO 205 J=0,NP
      WRITE(*,972)J,TDBAD(1,J),TDBAD(2,J),TDBAD(3,J),TDBAD(4,J),
     $            TDBAD(5,J),J,VCBAD(1,J),VCBAD(2,J),VCBAD(3,J),
     $            VCBAD(4,J),VCBAD(5,J)
205   CONTINUE
      WRITE(*,*)
      WRITE(*,*)
      WRITE(*,974)
      WRITE(*,976)
```

```
      WRITE(*,*)
      WRITE(*,973)
      DO 225 J=0,NP
      WRITE(*,975)J,HCBAD(1,J),HCBAD(2,J),HCBAD(3,J),HCBAD(4,J),
     $           HCBAD(5,J)
 225  CONTINUE
C
C        FORMAT STATEMENTS
C
 5    FORMAT(2X,'Run No. ',I3)
 6    FORMAT(2X,'Completed Power Setting No.',I2,', Station No.',I2)
 490  FORMAT('1')
 500  FORMAT(5X,'Micro Craft Technology/AEDC',66X,'Date Computed',5X,
     $       I2,'-',I2,'-',I4)
 510  FORMAT(5X,'Arnold AFB, TN  37389',72X,'Time Computed',7X,I2,':',
     $       I2,':',I2)
 520  FORMAT(5X,'High Temperature Wall Laboratory (HTWL)',54X,
     $       'Date Recorded',5X,I2,'-',I2,'-',I4)
 530  FORMAT(5X,'Project No.  DD01VW, Job 0115',64X,'Time Recorded',
     $       7X,I2,':',I2,':',I2)
 540  FORMAT(50X,'*** HTWL REDUCED DATA ***')
 550  FORMAT(5X,'PAGE 1')
 560  FORMAT(8X,'RUN',10X,'WALL',11X,'HEATER TUBE',15X,'ANNULUS',13X,
     $       'TUBE LENGTH',10X,'FLOW')
 570  FORMAT(8X,'NO.',10X,'MATL',10X,'ID(MM)  OD(MM)',10X,
     $       'ID(MM)  OD(MM)',12X,'(MM)',14X,'LOOP')
 571  FORMAT(8X,'NO.',10X,'MATL',10X,'ID(IN)  OD(IN)',10X,
     $       'ID(IN)  OD(IN)',12X,'(IN)',14X,'LOOP')
 580  FORMAT(8X,I3,11X,'SS',11X,F6.3,2X,F6.3,10X,F6.3,2X,F6.3,11X,
     $       F6.2,13X,'CLSD')
 590  FORMAT(8X,I3,11X,'SS',11X,F6.3,2X,F6.3,10X,F6.3,2X,F6.3,11X,
     $       F6.2,13X,'OPEN')
 600  FORMAT(8X,I3,11X,'CU',11X,F6.3,2X,F6.3,10X,F6.3,2X,F6.3,11X,
     $       F6.2,13X,'CLSD')
 610  FORMAT(8X,I3,11X,'CU',11X,F6.3,2X,F6.3,10X,F6.3,2X,F6.3,11X,
     $       F6.2,13X,'OPEN')
 620  FORMAT(8X,I3,11X,'AMZ',10X,F6.3,2X,F6.3,10X,F6.3,2X,F6.3,11X,
     $       F6.2,13X,'CLSD')
 630  FORMAT(8X,I3,11X,'AMZ',10X,F6.3,2X,F6.3,10X,F6.3,2X,F6.3,11X,
     $       F6.2,13X,'OPEN')
 640  FORMAT(8X,I3,11X,'INC',10X,F6.3,2X,F6.3,10X,F6.3,2X,F6.3,11X,
     $       F6.2,13X,'CLSD')
 650  FORMAT(8X,I3,11X,'INC',10X,F6.3,2X,F6.3,10X,F6.3,2X,F6.3,11X,
     $       F6.2,13X,'OPEN')
 660  FORMAT(15X,'*** CONDITIONS ***')
 670  FORMAT(8X,'PMAN-IN',10X,'TMAN-IN',13X,'WATER FLOW',15X,'G',16X,
     $       'VEL',11X,'R(WATER)')
 680  FORMAT(9X,'(BAR)',10X,'(DEG-C)',11X,'(LPM)    (KG/S)',9X,
     $       '(KG/M^2 S)',10X,'(M/S)',10X,'(uS/CM)')
 681  FORMAT(9X,'(PSIA)',10X,'(DEG-F)',11X,'(GPM)    (LB/S)',9X,
     $       '(LB/FT^2 S)',9X,'(FT/S)',10X,'(uS/CM)')
 690  FORMAT(8X,F7.1,10X,F7.2,10X,F6.1,3X,F6.2,10X,F8.1,10X,F6.1,
     $       10X,F6.2)
 700  FORMAT(20X,'AXIAL LOCATION FROM L.E. OF TUBE',39X,F6.2,' MM')
 701  FORMAT(20X,'AXIAL LOCATION FROM L.E. OF TUBE',39X,F6.2,' IN')
 710  FORMAT(9X,'POWER',5X,'QDOT-TS',4X,'QDOT-SYS',5X,'QDOT-TOT',6X,
     $       'QDOT-CALC',7X,'TWALL',5X,'TW1D',5X,'TBULK',5X,'TSAT',5X,
     $       'DTSAT',4X,'DTSUB')
 720  FORMAT(8X,'SETTING',3X,'(KW/M^2)',4X,'(KW/M^2)',5X,'(KW/M^2)',6X,
     $       '(KW/M^2)',7X,'(DEG-C)',3X,'(DEG-C)',2X,'(DEG-C)',2X,
     $       '(DEG-C)',2X,'(DEG-C)',3X,'(DEG-C)')
 721  FORMAT(8X,'SETTING',2X,'(BTU/FT^2S)',1X,'(BTU/FT^2S)',2X,
     $       '(BTU/FT^2S)',3X,'(BTU/FT^2S)',4X,'(DEG-F)',3X,'(DEG-F)',
     $       3X,'(DEG-F)',2X,'(DEG-F)',2X,'(DEG-F)',3X,'(DEG-F)')
```

```
730   FORMAT(9X,I2,7X,F8.1,4X,F8.1,5X,F8.1,6X,F8.1,6X,F7.2,3X,
  $          F7.2,3X,F6.2,3X,F6.2,3X,F7.2,3X,F7.2)
735   FORMAT(30X,'* * *  UPSTREAM BURNOUT OCCURRED IN TRANSIENT TO NEXT
  $ SET POINT  * * *')
736   FORMAT(30X,'* * *  NO BURNOUT OCCURRED  * * *')
737   FORMAT(30X,'* * *  DOWNSTREAM BURNOUT OCCURRED IN TRANSIENT TO NE
  $XT SET POINT  * * *')
740   FORMAT(5X,'PAGE 2')
760   FORMAT(5X,'PAGE 3')
780   FORMAT(5X,'PAGE 4')
790   FORMAT(9X,'POWER',4X,'E-TS',6X,'E-SYS',6X,'E-TOT',6X,'E-CALC',5X,
  $          'IREC-TOT',4X,'IRMS-TOT',4X,'VREC-TOT',3X,'VRMS-TOT',5X,
  $          'DVTS-DC',3X,'DVTS-RMS')
800   FORMAT(8X,'SETTING',3X,'(KW)',6X,'(KW)',7X,'(KW)',7X,'(KW)',8X,
  $          '(AMPS)',7X,'(AMPS)',5X,'(VOLTS)',4X,'(VOLTS)',4X,
  $          '(VOLTS)',4X,'(VOLTS)')
810   FORMAT(9X,I2,5X,F7.1,4X,F7.1,4X,F7.1,4X,F7.1,4X,F8.1,5X,F8.1,5X,
  $          F6.1,5X,F6.1,5X,F6.1,5X,F6.1)
820   FORMAT(5X,'PAGE 5')
830   FORMAT(9X,'POWER',5X,'PTS1',7X,'PTS2',8X,'PTS3',8X,'PTS4',7X,
  $          'DPTS',5X,'PMAN-OUT',6X,'TMAN-OUT',4X,'DTMAN')
840   FORMAT(8X,'SETTING',3X,'(BAR)',6X,'(BAR)',7X,'(BAR)',7X,
  $          '(BAR)',6X,'(BAR)',7X,'(BAR)',7X,'(DEG-C)',4X,'(DEG-C)')
841   FORMAT(8X,'SETTING',3X,'(PSIA)',5X,'(PSIA)',6X,'(PSIA)',6X,
  $          '(PSIA)',5X,'(PSI)',6X,'(PSIA)',7X,'(DEG-F)',4X,'(DEG-F)')
850   FORMAT(9X,I2,5X,F7.1,5X,F7.1,5X,F7.1,5X,F7.1,5X,F6.2,5X,F7.1,5X,
  $          F7.2,5X,F6.2)
860   FORMAT(5X,'PAGE 6')
891   FORMAT(8X,'ST 1',3X,'QDOT TOT = ',F7.1,' BTU/FT^2 S',3X,
  $          'QGEN TOT = ',F12.1,' BTU/FT^3 S',3X,'CURR TOT = ',
  $          F7.1,' AMPS',3X,'VOLT CORR = ',F6.2,' VOLTS',3X,
  $          'H CORR = ',F5.2,' BTU/FT^2 S F')
892   FORMAT(8X,'ST 2',3X,'QDOT TOT = ',F7.1,' BTU/FT^2 S',3X,
  $          'QGEN TOT = ',F12.1,' BTU/FT^3 S',3X,'CURR TOT = ',
  $          F7.1,' AMPS',3X,'VOLT CORR = ',F6.2,' VOLTS',3X,
  $          'H CORR = ',F5.2,' BTU/FT^2 S F')
893   FORMAT(8X,'ST 3',3X,'QDOT TOT = ',F7.1,' BTU/FT^2 S',3X,
  $          'QGEN TOT = ',F12.1,' BTU/FT^3 S',3X,'CURR TOT = ',
  $          F7.1,' AMPS',3X,'VOLT CORR = ',F6.2,' VOLTS',3X,
  $          'H CORR = ',F5.2,' BTU/FT^2 S F')
894   FORMAT(8X,'ST 4',3X,'QDOT TOT = ',F7.1,' BTU/FT^2 S',3X,
  $          'QGEN TOT = ',F12.1,' BTU/FT^3 S',3X,'CURR TOT = ',
  $          F7.1,' AMPS',3X,'VOLT CORR = ',F6.2,' VOLTS',3X,
  $          'H CORR = ',F5.2,' BTU/FT^2 S F')
895   FORMAT(8X,'ST 5',3X,'QDOT TOT = ',F7.1,' BTU/FT^2 S',3X,
  $          'QGEN TOT = ',F12.1,' BTU/FT^3 S',3X,'CURR TOT = ',
  $          F7.1,' AMPS',3X,'VOLT CORR = ',F6.2,' VOLTS',3X,
  $          'H CORR = ',F5.2,' BTU/FT^2 S F')
896   FORMAT(8X,'MEASURED VALUES:  RMS CURRENT = ',F8.1,' AMPS',5X,
  $          'TEST SECTION VOLTAGE = ',F6.2,' VOLTS',10X,
  $          'H ESTIMATE = ',F5.2,' BTU/FT^2 S F')
900   FORMAT(8X,'POWER SETTING NO.',2X,I2)
901   FORMAT(8X,'ST 1',3X,'QDOT TOT = ',F7.1,' KW/M^2',3X,
  $          'QGEN TOT = ',F12.1,' KW/M^3',3X,'CURR TOT = ',
  $          F7.1,' AMPS',3X,'VOLT CORR = ',F6.2,' VOLTS',3X,
  $          'H CORR = ',F6.1,' KW/M^2 C')
902   FORMAT(8X,'ST 2',3X,'QDOT TOT = ',F7.1,' KW/M^2',3X,
  $          'QGEN TOT = ',F12.1,' KW/M^3',3X,'CURR TOT = ',
  $          F7.1,' AMPS',3X,'VOLT CORR = ',F6.2,' VOLTS',3X,
  $          'H CORR = ',F6.1,' KW/M^2 C')
903   FORMAT(8X,'ST 3',3X,'QDOT TOT = ',F7.1,' KW/M^2',3X,
  $          'QGEN TOT = ',F12.1,' KW/M^3',3X,'CURR TOT = ',
  $          F7.1,' AMPS',3X,'VOLT CORR = ',F6.2,' VOLTS',3X,
  $          'H CORR = ',F6.1,' KW/M^2 C')
```

```
 904   FORMAT(8X,'ST 4',3X,'QDOT TOT = ',F7.1,' KW/M^2',3X,
     $        'QGEN TOT = ',F12.1,' KW/M^3',3X,'CURR TOT = ',
     $        F7.1,' AMPS',3X,'VOLT CORR = ',F6.2,' VOLTS',3X,
     $        'H CORR = ',F6.1,' KW/M^2 C')
 905   FORMAT(8X,'ST 5',3X,'QDOT TOT = ',F7.1,' KW/M^2',3X,
     $        'QGEN TOT = ',F12.1,' KW/M^3',3X,'CURR TOT = ',
     $        F7.1,' AMPS',3X,'VOLT CORR = ',F6.2,' VOLTS',3X,
     $        'H CORR = ',F6.1,' KW/M^2 C')
 906   FORMAT(8X,'MEASURED VALUES:  RMS CURRENT = ',F8.1,' AMPS',5X,
     $        'TEST SECTION VOLTAGE = ',F6.2,' VOLTS',10X,
     $        'H ESTIMATE = ',F6.1,' KW/M^2 C')
 907   FORMAT(26X,'TC1 = ',F6.1,' DEG-F',4X,'TC2 = ',F6.1,' DEG-F',4X,
     $             'TC3 = ',F6.1,' DEG-F',4X,'TC4 = ',F6.1,' DEG-F',4X,
     $             'TC5 = ',F6.1,' DEG-F')
 908   FORMAT(26X,'TC1 = ',F6.1,' DEG-C',4X,'TC2 = ',F6.1,' DEG-C',4X,
     $             'TC3 = ',F6.1,' DEG-C',4X,'TC4 = ',F6.1,' DEG-C',4X,
     $             'TC5 = ',F6.1,' DEG-C')
 909   FORMAT(8X,'CALCULATED VALUES:')
 910   FORMAT(8X,'RADIUS',5X,'T1',10X,'QDOT',8X,'QGEN',5X,'RESIDUAL',
     $        18X,'T2',10X,'QDOT',8X,'QGEN',5X,'RESIDUAL')
 911   FORMAT(8X,'RADIUS',5X,'T3',10X,'QDOT',8X,'QGEN',5X,'RESIDUAL',
     $        18X,'T4',10X,'QDOT',8X,'QGEN',5X,'RESIDUAL')
 912   FORMAT(8X,'RADIUS',5X,'T5',10X,'QDOT',8X,'QGEN',5X,'RESIDUAL')
 920   FORMAT(9X,'(MM)',3X,'(DEG-C)',6X,'(KW/M^2)',4X,'(KW/M^3)',
     $        4X,'(DEG-C)',15X,'(DEG-C)',6X,'(KW/M^2)',4X,'(KW/M^3)',
     $        4X,'(DEG-C)')
 921   FORMAT(9X,'(MM)',3X,'(DEG-C)',6X,'(KW/M^2)',4X,'(KW/M^3)',
     $        4X,'(DEG-C)')
 922   FORMAT(9X,'(IN)',3X,'(DEG-F)',4X,'(BTU/FT^2 S)',1X,'(BTU/FT^3 S)'
     $        ,1X,'(DEG-F)',15X,'(DEG-F)',4X,'(BTU/FT^2 S)',1X,
     $        '(BTU/FT^3 S)',1X,'(DEG-F)')
 923   FORMAT(9X,'(IN)',3X,'(DEG-F)',4X,'(BTU/FT^2 S)',1X,'(BTU/FT^3 S)'
     $        ,1X,'(DEG-F)')
 930   FORMAT(8X,F6.3,3X,F7.1,3X,F10.1,3X,F10.0,3X,F6.4,17X,F7.1,
     $        3X,F10.1,3X,F10.0,3X,F6.4)
 940   FORMAT(5X,'PAGE 7')
 970   FORMAT(4X,'TEMP DISTRIBUTION DID NOT CONVERGE IF "1" APPEARS',
     $        33X,'VOLTAGE CORRECTION DID NOT CONVERGE IF "1" APPEARS')
 971   FORMAT(4X,'NP \ STATION',10X,'1',10X,'2',10X,'3',10X,'4',10X,
     $        '5',15X,'NP \ STATION',10X,'1',10X,'2',10X,'3',10X,'4',
     $        10X,'5')
 972   FORMAT(4X,I2,20X,I1,10X,I1,10X,I1,10X,I1,10X,I1,15X,I2,20X,I1,
     $        10X,I1,10X,I1,10X,I1,10X,I1)
 973   FORMAT(4X,'NP \ STATION',10X,'1',10X,'2',10X,'3',10X,'4',10X,
     $        '5')
 974   FORMAT(4X,'H CORRECTION DID NOT CONVERGE IF "1" APPEARS; IF "2" A
     $PPEARS THE TC MEASUREMENT IS SUSPECT - Q INSTEAD OF H CORRECTION P
     $ERFORMED;')
 976   FORMAT(10X,'Q CORRECTION DID NOT CONVERGE IF "3" APPEARS')
 975   FORMAT(4X,I2,20X,I1,10X,I1,10X,I1,10X,I1,10X,I1)
 999   FORMAT(I2,1X,I2,1X,I4,1X,I2,1X,I2,1X,I2)
       STOP
       END
C
C
C        SUBROUTINES
C
      SUBROUTINE SAT(P,TSAT)
      IMPLICIT REAL*8(A-H,M-Z)
      IF(P.GT.400.) GO TO 10
      TSAT = 240. + P - 0.00125 * (P**2) - (660./(2.75 + P))
      GO TO 30
 10   CONTINUE
      IF(P.GT.1000.) GO TO 20
```

```
      TSAT = 390. + 0.16 * P
      GO TO 30
 20   CONTINUE
      TSAT = 470. + 0.082 * P
 30   CONTINUE
C       CONVERT TSAT IN DEG-F TO DEG-C
      TSAT = (5./9.) * (TSAT - 32.)
      RETURN
      END
C
C
      SUBROUTINE WATPROP(TMAN,RHO,CP)
      IMPLICIT REAL*8(A-H,M-Z)
      TW = TMAN
C       CONVERT TMAN IN DEG-C TO DEG-F
      TW = (TW * 9./5.) + 32.
      RHO = -5.3321D-05 * TW**2 - 1.10158D-03 * TW + 62.581
      IF(TW.GT.300.) GO TO 10
      CP = 1.0
      GO TO 20
 10   CONTINUE
      CP = 6.7143D-06 * TW**2 - 4.56429D-03 * TW + 1.81143
 20   CONTINUE
C       CONVERT RHO FROM LBM/CU FT TO KG/CU M
      RHO = RHO * 16.01845
C       CONVERT CP FROM BTU/LBM F TO J/KG C
      CP = CP * 4186.55
      RETURN
      END
C
C
C
      SUBROUTINE WALL2D(NOR,IMAT,CURRMS,TIN,DR,R1,R2,LTB,TB,H,VOLTI,
     $                  BETA,EPS,ERV,ERRT,ERQ,LLLL,QSYSE,TSURF,TCBD,
     $                  IICORR,IHCORR,T,QDOT,QGEN,RADI,RESID,N,QDTOT,
     $                  QGTOT,CURTOT,RESTOT,VOLTC,HC,KMT,TDBAD,VCBAD,
     $                  HCBAD)
      IMPLICIT REAL*8(A-H,M-Z)
      COMMON I,J,K
      DIMENSION T(10,0:20,0:300),TOLD(0:300),QDOT(10,0:20,300),
     $          RADI(10,0:20,300),QGEN(10,0:20,300),H(0:20),
     $          RESID(10,0:20,0:300),QDTOT(10,0:20),QSYSE(0:20),
     $          QGTOT(10,0:20),CURTOT(10,0:20),RESTOT(10,0:20),
     $          VOLTC(10,0:20),HC(10,0:20),KMT(10,0:20,0:300),
     $          TDBAD(10,0:20),VCBAD(10,0:20),HCBAD(10,0:20),
     $          TH(0:300),TL(0:300)
      REAL*8 LGTH,LTB,KMT
      INTEGER NOR,N,NMAX,TDBAD,VCBAD,HCBAD,N1,N2,N1MAX,N2MAX,TCBD
C       CONVERT TEMPS FROM DEGC TO DEGR
      TIN=TIN*(9./5.)+491.67
      DO 4 K=1,NOR
      TOLD(K)=TIN
      IF(LLLL.EQ.0)GO TO 2
      TOLD(K)=T(I,J-1,K)
  2   CONTINUE
  4   CONTINUE
      TB=TB*(9./5.)+491.67
      TMEAS=TSURF*(9./5.)+491.67
C       CONVERT LENGTHS FROM M TO FT
      DR=DR*3.281
      RI=R1*3.281
      RO=R2*3.281
      LGTH=LTB*3.281
      LL=0
```

```
      LM=0
      LN=0
      LO=0
      N1=0
      N1MAX=2000
      MMMM=0
      HINIT=H(J)
 3    CONTINUE
      LLL=0
      LMM=0
      LNN=0
      LOO=0
      N2=0
      N2MAX=1000
 5    CONTINUE
      N=0
      NMAX=10000
 20   CONTINUE
      N=N+1
      CALL GSI(TOLD,NOR,IMAT,DR,H,TB,VOLTI,RO,RI,LGTH,BETA,T,QDOT,
     $        QGEN,RADI,QDTOT,QGTOT,CURTOT,RESTOT,KMT)
      IF(N.GT.NMAX) GOTO 94
      DO 40 K=1,NOR
      RESID(I,J,K)=DABS(TOLD(K)-T(I,J,K))
 40   CONTINUE
      DO 50 K=2,NOR
      RESID(I,J,K)=DMAX1(RESID(I,J,K),RESID(I,J,K-1))
 50   CONTINUE
      IF(RESID(I,J,NOR).LE.EPS) GO TO 100
      DO 60 K=1,NOR
      TOLD(K)=T(I,J,K)
 60   CONTINUE
      GO TO 20
 94   CONTINUE
      TDBAD(I,J)=1
 100  CONTINUE
C
C        ADJUST VOLTAGE FOR CURRENT MATCH
C
      IF(IICORR.EQ.0)GO TO 90
      MMMM=1
      N2=N2+1
      IF(N2.GT.N2MAX) GOTO 96
      CURDEL=CURRMS-CURTOT(I,J)
      CURDAB=DABS(CURRMS-CURTOT(I,J))
      IF(CURDAB.LT.ERV) GO TO 90
      IF(CURDEL.LT.0.0) GO TO 82
      IF(LMM.EQ.1) GO TO 81
      IF(LNN.EQ.1) GO TO 81
      VL=VOLTI
      VOLTI=VL+0.5
      LLL=1
      GO TO 5
 81   CONTINUE
      VL=VOLTI
      VOLTI=VL+((VH-VL)/2.)
      LOO=1
      GO TO 5
 82   CONTINUE
      IF(LLL.EQ.1)GO TO 83
      IF(LOO.EQ.1)GO TO 83
      VH=VOLTI
      VOLTI=VH-0.5
      LNN=1
```

```
      GO TO 5
 83   CONTINUE
      VH=VOLTI
      VOLTI=VL+((VH-VL)/2.)
      LMM=1
      GO TO 5
 96   CONTINUE
      VCBAD(I,J)=1
 90   CONTINUE
C
C       ADJUST NEW T TO MATCH QCALC WITH QSYS (IF ALL THERMOCOUPLES
C       BAD DURING A GIVEN POWER SETTING)
C
      IF(LLLL.EQ.0)GO TO 200
      HCBAD(I,J)=2
      N1=N1+1
      IF(N1.GT.N1MAX)GO TO 198
      QDEL=QDTOT(I,J)-QSYSE(J)
      QDELAB=DABS(QDTOT(I,J)-QSYSE(J))
      IF(QDELAB.LT.ERQ) GO TO 200
      IF(QDEL.LT.0.0) GO TO 202
      IF(LM.EQ.1) GO TO 201
      IF(LN.EQ.1) GO TO 201
      DO 204 K=1,NOR
      TH(K)=T(I,J,K)
      TOLD(K)=TH(K)-20.0
 204  CONTINUE
      LL=1
      GO TO 3
 201  CONTINUE
      DO 205 K=1,NOR
      TH(K)=T(I,J,K)
      TOLD(K)=TL(K)+((TH(K)-TL(K))/2.)
 205  CONTINUE
      LO=1
      GO TO 3
 202  CONTINUE
      IF(LL.EQ.1)GO TO 203
      IF(LO.EQ.1)GO TO 203
      DO 206 K=1,NOR
      TL(K)=T(I,J,K)
      TOLD(K)=TL(K)+20.0
 206  CONTINUE
      LN=1
      GO TO 3
 203  CONTINUE
      DO 207 K=1,NOR
      TL(K)=T(I,J,K)
      TOLD(K)=TL(K)+((TH(K)-TL(K))/2.)
 207  CONTINUE
      LM=1
      GO TO 3
 198  CONTINUE
      HCBAD(I,J)=3
 200  CONTINUE
C
C       ADJUST H ESTIMATE FOR MEAS TEMP MATCH
C
      IF(IHCORR.EQ.0)GO TO 104
      IF(TCBD.EQ.1)GO TO 99
      N1=N1+1
      IF(N1.GT.N1MAX) GOTO 98
      IF(H(J).LE.0.0) GOTO 98
      IF(H(J).GT.100000.) GOTO 98
```

```
      TDEL=T(I,J,NOR)-TMEAS
      TDELAB=DABS(T(I,J,NOR)-TMEAS)
      IF(TDELAB.LT.ERRT) GO TO 104
      IF(TDEL.LT.0.0) GO TO 102
      IF(LM.EQ.1) GO TO 101
      IF(LN.EQ.1) GO TO 101
      HL=H(J)
      H(J)=HL+500.
      LL=1
      GO TO 3
 101  CONTINUE
      HL=H(J)
      H(J)=HL+((HH-HL)/2.)
      LO=1
      GO TO 3
 102  CONTINUE
      IF(LL.EQ.1)GO TO 103
      IF(LO.EQ.1)GO TO 103
      HH=H(J)
      H(J)=HH-500.
      LN=1
      GO TO 3
 103  CONTINUE
      HH=H(J)
      H(J)=HL+((HH-HL)/2.)
      LM=1
      GO TO 3
 98   CONTINUE
      HCBAD(I,J)=1
 99   CONTINUE
 104  CONTINUE
C       CONVERT TEMP FROM DEGR TO DEGC, QDOT FROM BTU/FT^2 S TO KW/M^2,
C       QGEN FROM BTU/FT^3 S TO KW/M^3, AND RAD FROM FT TO M
      DO 150 K=1,NOR
      T(I,J,K)=(T(I,J,K)-491.67)*(5./9.)
      QDOT(I,J,K)=QDOT(I,J,K)/8.827D-02
      QGEN(I,J,K)=QGEN(I,J,K)/(8.827D-02*0.3048)
      RADI(I,J,K)=RADI(I,J,K)*0.3048
      VOLTC(I,J)=VOLTI
      HC(I,J)=H(J)
 150  CONTINUE
C       CONVERT QDOT TOTAL FROM BTU/FT^2 S TO KW/M^2, QGEN TOT FROM
C       BTU/FT^3 S TO KW/M^3
      QDTOT(I,J)=QDTOT(I,J)/8.827D-02
      QGTOT(I,J)=QGTOT(I,J)/(8.827D-02*0.3048)
      RETURN
      END
C
C
      SUBROUTINE GSI(TOLD,NOR,IMAT,DR,H,TB,VOLTI,RO,RI,LGTH,BETA,T,
     $          QDOT,QGEN,RADI,QDTOT,QGTOT,CURTOT,RESTOT,KMT)
C
C       GAUSS-SEIDEL ITERATION OF TEMPERATURES AT NOR NODES THRU WALL.
C       RELAXATION IS USED TO DECREASE COMPUTATION TIME: 1. < BETA < 2.
C
      IMPLICIT REAL*8(A-H,M-Z)
      COMMON I,J,K
      DIMENSION T(10,0:20,0:300),TOLD(0:300),QDOT(10,0:20,300),
     $         RADI(10,0:20,300),QGEN(10,0:20,300),
     $         QDTOT(10,0:20),QGTOT(10,0:20),CURTOT(10,0:20),
     $         RHO(0:300),KMAT(0:300),RES(300),H(0:20),
     $         RESTOT(10,0:20),KMT(10,0:20,0:300),QDOTT(10,0:20)
      REAL*8 KMAT,LGTH,KMT
      INTEGER NOR
```

```
      PI=3.14159
      DO 10 K=1,NOR
      T(I,J,K)=TOLD(K)
      CALL PROP(IMAT,T,RHO,KMAT)
 10   CONTINUE
      DEL=0.0
      QDOTT(I,J)=0.0
      QDTOT(I,J)=0.0
      QGTOT(I,J)=0.0
      CURTOT(I,J)=0.0
      VOLTOT=0.0
      RESTOT(I,J)=0.0
      VOLT=VOLTI
      DO 50 K=1,NOR
      RADI(I,J,K)=RO-DEL*DR
      T(I,J,NOR+1)=T(I,J,NOR-1)
 25   CONTINUE
      KMAT(NOR+1)=KMAT(NOR-1)
 30   CONTINUE
      IF(K.NE.1) GOTO 35
C
C        OUTER WALL NODE
C
      AS=2.*PI*RO*LGTH
      ACS=PI*DR*RO
      RES(K)=(RHO(K)*LGTH)/ACS
      QD=(3600.*0.948*(VOLT**2.))/(RES(K)*AS*1000.)
      VOL=LGTH*ACS
      QG=(QD*AS)/VOL
      A=1./(H(J)+((KMAT(K+1)+KMAT(K))/(2.*DR))-((KMAT(K+1)+KMAT(K))/
     $  (4.*RO)))
      B=H(J)*TB
      C=((KMAT(K+1)+KMAT(K))/2.)*((T(I,J,K+1)/DR)-(T(I,J,K+1)/(2.*RO)))
      D=QG*(DR/2.)
      IF(J.NE.9)GO TO 34
 34   CONTINUE
      T(I,J,K)=A*(B+C+D)
      GO TO 45
 35   CONTINUE
      IF(K.NE.NOR) GOTO 40
C
C        INNER WALL NODE
C
      AS=2.*PI*RI*LGTH
      ACS=PI*DR*RI
      RES(K)=(RHO(K)*LGTH)/ACS
      QD=(3600.*0.948*(VOLT**2.))/(RES(K)*AS*1000.)
      VOL=LGTH*ACS
      QG=(QD*AS)/VOL
      A=1./((KMAT(K-1)+KMAT(K))*((RI/DR)+(1./2.)))
      B=(KMAT(K-1)+KMAT(K))*((RI/DR)+(1./2.))*T(I,J,K-1)
      C=QG*DR*RI
      T(I,J,K)=A*(B+C)
      GO TO 45
 40   CONTINUE
C
C        INTERIOR NODES
C
      AS=2.*PI*RADI(I,J,K)*LGTH
      ACS=2.*PI*DR*RADI(I,J,K)
      RES(K)=(RHO(K)*LGTH)/ACS
      QD=(3600.*0.948*(VOLT**2.))/(RES(K)*AS*1000.)
      VOL=LGTH*ACS
      QG=(QD*AS)/VOL
```

```
      A=1./(((KMAT(K-1)+(2.*KMAT(K))+KMAT(K+1))/(2.*DR))+((KMAT(K-1)-
     $     KMAT(K+1))/(4.*RADI(I,J,K))))
      B=(((KMAT(K-1)+KMAT(K))/(2.*DR))+((KMAT(K-1)+KMAT(K))/
     $     (4.*RADI(I,J,K))))*T(I,J,K-1)
      C=(((KMAT(K+1)+KMAT(K))/(2.*DR))-((KMAT(K+1)+KMAT(K))/
     $     (4.*RADI(I,J,K))))*T(I,J,K+1)
      D=QG*DR
      T(I,J,K)=A*(B+C+D)
 45   CONTINUE
      QDOT(I,J,K)=QD/3600.
      QGEN(I,J,K)=QG/3600.
      QDT=(QD*AS)/3600.
      QDOTT(I,J)=QDOTT(I,J)+QDT
      ASO=2.*PI*RO*LGTH
      QDTOT(I,J)=QDOTT(I,J)/ASO
      ACSO=PI*(RO**2.-RI**2.)
      QGTOT(I,J)=(QDTOT(I,J)*ASO)/(LGTH*ACSO)
      CURTOT(I,J)=CURTOT(I,J)+(VOLT/RES(K))
      VOLTOT=VOL+VOLTOT
      KMT(I,J,K)=KMAT(K)
C       RELAXATION
      T(I,J,K)=BETA*T(I,J,K)+(1.-BETA)*TOLD(K)
      CALL PROP(IMAT,T,RHO,KMAT)
      DEL=DEL+1.
 50   CONTINUE
      RETURN
      END
C
C
      SUBROUTINE PROP(IMAT,T,RHO,KMAT)
      IMPLICIT REAL*8(A-H,M-Z)
      COMMON I,J,K
      DIMENSION T(10,0:20,0:300),RHO(0:300),KMAT(0:300),TM(0:300)
      REAL*8 KMAT
      TM(K)=T(I,J,K)-460.
      IF(TM(K).GT.60.)GO TO 5
      TM(K)=60.
 5    CONTINUE
      IF(IMAT.GT.1) GOTO 10
C       304 SS
      RHO(K)=-9.3199D-06*TM(K)**2+4.6853D-02*TM(K)+74.02
      KMAT(K)=-5.4055D-10*TM(K)**2+1.83635D-06*TM(K)+0.002191
      GO TO 40
 10   CONTINUE
      IF(IMAT.GT.2) GOTO 20
C       COPPER
      RHO(K) = 1.3092D-06 * TM(K)**2 + 2.5470D-03 * TM(K) + 1.7264
      KMAT(K) = -7.3176D-10 * TM(K)**2 - 4.2147D-06 * TM(K) + 0.064234
      GO TO 40
 20   CONTINUE
      IF(IMAT.GT.3) GOTO 30
C       AMZIRC
      RHO(K) = 1.6752D-06 * TM(K)**2 + 2.0008D-03 * TM(K) + 2.0714
      KMAT(K) = -1.534D-11 * TM(K)**3 + 2.006D-08 * TM(K)**2 -
     $        2.4263D-07 * TM(K) + 0.04205
      GO TO 40
 30   CONTINUE
C       INCONEL
      IF(TM(K).GT.1000.) GO TO 35
      RHO(K) = 2.58927D-06 * TM(K)**2 + 1.42497D-03 * TM(K) + 40.4211
      GO TO 38
 35   CONTINUE
      IF(TM(K).GT.1500.) GO TO 36
      RHO(K) = 44.5
```

```
      GO TO 38
 36   CONTINUE
      RHO(K) =-4.76131D-06 * TM(K)**2 + 1.98756D-02 * TM(K) + 25.3955
 38   CONTINUE
C       CONVERT INCONEL RESISTIVITY FROM MICRO OHM-IN TO MICRO OHM-CM
      RHO(K) = RHO(K) * 2.54
      KMAT(K) = 1.4806D-06 * TM(K) + 0.0022
 40   CONTINUE
C       CONVERT R FROM MICRO OHM-CM TO OHM-FT
      RHO(K)=RHO(K)*1.0D-06*0.03281
C       CONVERT K FROM BTU/FT S F TO BTU/FT HR F
      KMAT(K)=KMAT(K)*3600.
      RETURN
      END
```

APPENDIX 3. Concluded

c. Input File

```
       25        13        53        38        09        06      1994         1         2        10
        5        14         2         1         1      100.       101       1.6      0.01       10.         1         1       10.       50.
     0.71      0.75      0.95        6.       44.         0     1000.       77.      84.5
   633.63  853.7563  828.2037  816.3025  793.2175  55.14045   79.1676  0.029725  0.028878  15.97095  10.88588  37.87353  22.58263  0.157004  0.124645  0.001124        0.        0.     2500.
 634.2838  853.0225    827.84   816.005    792.83  54.92823  79.61064  0.036964   0.03577  323.0362  780.9288  783.8825  982.6637  4.867846  4.527926  2.813166     2500.     2100.     4200.
 636.8412  853.0713  827.7212   816.035  794.1338  54.55207  80.43555  0.059511   0.05753  650.4275  1447.891   1405.46  1787.014  10.59414  9.518516  6.151276     6900.     5000.     5400.
 636.8625  852.1913  826.6113  815.2575  792.7287  54.30951  82.09371  0.096168  0.097149  981.4775  2153.107  1938.977  2447.976  17.28646  15.82082  10.33265    16100.    11800.     6700.
 635.8375   850.365   823.965  813.7825  792.2375  54.11674  84.65298  0.161768   0.16284  1364.606  2787.912  2401.549   3076.98  25.38047  23.72396  15.62902    32700.    25000.     8000.
 635.8212  849.7287  823.7187    812.73  792.0987  54.11263  88.95045  0.262643  0.269861  1797.466  3234.336  2795.474  3547.199  34.54892  34.07561  22.30774    57300.    51200.    10000.
 635.5125   849.665   823.265  811.9238    790.28  54.70548  94.45484  0.405356  0.416041  2276.626  3573.308   3213.77  3923.914  44.32634  44.85943   29.6128    90400.    87800.    12000.
 636.2425  849.6963  822.9037    811.46  791.3812  54.72182   98.2171  0.498258  0.505233  2524.456  3739.951  3426.821  4107.722   49.6115  50.53749  33.65447   110900.   110200.    13000.
 637.0037  849.6775  822.4025  811.0262    789.41  54.91556  101.7362  0.578346  0.596108  2767.799  3883.032  3638.382  4262.288  54.42775  55.47657  37.27871   131800.   131700.    14000.
 636.1113  848.3575  821.3337    809.72  787.9425  55.50662  105.7291  0.675076  0.692879  3039.895  4022.312  3875.179  4411.259   59.5305  60.52173  41.05567   156000.   155000.    15000.
 635.3937   848.225  821.2075   809.255  786.4388  55.63834   110.055   0.78193  0.803505  3296.757  4141.629  4093.474  4566.163  64.60586  65.65656  44.85564   181400.   180500.    16000.
   634.98  847.5213  819.7663  807.8588  786.3888   55.5217  112.0463  0.828536   0.85234  3418.076  4205.317  4195.135  4644.327  66.73448  67.85773  46.40832   193000.   192200.    17000.
 634.9937  847.1025  819.1125   806.995  786.9725  55.60354  114.4725  0.886525  0.914643  3557.564  4265.759  4311.313  4726.818  69.39959  70.49523  48.38977   207500.   207000.    18000.
 636.3075  847.3813  819.9875  808.1637   786.465  55.61068  117.3187  0.957877  0.988224  3699.219  4316.225    4425.9   4811.67  72.26642  73.47911   50.6503   223500.   223600.    19000.
 635.7088  846.9638  820.2888  808.3468  786.4925  56.58424  120.5825   1.03507  1.077516  3840.668  4357.427  4534.138  4889.661  75.64839  76.86768  53.34202   242000.   242000.    20000.
      0.5  81.17814         0
     1.75  81.23014         0
       3.  80.80918         0
     4.25  81.27375         0
      5.5  80.98421         0
      0.5  98.73266         0
     1.75  116.1361         0
       3.  99.69065         0
     4.25  97.38865         0
      5.5  101.8045         0
      0.5  147.8006         0
     1.75  160.0438         0
       3.  139.4519         0
     4.25  137.0795         0
      5.5  129.5323         0
      0.5    224.22         0
     1.75  231.4363         0
       3.  210.6775         0
     4.25   204.235         0
      5.5  197.8241         0
      0.5  320.3462         0
     1.75  318.4137         0
       3.   298.315         0
     4.25  298.0913         0
      5.5  316.9588         0
      0.5    449.47         0
     1.75  445.6187         0
       3.  444.5913         0
     4.25  405.0913         0
      5.5  419.7191         0
      0.5  663.0612         0
     1.75  659.1888         0
       3.  674.6925         0
     4.25  633.5388         0
      5.5  672.4072         0
      0.5  863.6975         0
     1.75  867.7825         0
       3.  800.0525         0
     4.25  823.7512         0
      5.5  830.8747         0
      0.5   1005.32         0
     1.75   1018.45         0
       3.  1012.094         0
     4.25  1008.199         0
      5.5  1014.553         0
      0.5   1156.42         0
     1.75  1159.285         0
       3.   1179.62         0
     4.25  1175.208         0
      5.5   1182.47         0
      0.5   1352.47         0
     1.75  1371.237         0
       3.   1362.87         0
     4.25  1358.691         0
      5.5   1365.69         0
      0.5  1461.088         0
     1.75  1459.108         0
       3.   1453.18         0
     4.25    1448.9         0
      5.5   1455.76         0
```

0.5	1530.22	0
1.75	1540.346	0
3.	1543.628	0
4.25	1538.684	0
5.5	1545.225	0
0.5	1594.55	0
1.75	1619.214	0
3.	1630.3	0
4.25	1625.67	0
5.5	1632.86	0
0.5	1695.65	0
1.75	1704.33	0
3.	1712.76	0
4.25	1707.44	0
5.5	1714.32	0

APPENDIX 4. Sample Data Tabulations

a. Sample Raw Data for a Power Setting

From File: TEST5.RAW recorded SEP 6, 1994

SCAN #	--TIME--- HR	MN	SEC	EMANPRES PSIG	WMANPRES PSIG	EMANTEMP DEGF	WMANTEMP DEGF	TSPRES1 PSIG	TSPRES2 PSIG	TSPRES3 PSIG	TSPRES4 PSIG	A-VDC VOLTS	A-ARMS ARMS	A-ADC ADC	B-VDC VOLTS	B-ARMS ARMS	B-ADC ADC	TS-VDC VOLTS	WATFLOW GPM	TSTEMP1 DEGF	TSTEMP2 DEGF	TSTEMP3 DEGF	TSTEMP4 DEGF	TSTEMP5 DEGF	TSTEMP6 DEGF
Begin Raw File Without Title																									
0	13	59	12.758	994.8	635.2	77.9952	88.7153	849.3	823.8	812.7	791.4	34.5968	2795.9	1797.7	34.1266	3547.4	3235.4	22.306	84.189	496.1	487.9	392.7	351.3	357.3	357.6
1	13	59	12.808	995	632.9	77.9427	88.77	849.6	824	812	791.1	34.5809	2795.9	1798	34.1107	3547.4	3235.4	22.3122	84.1609	496.9	491.4	393	350.8	356.2	358.2
2	13	59	12.858	996.5	635.7	77.8961	88.937	850.9	824.6	814	793.3	34.6048	2795.9	1797.7	34.1346	3547.4	3235.2	22.3091	84.1328	495.7	495.6	393.2	351.9	357.3	359
3	13	59	12.908	995.4	637	77.7751	89.0305	850	823.5	813.3	791.9	34.6048	2796.7	1798	34.1266	3548.2	3235.2	22.3122	84.0625	492.8	498.7	393.1	353.6	360	358.9
4	13	59	12.958	994.8	635.1	77.9865	89.0262	849.9	824.1	812.4	791.3	34.5968	2795.9	1797.5	34.1505	3548.2	3235.4	22.3184	84.0203	495.4	499.3	393.8	352.6	359.3	360.1
5	13	59	13.008	996.6	637.1	77.7707	89.0262	850.6	825.4	813.8	792	34.6048	2795.9	1797.7	34.1266	3549	3235.4	22.3184	83.9992	494.8	497.4	393.8	353	360	360.4
6	13	59	13.058	995	638.9	77.7751	89.0305	849.9	824.4	812.4	792	34.5809	2796.7	1798	34.1266	3547.4	3235.2	22.3091	83.95	493.6	494.2	393.9	354.3	361.7	360.7
7	13	59	13.108	996	635.5	77.9909	88.8175	850.9	825.8	813.9	793	34.5889	2795.9	1797.7	34.1186	3546.6	3235.2	22.3122	83.9218	492.9	490.3	393.6	355.5	363.6	360.3
8	13	59	13.158	994.9	634.9	77.9821	88.7023	851.3	823.8	814.1	793.3	34.5809	2795.9	1797.7	34.1266	3545.1	3233.9	22.3091	83.8726	491.3	487.6	393.3	356.1	364.4	358.3
9	13	59	13.208	995	637	77.7707	89.0262	850.6	824.7	812.8	791.6	34.5968	2795.2	1797.5	34.1186	3547.4	3233.9	22.3091	83.8656	497.8	487	393.6	352.9	360	358.7
10	13	59	13.258	996.3	639.7	77.9865	88.8132	851.1	825.1	814	792.7	34.5889	2795.2	1798.2	34.1107	3548.2	3233.9	22.2967	83.8445	497.6	489.5	392.9	353	360.5	357.3
11	13	59	13.308	994.3	634.9	77.8742	88.7023	849.8	824.4	811.9	791.4	34.5968	2795.9	1797.7	34.1266	3546.6	3234.2	22.3184	83.8937	498.9	494.1	393.6	352.3	361.4	357.7
12	13	59	13.358	995.8	634	77.9909	88.924	850.4	824.6	813.5	792.5	34.6048	2795.2	1797.2	34.1186	3546.6	3234.4	22.3153	83.9781	502.8	498.5	393.9	349.3	359.4	358.9
13	13	59	13.408	994.8	636.3	77.8786	88.8132	849.9	824.5	813.3	792.2	34.5809	2795.2	1797.2	34.1107	3547.4	3235.2	22.3153	83.9359	502.9	501.7	393.4	349.8	359.9	359.9
14	13	59	13.458	995.8	635.9	77.8786	89.0262	850.3	823.6	812.8	792.1	34.5968	2795.9	1797.2	34.1186	3546.6	3234.2	22.2998	84.1187	500.6	502.2	393.2	351.1	361.6	360
15	13	59	13.508	995.9	636.9	77.9909	89.137	850.1	824.2	813.5	792.8	34.5809	2795.9	1797.7	34.1107	3547.4	3234.4	22.3029	84.1398	498.5	499.8	391.4	352.3	362.6	358.4
16	13	59	13.558	996.5	636.2	77.9821	89.0219	850.8	824.9	814	792.2	34.5809	2795.9	1797.2	34.1107	3547.4	3233.9	22.3122	84.1258	500.4	495.3	390.9	352.2	362.6	356.8
17	13	59	13.608	995.3	635.4	77.883	88.8175	850.3	824.5	813.5	791.4	34.5889	2795.2	1797.7	34.0947	3545.8	3232.4	22.3122	84.1117	499.1	490.8	390.7	353.4	364	355.9
18	13	59	13.658	995.5	635.1	77.7663	88.7023	849.9	823.7	813.1	792.9	34.5889	2795.2	1797.5	34.1027	3548.2	3232.9	22.3091	84.0976	495	487.8	390.4	355.7	366.9	355.9
19	13	59	13.708	995.2	637.9	77.9821	89.1284	849.7	824	812.7	791.6	34.5889	2795.2	1797.2	34.1107	3549	3233.7	22.3091	84.0484	494.1	486.9	390.1	356.3	367.5	355.4
20	13	59	13.758	996.4	636.9	77.883	88.8175	849.9	824.7	813.3	793	34.5889	2795.9	1797.5	34.0947	3545.1	3234.4	22.3122	84.1047	494.6	489.2	390.3	356	366.8	353.7
21	13	59	13.808	994.5	635.1	77.8742	88.8089	849	823.4	811.9	791.2	34.565	2795.9	1797.5	34.0947	3551.3	3234.2	22.306	84.0625	496.7	493.8	390.7	355	365.7	348.5
22	13	59	13.858	997.3	635.5	77.9996	88.9327	851.2	825.5	814.6	794.2	34.5809	2795.2	1797.2	34.0788	3541.9	3234.4	22.306	84.0414	498.4	498.5	390.9	353.9	364.6	349.2
23	13	59	13.908	995.6	634.7	77.9909	88.8175	849.5	824	812.5	791.5	34.557	2794.4	1797	34.0389	3545.1	3234.7	22.3029	84.0062	500.3	500.7	390.7	353	363.7	350
24	13	59	13.958	993.9	635.7	77.8917	88.9327	849.1	823.6	811.9	792.3	34.5729	2795.9	1796.7	34.1983	3547.4	3234.2	22.3029	83.9781	502.2	500.6	390.9	352.1	362.5	347
25	13	59	14.008	994.2	636.2	77.7707	88.9197	850.7	824.9	813.7	791.4	34.565	2795.9	1797	33.9991	3548.2	3233.7	22.306	83.9781	500.1	498.6	390.9	353.6	364.1	346.1
26	13	59	14.058	997.2	638	77.9952	88.9284	851.2	825.8	815.2	793.1	34.5809	2794.4	1797.2	34.0469	3549	3233.9	22.306	84.0414	498.8	494.3	391.4	354.9	364.7	345.5
27	13	59	14.108	994.7	635.5	77.8786	88.8132	849.5	823.7	812.4	789.8	34.565	2795.2	1797.5	34.0071	3547.4	3234.7	22.3029	84.0484	499.1	489.5	391.6	356.1	365.5	346.9
28	13	59	14.158	996	636.9	77.9909	88.711	851.2	825.7	814	792.5	34.549	2795.2	1797.2	34.0708	3547.4	3234.4	22.306	84.0414	499.2	487.5	392	356.6	365.7	350
29	13	59	14.208	996	637.5	77.7751	88.711	851.6	826.1	814	793.3	34.5729	2795.9	1797.2	34.0868	3547.4	3234.9	22.306	84.1187	499.6	488.6	392.5	356.5	365.5	351.9
30	13	59	14.258	995	637.1	77.9865	88.9197	849.7	823.5	812.3	792.7	34.565	2795.9	1797.7	34.0629	3549	3234.7	22.306	84.1117	498.4	492.1	392.7	356.6	366.5	353
31	13	59	14.308	996.1	637.5	77.8786	88.8132	851.7	827	814.1	793.3	34.557	2795.9	1797.7	34.0708	3549	3235.2	22.3091	84.0976	499	497.2	392.9	356.4	367.1	355
32	13	59	14.358	995	635	77.8874	88.8218	849.6	823.8	811.9	792	34.565	2796.7	1797.5	34.0708	3547.4	3235.2	22.3029	84.0765	498.5	501.7	393.2	356.8	367.1	355
33	13	59	14.408	995.8	636.4	78.1031	88.8218	851.6	825.1	813.9	793.5	34.5968	2794.4	1797.2	34.0629	3547.4	3235.4	22.3091	84.0484	501.4	502.8	393.8	355.3	364.9	355.3
34	13	59	14.458	995.3	633.3	77.8786	88.9197	849.7	823.1	812.6	791.5	34.4773	2795.2	1797.7	34.0708	3548.2	3235.2	22.306	84.1328	506.4	501.6	393.9	353.2	364.1	354.6
35	13	59	14.508	995.3	633.4	77.8917	88.8262	850.5	824.6	814.1	792.8	34.6526	2796.7	1798	34.0629	3548.2	3235.2	22.3122	84.1398	502	498.2	393	355.4	367.5	353
36	13	59	14.558	996.2	631.9	77.8874	88.8218	850.3	825.5	813.3	792.3	34.5171	2796.7	1797.7	34.0708	3547.4	3234.9	22.3153	84.0695	503.5	493.6	393.1	355	367.3	353.9
37	13	59	14.608	995.2	633.2	77.8917	88.9327	850.3	824.8	812.7	781.2	34.4853	2796.7	1798.5	34.0708	3546.6	3234.9	22.3153	84.0273	502.4	489.7	393.2	356	369.1	355.3
38	13	59	14.658	996.1	637.3	77.7663	88.8089	850.5	825.3	814.1	826.9	34.5092	2795.2	1798	34.0549	3547.4	3234.7	22.3091	84.0132	506.8	488	393.6	354.6	367.3	357
39	13	59	14.708	995.8	636	77.8786	88.9197	850.1	824	812.8	761.4	34.541	2795.2	1797.5	34.0629	3548.2	3235.2	22.3153	84.0062	510.6	490.4	394	353	364.5	357.3
40	13	59	14.758	995.9	638.1	77.883	89.0305	850.2	825	812.8	820.8	34.557	2795.2	1797.5	34.0629	3549	3234.9	22.3153	84.0484	504.1	495.9	393.8	355.7	367.3	356.2
41	13	59	14.808	994.7	635.9	77.6716	88.8218	849.7	824.9	812	775.5	34.5331	2795.2	1797.5	34.0549	3547.4	3234.7	22.3122	84.0343	502.9	502.1	393.8	356.3	367.8	354.4
42	13	59	14.858	995.8	637.2	77.883	88.924	850.9	826.2	787.7	787.3	34.5331	2794.4	1797.5	34.0549	3548.2	3234.7	22.3122	84.0132	500	506.4	393.5	357.6	368.8	353.2
43	13	59	14.908	995.3	635.8	77.9952	88.9284	849.5	824.5	801.9	794.7	34.5171	2795.2	1798	34.0469	3546.6	3234.4	22.3091	83.9781	499.1	507	393.6	357.6	368.6	353.9
44	13	59	14.958	994.7	634.5	77.7751	88.6045	849.6	820.2	821.9	793.4	34.5171	2796.7	1797.5	34.0469	3545.1	3233.9	22.306	83.964	499.8	504.8	394.5	357.3	368.2	354
45	13	59	15.008	996	637.4	77.883	89.137	851.2	823.4	807	793.8	34.5171	2795.9	1797.5	34.0549	3545.8	3233.7	22.3091	83.964	499.8	500	394.7	357.3	367.3	355.2
46	13	59	15.058	996.2	634.9	77.6716	88.7153	849.6	762.5	810.6	791.8	34.5092	2795.9	1797.5	34.0389	3545.1	3233.7	22.306	83.95	500.4	494.8	395	356.4	366.7	356.2
47	13	59	15.108	995.3	634	77.9909	89.0305	849.3	810.5	813.9	790.9	34.5171	2795.2	1797.2	34.0549	3546.6	3233.9	22.306	83.9711	498.8	489.8	395.2	354.8	367.6	356
48	13	59	15.158	996	636.7	77.883	89.0305	849	846.3	814.3	792.8	34.5092	2795.2	1797.5	34.0469	3546.6	3233.9	22.306	83.964	497.9	487.4	395.1	354.3	368.1	355.4
49	13	59	15.208	993.7	634.8	77.5636	88.9284	848.7	810.2	812.5	790.9	34.5251	2795.2	1797.5	34.0549	3546.6	3233.7	22.306	83.957	498.4	488.1	395.3	354	367.9	355.2
50	13	59	15.258	996.6	636.4	77.8786	88.9197	821.7	820.6	814.1	791.9	34.5171	2795.2	1798.2	34.0469	3546.6	3233.2	22.306	83.9429	502.1	492.2	395.7	351.9	367.1	353.3
51	13	59	15.308	996.2	635	77.8874	89.0349	840.2	827.9	813.7	792.1	34.5171	2795.9	1797.7	34.0469	3546.6	3233.7	22.3122	83.9218	502.2	497.4	396.1	351.4	366.2	352.5
52	13	59	15.358	995.4	634.6	77.883	89.5629	859.3	827.2	812.8	792	34.5092	2795.9	1798	34.0549	3546.6	3234.4	22.306	83.9429	499.8	502.4	396	353.2	367.3	354.3
53	13	59	15.408	995	634.8	77.8786	89.2392	841.9	826.3	813.6	792.2	34.5171	2794.4	1797.7	34.0549	3547.4	3234.2	22.306	83.95	500.6	504.6	396.5	352.8	367.2	356.1
54	13	59	15.458	996.2	635.3	77.7751	93.3859	846.8	825	813.2	791	34.5171	2794.4	1797.2	34.0708	3548.2	3234.7	22.3091	83.9711	499.6	504.3	396.5	353.7	367.8	355.5
55	13	59	15.508	994.8	633.9	77.6672	86.5776	851.7	824.7	813.7	792.1	34.5171	2795.9	1797.2	34.0629	3547.4	3235.2	22.3091	83.95	498.8	501.4	396.6	354.3	367.8	353.7
56	13	59	15.558	996.2	635	77.883	88.8175	851.4	826.1	813.9	792.7	34.5092	2796.7	1797.2	34.0389	3545.8	3234.9	22.306	83.9148	498.1	496.9	397.5	355.4	368.3	353.4
57	13	59	15.608	995	634.4	78.75	85.7272	849.7	825.1	812.7	791.1	34.5092	2795.2	1797	34.0469	3547.4	3234.9	22.2998	83.8585	502.6	491.7	397.8	353	365.9	353.6
58	13	59	15.658	995	633.7	82.7199	88.1738	849.9	824.4	812.9	790.9	34.5092	2793.6	1797	34.031	3548.2	3234.9	22.3029	83.9218	504.7	488.2	397.9	352.4	365.2	352.3
59	13	59	15.708	996.2	637.7	72.1456	90.2012	851.6	825.2	814.8	792.8	34.5092	2795.2	1797	34.0469	3546.6	3234.2	22.2998	83.9148	498.7	489	397.2	356.6	369.4	348.2
60	13	59	15.758	995.7	635.7	**ou**	89.4607	850.5	825.6	814.2	792	34.5092	2795.2	1798	34.0389	3546.6	3233.9	22.2998	83.9359	499.3	492.2	396.9	355.5	367.8	349.1
61	13	59	15.808	996.2	637.3	79.1767	89.4564	849.5	823.9	811.9	790.1	34.5012	2794.4	1797	34.0469	3547.4	3233.7	22.3029	83.9429	502.8	496.9	397.3	353.9	366.9	347
62	13	59	15.858	994.4	636.8	80.5716	89.1327	849.5	823.7	812	789.6	34.5092	2795.2	1797.5	34.0389	3546.6	3233.9	22.2998	83.9148	505.1	501.2	396.9	354.2	368.2	348.8
63	13	59	15.908	995.6	637.2	78.3101	89.1327	850.3	824.8	813.9	792.2	34.5092	2795.2	1797.2	34.0389	3548.2	3234.2	22.3029	83.8585	502.9	503.9	396.5	355.5	371.2	351.1
64	13	59	15.958	995.8	636.4	77.9865	89.665	849.9	825.3	813.2	791.9	34.5171	2795.9	1797.2	34.0629	3547.4	3233.9	22.3029	83.8796	502.8	503.4	396.8	355.9	372.5	357.2
65	13	59	16.008	995.2	636	77.9952	89.1413	849.4	823.1	811.6	790.9	34.5092	2793.6	1797	34.031	3547.4	3233.7	22.3029	83.8867	501.3	499.7	396.3	356.9	374.3	359.1
66	13	59	16.058	995.5	635.9	77.5549	89.0262	850.5	824	812.4	790.5	34.5251	2795.2	1797.2	34.0549	3546.6	3233.7	22.2998	83.9007	496.7	495.8	396.7	359.7	376.9	354.9
67	13	59	16.108	996.9	635.7	78.09	89.1284	850.5	825.6	813.5	792.6	34.5171	2794.4	1797.5	34.0469	3547.4	3233.4	22.3029	83.9218	494.3	491.8	397	361	378.4	355.6
68	13	59	16.158	994.7	632.9	77.7751	89.0305	849.5	824.5	812.4	790.7	34.5171	2795.2	1797.2	34.0629	3545.1	3233.2	22.306	83.8937	497.1	489.3	397	358.8	376.3	357.3
69	13	59	16.208	995	634.7	77.883	89.2435	850.8	823.9	812.2	791.6	34.5251	2795.9	1798	34.0629	3548.2	3232.7	22.3029	83.8163	500.4	490.5	397.9	357.4	375.3	359.1
70	13	59	16.258	994.5	636.6	77.6584	88.9154	850	824	812.2	792.3	34.5251	2795.9	1797.7	34.0549	3547.4	3232.9	22.3029	83.7601	504.6	495.2	398.5	355.2	372.9	362.1
71	13	59	16.308	995	637	77.9865	89.0262	849.7	823.7	812.6	791.5	34.541	2795.2	1797.5	34.0788	3546.6	3233.7	22.3122	83.7741	503.8	500.6	398.8	358.2	375.2	367.7
72	13	59	16.358	995.1	636.5	77.9865	88.8132	850.6	825.8	813.5	792.2	34.5331	2794.4	1797	34.0788	3545.1	3233.4	22.306	83.7952	500.4	504.3	398.4	359.3	375.5	364.3
73	13	59	16.408	994.2	633.3	77.7751	89.0305	849	823.6	811.4	791	34.541	2795.9	1797	34.0788	3545.8	3233.2	22.3122	83.8304	497.4	505	398.6	360.2	375.9	363.6
74	13	59	16.458	996.5	635.4	77.6672	89.0305	852.1	827.2	815.8	795	34.541	2795.2	1797	34.0788	3548.2	3233.7	22.306	83.8374	496.5	502.4	398.6	360	374.4	362.2
75	13	59	16.508	994.7	637.5	77.883	89.0305	849.7	823.7	812.8	790.5	34.5331	2795.2	1797	34.0629	3547.4	3234.4	22.3091	83.8234	497.1	497.9	398.8	358.8	371.8	360.3
76	13	59	16.558	995.9	636.8	77.9996	88.8262	850.8	824	812.5	793.1	34.5331	2795.2	1797.2	34.0708	3546.6	3234.9	22.306	83.8867	496.3	492.6	398.1	359.3	371.6	358.4
77	13	59	16.608	995.6	637.7	78.1075	88.9327	850.1	823.5	813.3	792.1	34.549	2795.9	1797.7	34.0868	3548.2	3234.7	22.3091	83.9148	498.9	488.6	398.4	357.3	369.8	358.6
78	13	59	16.658	994.8	635.5	77.9865	89.0262	849.9	824.5	812.6	791.1	34.557	2795.2	1797	34.0947	3546.6	3234.7	22.3122	83.9781	498.1	488.7	398.7	358.1	371	359.1
79	13	59	16.708	996.8	636	77.9909	89.0305	851.9	825.2	815.4	793.7	34.557	2795.9	1797.2	34.1027	3549	3235.7	22.3122	84.0625	498.2	492.5	399	358.7	372.1	360.1

TSTEMP7	TSTEMP8	DVTS1	DVTS2	DVTS3	TMPREF1	TMPREF2	BPTEMP1	BPTEMP2	BPTEMP3	BPTEMP4	BPTEMP5	BPTEMP6	BPTEMP7	BPTEMP8	TSTEMP9	TSTEMP10	TSPRESS5	DYNPRES	EGPTEMP	WGPTEMP	SDELTEMP	NDELTEMP	REFTMP1	REFTMP3	REFTMP5
DEGF	DEGF	VOLTS	VOLTS	VOLTS	DEGF	DEGF	DEGF	DEGF	DEGF	DEGF	DEGF	DEGF	DEGF	DEGF	DEGF	DEGF	PSID	PSI	DEGF	DEGF	MV	MV	DEGC	DEGC	DEGC
401.7	367.5	0.1751	0.282	0	78.7904	79.4378	90.993	90.3553	**eu**	**eu**	**eu**	**eu**	92.6914	**eu**	604.4	713	54.5301	810.6	73.5609	72.8015	0.2612	0.2734	23.3076	23.3662	24.2328
401	367.5	0.1751	0.282	0	79.0106	78.9027	90.7805	90.2489	**eu**	**eu**	**eu**	**eu**	92.9035	**eu**	604.3	713	54.1017	810.2	73.3997	72.8572	0.2612	0.2661	23.31	23.3369	24.2328
403	366.4	0.1703	0.282	0	78.3587	79.0062	90.5636	90.3509	**eu**	**eu**	**eu**	**eu**	93.0052	**eu**	604.4	712.9	53.9661	811.3	73.5697	72.9188	0.2637	0.271	23.3076	23.371	24.2304
411.5	365.9	0.1751	0.282	0	79.2637	79.3716	90.5636	90.2446	**eu**	**eu**	**eu**	**eu**	93.0052	**eu**	604.5	713.1	54.5872	811.1	73.5565	73.0141	0.2661	0.271	23.4516	23.3637	24.2304
395.1	367.8	0.1751	0.282	0	78.9713	79.295	90.7762	90.2446	**eu**	**eu**	**eu**	**eu**	92.8992	**eu**	604.6	713.2	54.3302	810.5	73.4436	72.7927	0.2685	0.271	23.288	23.3613	24.2304
395.7	368.9	0.1751	0.282	0	78.2929	78.7246	90.5636	90.1383	**eu**	**eu**	91.4136	**eu**	92.8992	**eu**	604.6	713.4	54.0446	811.3	73.6605	73.0097	0.2661	0.2637	23.0293	23.3613	24.2304
400.4	368.7	0.1751	0.2868	0	78.6932	79.1248	90.5679	90.1426	**eu**	**eu**	**eu**	**eu**	92.7975	**eu**	604.4	712.9	53.7305	811.1	73.448	72.6885	0.2637	0.2734	23.1928	23.3637	24.2328
400.3	369.4	0.18	0.2868	0.0049	79.0193	79.1272	90.6742	90.2489	**eu**	**eu**	**eu**	**eu**	92.7975	**eu**	604.3	712.9	54.2445	811.5	73.5565	72.7971	0.2685	0.2002	23.3149	23.3637	24.2328
413.8	370.1	0.1751	0.2771	0	78.9975	79.4291	90.5593	90.1339	**eu**	**eu**	91.5155	**eu**	92.8949	**eu**	604.5	713.4	54.1232	811.3	73.2223	72.8968	0.2588	0.2759	23.3027	23.3588	24.228
390.6	369.6	0.1751	0.282	0	78.8939	79.3255	90.7848	90.3596	**eu**	**eu**	**eu**	**eu**	92.9078	**eu**	604.5	713	54.1232	810.7	73.7689	72.9012	0.2661	0.3198	23.3051	23.3613	24.2353
395.9	369.4	0.1703	0.282	-0.0049	78.7904	79.3299	90.7675	90.236	**eu**	**eu**	91.405	**eu**	92.7846	**eu**	604.3	713	54.4659	811.5	73.6605	72.7927	0.2661	0.2368	23.3076	23.3613	24.2255
390.4	370.4	0.1703	0.2868	0	78.8852	78.8852	90.5636	90.3509	**eu**	**eu**	91.5198	**eu**	93.0052	**eu**	604.6	713.4	54.3302	810.1	73.7645	73.0053	0.2393	**ad**	23.3002	23.3588	24.2304
378.7	369.6	0.1751	0.282	-0.0049	78.7773	79.3168	90.7762	90.4573	**eu**	**eu**	91.626	**eu**	92.8992	**eu**	604.4	712.9	54.6158	810.8	73.5565	72.7971	0.354	0.3296	23.3002	23.3637	24.2304
384.4	370.1	0.1751	0.282	-0.0049	79.0106	79.3343	90.5722	90.2532	**eu**	**eu**	91.4223	**eu**	92.9078	**eu**	604.4	713.3	54.7086	810.3	73.3352	72.7927	0.3198	0.2661	23.31	23.3613	24.2353
390.4	369.4	0.1751	0.282	0	78.6781	79.2177	90.6699	90.3509	**eu**	**eu**	91.5198	**eu**	92.7932	**eu**	604.6	713.2	53.8019	810.7	73.6605	72.9012	0.1807	0.2783	23.3051	23.3613	24.2304
399.1	369.1	0.1703	0.2868	0	79.0062	79.3299	90.7805	90.3553	**eu**	**eu**	91.6303	**eu**	92.7975	**eu**	604.4	713.2	54.3017	811	73.6649	74.2069	-0.061	0.2759	23.3076	23.3637	24.2328
393.7	373.4	0.1751	0.2868	0	79.0018	79.2177	90.5636	90.2446	**eu**	**eu**	91.626	**eu**	92.7932	**eu**	604.6	713	54.3302	811	73.5477	76.3624	**ad**	0.2783	23.3051	23.3588	24.2304
394.6	371.4	0.1751	0.2868	0	78.786	79.3255	90.5722	90.1469	**eu**	**eu**	91.5285	**eu**	92.8018	**eu**	604.6	713.2	53.809	810.5	73.5565	79.8228	0.2759	0.2759	23.3051	23.3637	24.2353
404.4	369.4	0.1703	0.2868	0	78.7991	79.4465	90.7605	90.2489	**eu**	**eu**	91.4179	**eu**	92.7975	**eu**	604.4	713.3	54.2445	810.2	73.6561	71.8109	0.271	0.2637	23.3125	23.3588	24.2328
403.2	368.2	0.1703	0.282	0	78.8983	79.222	90.5636	90.2446	**eu**	**eu**	91.4136	**eu**	92.6871	**eu**	604.4	713.3	54.2802	810.8	74.0897	62.6338	0.2759	0.2685	23.3076	23.3588	24.2304
400.4	367	0.1751	0.282	0.0049	78.8939	79.1098	90.6656	90.1339	**eu**	**eu**	91.5155	**eu**	92.7889	**eu**	604.8	713.2	54.5301	811.1	65.6033	70.7324	0.2759	0.2759	23.3051	23.3637	24.228
391.4	366.9	0.1703	0.2868	-0.0049	78.8896	79.3212	90.6785	90.1469	**eu**	**eu**	91.5285	**eu**	92.6958	**eu**	604.5	713.5	54.423	809.6	78.6291	73.4392	0.2685	0.2734	23.3027	23.3588	24.2353
385.9	367.4	0.1751	0.282	0	78.7948	79.2264	90.453	90.3466	**eu**	**eu**	91.4093	**eu**	92.7889	**eu**	604.6	713.3	54.4516	811.6	72.6973	73.0229	0.2612	0.271	23.31	23.3686	24.228
384.8	366.8	0.1751	0.282	-0.0049	79.222	79.3299	90.5722	90.3596	**eu**	**eu**	91.5285	**eu**	93.1198	**eu**	604.5	713.4	54.3088	808.4	66.8065	73.1226	0.2612	0.2685	23.3076	23.3637	24.2353
380.7	367.1	0.1751	0.2771	0	78.7817	79.3212	90.7805	90.4616	**eu**	**eu**	91.5241	**eu**	92.9035	**eu**	604.5	713.2	54.266	828.1	72.1544	73.3484	0.2685	0.2685	23.3027	23.3686	24.2328
388.8	367.1	0.1751	0.2917	-0.0097	78.9027	78.9027	90.8954	90.1512	**eu**	**eu**	91.3204	**eu**	92.7001	**eu**	604.7	713.3	54.5515	812.7	73.8773	73.1182	0.271	0.2661	23.31	23.3613	24.2377
389.3	367.6	0.1703	0.2868	0	78.9114	79.4509	90.5593	90.5593	**eu**	**eu**	91.6217	**eu**	92.8949	**eu**	604.6	713.1	53.1593	813.2	73.8861	72.6929	0.2661	0.2685	23.3149	23.3662	24.228
383.1	369.5	0.18	0.2868	0	78.786	79.2177	90.6656	90.3466	**eu**	**eu**	91.5155	**eu**	92.8949	**eu**	604.7	713.3	54.0946	806.5	73.7689	73.1182	0.271	0.2685	23.3051	23.3613	24.228
381.9	369	0.1703	0.2771	0.0049	79.0018	79.5413	90.3553	90.3553	**eu**	**eu**	91.4179	**eu**	92.7975	**eu**	604.8	713.3	46.1555	810.2	73.7733	73.3396	0.2685	0.2685	23.3051	23.3637	24.2328
382.5	367.3	0.1751	0.282	0.0049	79.0106	79.4422	90.6742	90.4616	**eu**	**eu**	91.4179	**eu**	92.9035	**eu**	604.8	713.3	52.6667	811.8	73.7733	72.7971	0.2685	0.2734	23.31	23.3637	24.2328
387.7	366.6	0.1703	0.2771	-0.0049	78.8983	79.3299	90.6742	90.3553	**eu**	**eu**	91.4179	**eu**	92.9035	**eu**	604.6	713.6	51.7314	811	73.5521	72.9012	0.2661	0.2661	23.3076	23.3613	24.2328
388.1	367.5	0.1703	0.2868	-0.0049	79.1098	79.2177	90.7891	90.3639	**eu**	**eu**	91.639	**eu**	92.8061	**eu**	604.8	714.2	54.7443	811.8	73.8773	73.3352	0.2661	0.2685	23.3051	23.3613	24.2377
390.9	367.3	0.1751	0.2868	-0.0049	78.7948	79.2264	90.6742	90.2489	**eu**	**eu**	91.5241	**eu**	92.7975	**eu**	604.6	714.3	54.0089	810.6	73.8861	73.127	0.271	0.271	23.31	23.3662	24.2328
380.8	368	0.18	0.2868	0	78.9027	79.3343	90.5766	90.1512	**eu**	**eu**	91.5328	**eu**	92.9121	**eu**	604.8	713.6	54.7514	811.1	73.4524	73.0185	0.2661	0.271	23.31	23.3662	24.2377
356.2	369.4	0.1703	0.282	0.0049	78.8939	79.3255	90.5679	90.4616	**eu**	**eu**	91.6303	**eu**	92.9035	**eu**	604.6	713.1	54.1517	810.2	73.8773	72.7927	0.2661	0.271	23.3051	23.3613	24.2328
373.7	368.8	0.1751	0.2868	0	79.1185	79.55	90.5679	90.5679	**eu**	**eu**	91.6303	**eu**	92.9035	**eu**	605.5	713.2	54.6015	811.4	73.6737	73.0229	0.2685	0.271	23.31	23.3686	24.2328
371.2	368.8	0.1751	0.282	0.0049	78.9027	79.4422	90.5679	90.4616	**eu**	**eu**	91.6303	**eu**	92.9035	**eu**	605.7	713.2	54.3017	811	73.9945	72.91	0.2612	0.2759	23.31	23.3662	24.2328
380.8	370.3	0.1703	0.2868	0	79.1141	79.5457	90.3553	90.3553	**eu**	**eu**	91.4179	**eu**	93.0095	**eu**	604.6	713.2	54.5658	810.5	73.5653	73.0229	0.2685	0.2734	23.3076	23.3686	24.2328
361.2	372.8	0.1703	0.2868	-0.0049	78.907	79.3386	90.6699	90.2446	**eu**	**eu**	91.5198	**eu**	92.7932	**eu**	604.4	713.1	54.5444	811.2	73.7645	73.0053	0.271	0.271	23.3125	23.3588	24.2304
342.2	371.6	0.1703	0.2868	0	79.0062	79.222	90.6828	90.1512	**eu**	**eu**	91.5328	**eu**	93.0181	**eu**	604.4	713.1	54.3373	811.1	73.6605	73.2267	0.2661	0.2734	23.3076	23.3613	24.2377
367.5	370.7	0.1703	0.2868	0	79.0193	79.343	90.3553	90.4616	**eu**	**eu**	91.5241	**eu**	92.9035	**eu**	604.6	713	54.3302	810.8	73.6649	72.9056	0.2685	0.2734	23.3149	23.3637	24.2328
376.3	369.8	0.1751	0.282	0.0049	79.1185	79.6579	90.5679	90.2489	**eu**	**eu**	91.5241	**eu**	89.2913	**eu**	604.6	713	53.8876	810.4	73.7777	73.127	0.2661	0.2612	23.31	23.3662	24.2328
390.6	368.7	0.1751	0.282	0.0049	79.0149	79.3386	90.2446	90.3509	**eu**	**eu**	91.626	**eu**	93.641	**eu**	604.4	712.9	54.4087	811.3	73.8817	73.1226	0.2808	0.2685	23.3125	23.3637	24.2304
397.8	368.2	0.18	0.2868	0	78.7904	79.222	90.4616	90.1426	**eu**	**eu**	91.5241	**eu**	96.7119	91.4179	605	712.8	54.2945	810.3	73.6693	72.91	0.271	0.2612	23.3076	23.3662	24.2328
393.8	368	0.1751	0.2771	-0.0049	79.1141	79.5457	90.5679	90.2489	**eu**	**eu**	91.4179	**eu**	95.4443	**eu**	604.4	712.8	54.4944	810.1	73.5565	72.9056	0.2637	0.271	23.3076	23.3637	24.2328
393.7	368.4	0.1703	0.2868	0	79.2307	79.3386	90.4702	90.4702	**eu**	**eu**	91.639	**eu**	**eu**	**eu**	604.3	712.9	54.0589	811.2	73.6649	72.9056	0.2661	0.2685	23.3125	23.3637	24.2377
392	369.4	0.1703	0.2868	0	79.2264	79.2264	90.5809	90.2619	**eu**	**eu**	91.4309	**eu**	**eu**	**eu**	604.3	712.8	53.9804	811.2	73.6693	73.0185	0.2637	0.2685	23.31	23.3662	24.2402
399.7	368.8	0.1751	0.2771	0	78.7817	79.2133	90.2619	90.3682	**eu**	**eu**	91.5371	**eu**	93.3404	**eu**	604.2	712.6	53.9804	810.4	73.5565	72.9056	0.2661	0.271	23.3027	23.3637	24.2402
404.4	367.4	0.18	0.2868	0	79.0018	79.2177	90.3596	90.2532	**eu**	**eu**	91.5285	**eu**	93.9674	**eu**	604.3	712.8	53.9518	810.9	73.5565	73.0141	0.2612	0.2685	23.3051	23.3637	24.2353
397.4	367.2	0.1751	0.2868	-0.0049	78.8983	79.3299	90.4659	90.4659	**eu**	**eu**	91.7408	**eu**	93.5437	**eu**	604.1	712.5	54.2731	810	73.7777	73.0185	0.2637	0.2563	23.3076	23.3662	24.2353
376.1	368.6	0.1751	0.2868	-0.0049	78.6868	79.55	90.4486	90.3423	**eu**	**eu**	91.405	**eu**	94.0561	**eu**	604.3	712.6	54.5373	810.9	73.6605	72.9012	0.2661	0.2661	23.31	23.3613	24.2255
378.9	368.7	0.1751	0.2868	0.0049	78.8983	79.4378	90.4702	90.3639	**eu**	**eu**	91.5328	89.1935	94.2893	**eu**	604.3	712.6	54.5587	811	73.7777	72.6929	0.2637	0.2759	23.3076	23.3662	24.2377
384.2	367.3	0.1751	0.2868	0	79.0106	79.55	90.4616	90.3553	**eu**	**eu**	**eu**	90.7805	93.4334	**eu**	604	712.7	54.4659	810.2	73.6649	73.0141	0.2808	0.2685	23.31	23.3637	24.2328
380.1	367.8	0.1654	0.282	0	79.1098	79.3255	90.7762	90.2446	**eu**	**eu**	**eu**	90.3509	93.4291	**eu**	603.9	712.8	53.7948	810.5	73.8773	72.6841	0.2685	0.2685	23.3051	23.3613	24.2304
392.3	368.2	0.1751	0.282	-0.0049	79.1185	79.3343	90.5679	90.1426	**eu**	**eu**	91.4179	91.0993	94.069	**eu**	604	712.6	54.3731	810.8	73.8817	73.1226	0.2637	0.2734	23.31	23.3637	24.2328
403	368	0.1751	0.2868	0.0049	78.8983	79.4378	90.4616	90.1426	**eu**	**eu**	**eu**	90.7805	94.069	**eu**	604.2	712.7	54.1946	810.7	73.6649	72.9056	0.2612	0.2685	23.3076	23.3637	24.2328
411.2	368	0.1703	0.2868	-0.0049	79.1185	79.3343	90.4573	90.2446	**eu**	**eu**	**eu**	89.9255	93.641	**eu**	604	712.6	54.4159	811	73.7733	73.1226	0.2661	0.2661	23.31	23.3637	24.2304
387.1	368.9	0.1751	0.2771	-0.0049	78.6825	79.3299	90.4573	90.1383	**eu**	**eu**	**eu**	89.8191	93.3232	**eu**	603.9	712.5	54.4516	810.5	73.5609	73.0185	0.2661	0.2685	23.3076	23.3662	24.2304
374.6	369.9	0.1751	0.282	0	79.1141	79.222	90.3596	90.2532	**eu**	**eu**	**eu**	90.5722	93.8615	**eu**	604	712.8	54.0375	810.3	73.5521	72.7927	0.2588	0.2734	23.3076	23.3613	24.2353
399.7	369.8	0.18	0.2771	0	79.0062	79.3299	90.5722	90.4659	**eu**	95.1314	**eu**	90.6785	93.8615	**eu**	604.1	712.7	54.6229	811.6	73.6649	73.0141	0.2661	0.2685	23.3076	23.3637	24.2353
389.5	369.3	0.1751	0.282	0	78.9027	79.7658	90.2489	90.2489	**eu**	95.1271	**eu**	90.2489	93.6453	**eu**	604	712.5	54.7157	810.5	73.5609	72.91	0.2685	0.2685	23.31	23.3662	24.2328
364.4	369.1	0.1751	0.282	0.0097	78.9027	79.2264	90.6742	93.7513	**eu**	94.8098	**eu**	89.8234	93.4334	**eu**	604.2	712.8	54.6943	810.4	73.6649	72.9056	0.2612	0.2759	23.31	23.3637	24.2328
355	368.8	0.1751	0.282	0	78.9027	79.55	90.3553	72.6287	**eu**	95.4443	**eu**	90.2489	93.4334	**eu**	604.1	712.5	54.5444	810.1	73.5521	72.7927	0.2685	0.2637	23.31	23.3613	24.2328
361.6	370.2	0.1654	0.282	0.0049	78.8983	79.3299	90.7762	**eu**	**eu**	95.017	**eu**	90.5636	93.747	**eu**	604	712.8	53.6163	811	73.7689	72.6841	0.2661	0.2685	23.3076	23.3613	24.2304
369.1	370.9	0.1703	0.2868	0	79.1141	79.5457	90.4746	85.6769	**eu**	94.0819	**eu**	90.4746	93.8701	**eu**	604	712.6	53.7662	810.9	73.7689	73.1182	0.2661	0.271	23.3076	23.3613	24.2402
377.8	371.6	0.1703	0.2868	0	78.8983	79.5457	91.8383	70.9944	**eu**	94.4881	**eu**	90.2446	93.641	**eu**	604	712.7	54.2088	809.9	73.5609	73.127	0.2685	0.2612	23.3076	23.3662	24.2304
396.6	375.7	0.1703	0.2771	0	78.7948	79.4422	108.7	86.1983	**eu**	95.0213	**eu**	90.0362	93.6453	**eu**	604	712.4	54.1089	810.6	73.7689	73.0097	0.2612	0.271	23.31	23.3613	24.2328
401.4	374.5	0.1751	0.2868	0	78.8983	79.7614	**eu**	90.4616	**eu**	94.704	**eu**	90.4616	93.7513	**eu**	603.9	712.5	54.5658	811.2	73.5477	73.0053	0.2637	0.2685	23.3076	23.3588	24.2328
382.3	372.1	0.1751	0.2868	0.0097	79.1141	78.7904	97.7711	90.7848	**eu**	94.3908	**eu**	90.3596	93.7556	**eu**	604.2	712.8	54.0232	810	73.6649	72.7971	0.2637	0.2685	23.3076	23.3637	24.2353
369.1	374.6	0.1703	0.282	0	79.0062	79.3299	88.2173	91.4093	**eu**	94.6954	**eu**	90.1339	93.4248	**eu**	604.1	712.5	54.3231	810.1	73.6649	72.9056	0.2637	0.2685	23.3076	23.3637	24.228
350.3	373.2	0.1703	0.2771	-0.0097	78.7948	60.9085	87.9061	91.4179	**eu**	94.9156	**eu**	90.1426	93.4334	**eu**	603.7	712.7	54.2303	810.1	73.5477	72.8968	0.2661	0.2685	23.31	23.3588	24.2328
366.6	377.7	0.1751	0.2868	0	79.1141	73.3878	92.1697	90.5766	**eu**	94.7126	**eu**	90.3639	93.6539	**eu**	603.9	712.8	53.9161	810.2	73.6605	72.9012	0.2637	0.2685	23.3076	23.3613	24.2377
382.4	376.6	0.1703	0.2868	0.0049	83.4305	81.2755	91.5285	90.4659	**eu**	94.3908	**eu**	90.2532	93.6496	**eu**	604.1	712.6	54.5515	810.6	73.5521	72.7927	0.2661	0.2783	23.31	23.3613	24.2353
393	373	0.1751	0.2868	0	78.8939	74.0325	92.1654	90.9974	**eu**	94.285	**eu**	90.0405	93.3318	**eu**	604	712.8	54.1232	809.9	73.6649	73.1226	0.2637	0.2685	23.3051	23.3637	24.2353
397.4	370.4	0.1751	0.282	-0.0049	66.3381	78.1384	92.0592	91.3161	**eu**	94.4967	**eu**	89.9342	93.4378	**eu**	604.1	712.5	53.9018	811.8	73.6649	72.7971	0.2612	0.2685	23.3051	23.3637	24.2353
392.8	371.2	0.18	0.282	0	79.878	79.4465	91.4179	90.993	**eu**	94.8098	**eu**	90.2489	93.7513	**eu**	604.1	712.6	53.8304	810.4	73.5565	73.0141	0.2637	0.2637	23.3125	23.3637	24.2328
394.3	370.5	0.1751	0.282	0	79.3299	79.5457	90.993	90.6742	**eu**	94.2807	**eu**	90.1426	93.7513	**eu**	603.9	712.5	54.7157	810.9	73.5653	72.9144	0.2637	0.271	23.3076	23.3686	24.2328
378.7	373.2	0.1751	0.282	0	71.9896	79.6623	91.5198	90.4573	**eu**	94.5939	**eu**	90.1383	93.5351	**eu**	604	712.6	54.0161	810.8	73.5653	73.1314	0.2685	0.2685	23.3125	23.3686	24.2304
382.5	373.6	0.1751	0.2868	0.0049	77.0631	79.5457	92.0506	91.2012	**eu**	94.2764	**eu**	90.0319	93.641	**eu**	604.2	712.4	54.5872	810.2	73.5521	72.6841	0.2637	0.2734	23.3076	23.3613	24.2304
385.9	374.8	0.1751	0.2868	0	79.1228	79.5544	91.7365	91.0993	**eu**	94.704	**eu**	90.1426	93.4334	**eu**	603.9	712.6	54.4444	811.4	73.5565	72.7971	0.2685	0.2661	23.3125	23.3637	24.2328

APPENDIX 4. Concluded
b. Sample Reduced Data

Micro Craft Technology/AEDC
Arnold AFB, TN 37389
High Temperature Wall Laboratory (HTWL)
Project No. DD01VW, Job 0115

Date Computed	3-24-1995
Time Computed	10:53:57
Date Recorded	9- 6-1994
Time Recorded	13:53:38

*** HTWL REDUCED DATA ***

PAGE 1

RUN NO.	WALL MATL	HEATER TUBE ID (MM)	HEATER TUBE OD (MM)	ANNULUS ID (MM)	ANNULUS OD (MM)	TUBE LENGTH (MM)	FLOW LOOP
25	SS	18.034	19.050	19.050	24.130	152.40	CLSD

*** CONDITIONS ***

PMAN-IN (BAR)	TMAN-IN (DEG-C)	WATER FLOW (LPM)	WATER FLOW (KG/S)	G (KG/M^2 S)	VEL (M/S)	R(WATER) (uS/CM)
70.0	25.00	319.8	5.31	30818.2	30.9	44.00

AXIAL LOCATION FROM L.E. OF TUBE 12.70 MM

POWER SETTING	QDOT-TS (KW/M^2)	QDOT-SYS (KW/M^2)	QDOT-TOT (KW/M^2)	QDOT-CALC (KW/M^2)	TWALL (DEG-C)	TW1D (DEG-C)	TBULK (DEG-C)	TSAT (DEG-C)	DTSAT (DEG-C)	DTSUB (DEG-C)
0	.0	1825.9	.9	1.7	27.26	27.29	25.08	271.99	-244.73	246.91
1	544.9	2260.8	909.9	1391.4	27.28	12.91	25.10	271.96	-244.68	246.86
2	2153.1	3623.8	1665.9	4719.7	32.94	-14.50	25.16	271.95	-239.01	246.80
3	7734.4	5968.8	12538.9	9321.4	41.23	-41.80	25.26	271.86	-230.63	246.60
4	13441.4	10000.3	21278.8	15335.7	52.56	-72.14	25.43	271.62	-219.06	246.19
5	20570.1	16372.0	31677.2	21536.7	62.90	-82.64	25.71	271.60	-208.70	245.89
6	29081.0	25201.2	43759.3	28400.3	75.65	-49.43	26.09	271.56	-195.91	245.47
7	34137.4	30751.6	50743.5	32335.9	83.17	14.66	26.33	271.52	-188.36	245.20
8	38947.6	35952.1	57363.0	36150.6	89.73	47.38	26.55	271.48	-181.74	244.92
9	44228.2	41826.1	64624.5	41197.7	128.21	81.05	26.81	271.38	-143.17	244.57
10	49916.8	48412.5	72445.4	46833.8	183.11	138.15	27.09	271.36	-88.26	244.27
11	52437.4	51297.8	76005.3	50036.0	217.32	169.75	27.22	271.24	-53.91	244.02
12	55622.8	54929.8	80374.5	52839.2	235.21	178.99	27.37	271.18	-35.97	243.81
13	59282.0	59299.1	85266.6	55515.4	234.40	182.17	27.56	271.26	-36.85	243.70
14	63456.2	64309.1	90698.9	58698.1	261.48	206.67	27.78	271.27	-9.80	243.50

Micro Craft Technology/AEDC
Arnold AFB, TN 37389
High Temperature Wall Laboratory (HTWL)
Project No. DD01VW, Job 0115

Date Computed 3-24-1995
Time Computed 10:53:57
Date Recorded 9- 6-1994
Time Recorded 13:53:38

*** HTWL REDUCED DATA ***

PAGE 2

AXIAL LOCATION FROM L.E. OF TUBE 44.45 MM

POWER SETTING	QDOT-TS (KW/M^2)	QDOT-SYS (KW/M^2)	QDOT-TOT (KW/M^2)	QDOT-CALC (KW/M^2)	TWALL (DEG-C)	TW1D (DEG-C)	TBULK (DEG-C)	TSAT (DEG-C)	DTSAT (DEG-C)	DTSUB (DEG-C)
0	.0	1825.9	.9	1.7	27.30	27.32	25.28	270.70	-243.40	245.43
1	544.9	2260.8	909.9	1391.1	27.53	22.59	25.34	270.68	-243.15	245.33
2	2153.1	3623.8	1665.9	4718.1	33.33	-7.64	25.55	270.68	-237.35	245.13
3	7734.4	5968.8	12538.9	9377.0	41.86	-38.58	25.90	270.59	-228.72	244.68
4	13441.4	10000.3	21278.8	15400.4	53.62	-73.99	26.51	270.36	-216.74	243.85
5	20570.1	16372.0	31677.2	21516.3	64.63	-84.06	27.48	270.34	-205.70	242.86
6	29081.0	25201.2	43759.3	28364.0	78.30	-50.35	28.81	270.28	-191.97	241.47
7	34137.4	30751.6	50743.5	32391.9	86.40	17.08	29.65	270.24	-183.84	240.60
8	38947.6	35952.1	57363.0	36308.4	93.51	53.67	30.44	270.19	-176.68	239.76
9	44228.2	41826.1	64624.5	41201.4	127.97	82.53	31.32	270.08	-142.11	238.76
10	49916.8	48412.5	72445.4	47073.8	190.73	148.16	32.32	270.06	-79.33	237.74
11	52437.4	51297.8	76005.3	50042.0	216.95	168.48	32.75	269.94	-52.99	237.18
12	55622.8	54929.8	80374.5	52852.0	234.42	184.25	33.30	269.88	-35.46	236.57
13	59282.0	59299.1	85266.6	56008.8	243.61	192.38	33.96	269.96	-26.35	235.99
14	63456.2	64309.1	90698.9	58980.3	268.96	209.89	34.72	269.95	-.99	235.23

Micro Craft Technology/AEDC
Arnold AFB, TN 37389
High Temperature Wall Laboratory (HTWL)
Project No. DD01VW, Job 0115

Date Computed 3-24-1995
Time Computed 10:53:57
Date Recorded 9- 6-1994
Time Recorded 13:53:38

*** HTWL REDUCED DATA ***

PAGE 3

AXIAL LOCATION FROM L.E. OF TUBE 76.20 MM

POWER SETTING	QDOT-TS (KW/M^2)	QDOT-SYS (KW/M^2)	QDOT-TOT (KW/M^2)	QDOT-CALC (KW/M^2)	TWALL (DEG-C)	TW1D (DEG-C)	TBULK (DEG-C)	TSAT (DEG-C)	DTSAT (DEG-C)	DTSUB (DEG-C)
0	.0	1825.9	.9	1.7	27.08	27.09	25.47	269.41	-242.33	243.94
1	544.9	2260.8	909.9	1390.7	27.77	13.47	25.59	269.39	-241.62	243.81
2	2153.1	3623.8	1665.9	4716.5	33.72	-19.02	25.94	269.40	-235.69	243.46
3	7734.4	5968.8	12538.9	9372.6	42.50	-49.95	26.55	269.32	-226.82	242.77
4	13441.4	10000.3	21278.8	15390.3	54.68	-84.79	27.59	269.09	-214.41	241.50
5	20570.1	16372.0	31677.2	21496.0	66.36	-83.92	29.24	269.07	-202.71	239.83
6	29081.0	25201.2	43759.3	28522.9	80.96	-43.24	31.53	269.00	-188.04	237.47
7	34137.4	30751.6	50743.5	32447.9	89.64	-20.39	32.97	268.96	-179.32	235.99
8	38947.6	35952.1	57363.0	36556.4	98.59	49.17	34.32	268.91	-170.32	234.59
9	44228.2	41826.1	64624.5	41445.9	134.14	93.18	35.84	268.78	-134.64	232.94
10	49916.8	48412.5	72445.4	47103.8	188.86	142.62	37.55	268.76	-79.90	231.22
11	52437.4	51297.8	76005.3	49742.1	212.36	167.32	38.29	268.64	-56.28	230.35
12	55622.8	54929.8	80374.5	52858.4	234.03	185.90	39.24	268.58	-34.55	229.34
13	59282.0	59299.1	85266.6	55909.5	249.63	201.30	40.37	268.65	-19.02	228.29
14	63456.2	64309.1	90698.9	59131.5	275.48	214.30	41.67	268.63	6.85	226.96

Micro Craft Technology/AEDC
Arnold AFB, TN 37389
High Temperature Wall Laboratory (HTWL)
Project No. DD01VW, Job 0115

Date Computed 3-24-1995
Time Computed 10:53:57
Date Recorded 9- 6-1994
Time Recorded 13:53:38

*** HTWL REDUCED DATA ***

PAGE 4

AXIAL LOCATION FROM L.E. OF TUBE 107.95 MM

POWER SETTING	QDOT-TS (KW/M^2)	QDOT-SYS (KW/M^2)	QDOT-TOT (KW/M^2)	QDOT-CALC (KW/M^2)	TWALL (DEG-C)	TW1D (DEG-C)	TBULK (DEG-C)	TSAT (DEG-C)	DTSAT (DEG-C)	DTSUB (DEG-C)
0	.0	1825.9	.9	1.7	27.34	27.34	25.67	268.12	-240.78	242.45
1	544.9	2260.8	909.9	1390.4	28.01	12.20	25.83	268.11	-240.09	242.28
2	2153.1	3623.8	1665.9	4714.9	34.10	-20.27	26.33	268.13	-234.02	241.80
3	7734.4	5968.8	12538.9	9368.3	43.14	-53.37	27.19	268.05	-224.91	240.85
4	13441.4	10000.3	21278.8	15455.1	55.74	-85.69	28.67	267.83	-212.08	239.15
5	20570.1	16372.0	31677.2	21475.7	68.10	-105.16	31.01	267.80	-199.71	236.79
6	29081.0	25201.2	43759.3	28486.6	83.62	-64.88	34.25	267.72	-184.10	233.46
7	34137.4	30751.6	50743.5	32503.8	92.88	-7.07	36.29	267.68	-174.81	231.39
8	38947.6	35952.1	57363.0	36498.6	102.37	48.91	38.20	267.62	-165.26	229.42
9	44228.2	41826.1	64624.5	41488.9	131.43	89.37	40.36	267.48	-136.06	227.13
10	49916.8	48412.5	72445.4	46838.3	182.81	141.46	42.77	267.46	-84.65	224.69
11	52437.4	51297.8	76005.3	49759.8	211.27	164.43	43.83	267.34	-56.07	223.51
12	55622.8	54929.8	80374.5	52858.7	234.00	183.14	45.17	267.28	-33.28	222.11
13	59282.0	59299.1	85266.6	56063.1	255.66	198.36	46.77	267.35	-11.69	220.58
14	63456.2	64309.1	90698.9	58958.2	270.31	212.21	48.61	267.30	3.01	218.69

Micro Craft Technology/AEDC
Arnold AFB, TN 37389
High Temperature Wall Laboratory (HTWL)
Project No. DD01VW, Job 0115

Date Computed 3-24-1995
Time Computed 10:53:57
Date Recorded 9- 6-1994
Time Recorded 13:53:38

*** HTWL REDUCED DATA ***

PAGE 5

AXIAL LOCATION FROM L.E. OF TUBE 139.70 MM

POWER SETTING	QDOT-TS (KW/M^2)	QDOT-SYS (KW/M^2)	QDOT-TOT (KW/M^2)	QDOT-CALC (KW/M^2)	TWALL (DEG-C)	TW1D (DEG-C)	TBULK (DEG-C)	TSAT (DEG-C)	DTSAT (DEG-C)	DTSUB (DEG-C)
0	.0	1825.9	.9	1.7	27.19	27.18	25.87	266.83	-239.64	240.96
1	544.9	2260.8	909.9	1390.1	28.26	14.67	26.07	266.82	-238.56	240.75
2	2153.1	3623.8	1665.9	4713.4	34.49	-24.40	26.72	266.85	-232.36	240.13
3	7734.4	5968.8	12538.9	9363.9	43.77	-56.77	27.84	266.78	-223.00	238.94
4	13441.4	10000.3	21278.8	15445.0	56.81	-74.84	29.75	266.56	-209.76	236.81
5	20570.1	16372.0	31677.2	21629.7	70.89	-97.80	32.78	266.54	-195.64	233.76
6	29081.0	25201.2	43759.3	28637.2	87.45	-43.49	36.97	266.44	-178.99	229.46
7	34137.4	30751.6	50743.5	32559.8	96.11	-2.97	39.61	266.40	-170.29	226.79
8	38947.6	35952.1	57363.0	36656.9	106.15	51.42	42.08	266.34	-160.19	224.26
9	44228.2	41826.1	64624.5	41419.6	135.79	95.59	44.87	266.18	-130.40	221.31
10	49916.8	48412.5	72445.4	47082.1	190.20	144.83	48.00	266.16	-75.96	218.16
11	52437.4	51297.8	76005.3	49746.6	212.07	168.62	49.37	266.04	-53.97	216.67
12	55622.8	54929.8	80374.5	52853.6	234.31	186.92	51.10	265.98	-31.67	214.88
13	59282.0	59299.1	85266.6	56031.4	257.60	203.22	53.17	266.05	-8.45	212.88
14	63456.2	64309.1	90698.9	59109.0	276.85	215.77	55.55	265.98	10.87	210.43

* * * DOWNSTREAM BURNOUT OCCURRED IN TRANSIENT TO NEXT SET POINT * * *

Micro Craft Technology/AEDC
Arnold AFB, TN 37389
High Temperature Wall Laboratory (HTWL)
Project No. DD01VW, Job 0115

Date Computed	3-24-1995
Time Computed	10:53:57
Date Recorded	9- 6-1994
Time Recorded	13:53:38

*** HTWL REDUCED DATA ***

PAGE 6

POWER SETTING	E-TS (KW)	E-SYS (KW)	E-TOT (KW)	E-CALC (KW)	IREC-TOT (AMPS)	IRMS-TOT (AMPS)	VREC-TOT (VOLTS)	VRMS-TOT (VOLTS)	DVTS-DC (VOLTS)	DVTS-RMS (VOLTS)
0	.0	16.7	.0	.0	26.9	60.5	.1	.1	.0	.0
1	5.0	20.6	8.3	12.7	1104.0	1766.5	4.7	4.7	2.8	2.8
2	19.6	33.1	15.2	43.0	2098.3	3192.5	10.1	4.8	6.2	6.2
3	70.5	54.4	114.4	85.4	3134.6	4387.0	16.6	26.1	10.3	16.1
4	122.6	91.2	194.1	140.9	4152.5	5478.5	24.6	35.4	15.6	22.4
5	187.6	149.3	288.9	197.3	5031.8	6342.7	34.3	45.6	22.3	29.6
6	265.2	229.9	399.1	261.2	5849.9	7137.7	44.6	55.9	29.6	37.2
7	311.4	280.5	462.8	297.0	6264.4	7534.5	50.1	61.4	33.7	41.3
8	355.2	327.9	523.2	334.3	6650.8	7900.7	55.0	66.2	37.3	45.0
9	403.4	381.5	589.4	377.8	7062.2	8286.4	60.0	71.1	41.1	48.7
10	455.3	441.6	660.8	429.4	7438.4	8659.6	65.1	76.3	44.9	52.6
11	478.3	467.9	693.2	453.7	7623.4	8839.5	67.3	78.4	46.4	54.1
12	507.3	501.0	733.1	482.1	7823.3	9038.1	69.9	81.1	48.4	56.1
13	540.7	540.9	777.7	511.0	8015.4	9237.6	72.9	84.2	50.7	58.5
14	578.8	586.5	827.2	539.1	8198.1	9423.8	76.3	87.8	53.3	61.4

Micro Craft Technology/AEDC
Arnold AFB, TN 37389
High Temperature Wall Laboratory (HTWL)
Project No. DD01VW, Job 0115

Date Computed 3-24-1995
Time Computed 10:53:57
Date Recorded 9- 6-1994
Time Recorded 13:53:38

*** HTWL REDUCED DATA ***

PAGE 7

POWER SETTING	PTS1 (BAR)	PTS2 (BAR)	PTS3 (BAR)	PTS4 (BAR)	DPTS (BAR)	PMAN-OUT (BAR)	TMAN-OUT (DEG-C)	DTMAN (DEG-C)
0	59.9	58.1	57.3	55.7	3.80	44.7	26.20	.75
1	59.8	58.1	57.3	55.7	3.79	44.8	26.45	.93
2	59.8	58.1	57.3	55.8	3.76	44.9	26.91	1.49
3	59.8	58.0	57.2	55.7	3.75	44.9	27.83	2.45
4	59.7	57.8	57.1	55.7	3.73	44.9	29.25	4.10
5	59.6	57.8	57.1	55.6	3.73	44.9	31.64	6.72
6	59.6	57.8	57.0	55.5	3.77	44.8	34.70	10.34
7	59.6	57.8	57.0	55.6	3.77	44.9	36.79	12.62
8	59.6	57.7	56.9	55.5	3.79	44.9	38.74	14.75
9	59.5	57.7	56.9	55.4	3.83	44.9	40.96	17.16
10	59.5	57.6	56.8	55.3	3.84	44.8	43.36	19.86
11	59.5	57.5	56.7	55.2	3.83	44.8	44.47	21.05
12	59.4	57.5	56.7	55.3	3.83	44.8	45.82	22.54
13	59.5	57.6	56.7	55.3	3.84	44.9	47.40	24.33
14	59.4	57.6	56.8	55.3	3.90	44.9	49.21	26.39

POWER SETTING NO. 0

ST 1	QDOT TOT = 1.7 KW/M^2	QGEN TOT = 3452.9 KW/M^3	CURR TOT = 62.4 AMPS	VOLT CORR = .25 VOLTS	H CORR = 14.2 KW/M^2 C
ST 2	QDOT TOT = 1.7 KW/M^2	QGEN TOT = 3452.8 KW/M^3	CURR TOT = 62.4 AMPS	VOLT CORR = .25 VOLTS	H CORR = 14.2 KW/M^2 C
ST 3	QDOT TOT = 1.7 KW/M^2	QGEN TOT = 3453.7 KW/M^3	CURR TOT = 62.5 AMPS	VOLT CORR = .25 VOLTS	H CORR = 14.2 KW/M^2 C
ST 4	QDOT TOT = 1.7 KW/M^2	QGEN TOT = 3452.7 KW/M^3	CURR TOT = 62.4 AMPS	VOLT CORR = .25 VOLTS	H CORR = 14.2 KW/M^2 C
ST 5	QDOT TOT = 1.7 KW/M^2	QGEN TOT = 3453.3 KW/M^3	CURR TOT = 62.4 AMPS	VOLT CORR = .25 VOLTS	H CORR = 14.2 KW/M^2 C

MEASURED VALUES: RMS CURRENT = 60.5 AMPS TEST SECTION VOLTAGE = .00 VOLTS H ESTIMATE = 14.2 KW/M^2 C

TC1 = 27.3 DEG-C TC2 = 27.4 DEG-C TC3 = 27.1 DEG-C TC4 = 27.4 DEG-C TC5 = 27.2 DEG-C

CALCULATED VALUES:

RADIUS (MM)	T1 (DEG-C)	QDOT (KW/M^2)	QGEN (KW/M^3)	RESIDUAL (DEG-C)	T2 (DEG-C)	QDOT (KW/M^2)	QGEN (KW/M^3)	RESIDUAL (DEG-C)
9.525	27.3	.0	3453.	.0099	27.3	.0	3453.	.0091
9.475	27.3	.0	3453.	.0099	27.3	.0	3453.	.0091
9.424	27.3	.0	3453.	.0099	27.3	.0	3453.	.0091
9.373	27.3	.0	3453.	.0099	27.3	.0	3453.	.0091
9.322	27.3	.0	3453.	.0099	27.4	.0	3453.	.0091
9.271	27.3	.0	3453.	.0099	27.4	.0	3453.	.0091
9.221	27.3	.0	3453.	.0099	27.4	.0	3453.	.0091
9.170	27.3	.0	3453.	.0099	27.4	.0	3453.	.0091
9.119	27.3	.0	3453.	.0099	27.4	.0	3453.	.0091
9.068	27.3	.0	3453.	.0099	27.4	.0	3453.	.0091
9.017	27.3	.0	3453.	.0099	27.4	.0	3453.	.0091

RADIUS (MM)	T3 (DEG-C)	QDOT (KW/M^2)	QGEN (KW/M^3)	RESIDUAL (DEG-C)	T4 (DEG-C)	QDOT (KW/M^2)	QGEN (KW/M^3)	RESIDUAL (DEG-C)
9.525	27.1	.0	3454.	.0096	27.3	.0	3453.	.0099
9.475	27.1	.0	3454.	.0096	27.4	.0	3453.	.0099
9.424	27.1	.0	3454.	.0096	27.4	.0	3453.	.0099
9.373	27.1	.0	3454.	.0096	27.4	.0	3453.	.0099
9.322	27.1	.0	3454.	.0096	27.4	.0	3453.	.0099
9.271	27.1	.0	3454.	.0096	27.4	.0	3453.	.0099
9.221	27.1	.0	3454.	.0096	27.4	.0	3453.	.0099
9.170	27.1	.0	3454.	.0096	27.4	.0	3453.	.0099
9.119	27.1	.0	3454.	.0096	27.4	.0	3453.	.0099
9.068	27.1	.0	3454.	.0096	27.4	.0	3453.	.0099
9.017	27.1	.0	3454.	.0096	27.4	.0	3453.	.0099

RADIUS (MM)	T5 (DEG-C)	QDOT (KW/M^2)	QGEN (KW/M^3)	RESIDUAL (DEG-C)
9.525	27.2	.0	3453.	.0097
9.475	27.2	.0	3453.	.0097
9.424	27.2	.0	3453.	.0097
9.373	27.2	.0	3453.	.0097
9.322	27.2	.0	3453.	.0097
9.271	27.2	.0	3453.	.0097
9.221	27.2	.0	3453.	.0097
9.170	27.2	.0	3453.	.0097
9.119	27.2	.0	3453.	.0097
9.068	27.2	.0	3453.	.0097
9.017	27.2	.0	3453.	.0097

POWER SETTING NO. 14

ST 1	QDOT TOT = 58698.1 KW/M^2	QGEN TOT = 118707389.5 KW/M^3	CURR TOT = 9414.5 AMPS	VOLT CORR = 57.00 VOLTS	H CORR = 249.2 KW/M^2 C
ST 2	QDOT TOT = 58980.3 KW/M^2	QGEN TOT = 119278056.4 KW/M^3	CURR TOT = 9418.4 AMPS	VOLT CORR = 57.25 VOLTS	H CORR = 252.1 KW/M^2 C
ST 3	QDOT TOT = 59131.5 KW/M^2	QGEN TOT = 119583840.6 KW/M^3	CURR TOT = 9422.0 AMPS	VOLT CORR = 57.38 VOLTS	H CORR = 252.1 KW/M^2 C
ST 4	QDOT TOT = 58958.2 KW/M^2	QGEN TOT = 119233245.9 KW/M^3	CURR TOT = 9414.9 AMPS	VOLT CORR = 57.25 VOLTS	H CORR = 266.2 KW/M^2 C
ST 5	QDOT TOT = 59109.0 KW/M^2	QGEN TOT = 119538254.7 KW/M^3	CURR TOT = 9418.4 AMPS	VOLT CORR = 57.38 VOLTS	H CORR = 266.2 KW/M^2 C

MEASURED VALUES: RMS CURRENT = 9423.8 AMPS TEST SECTION VOLTAGE = 61.42 VOLTS H ESTIMATE = 113.3 KW/M^2 C

TC1 = 924.3 DEG-C TC2 = 929.1 DEG-C TC3 = 933.8 DEG-C TC4 = 930.8 DEG-C TC5 = 934.6 DEG-C

CALCULATED VALUES:

RADIUS (MM)	T1 (DEG-C)	QDOT (KW/M^2)	QGEN (KW/M^3)	RESIDUAL (DEG-C)	T2 (DEG-C)	QDOT (KW/M^2)	QGEN (KW/M^3)	RESIDUAL (DEG-C)
9.525	261.5	372.3	146584263.	.0025	269.0	373.6	147094934.	.0001
9.475	404.5	680.1	133878960.	.0038	413.2	682.8	134399299.	.0063
9.424	521.5	640.4	126053389.	.0049	531.3	643.1	126584319.	.0063
9.373	619.2	613.9	120848610.	.0060	630.0	616.7	121392519.	.0063
9.322	700.9	595.6	117246616.	.0070	712.6	598.5	117805168.	.0063
9.271	768.6	582.8	114709515.	.0079	781.1	585.7	115283274.	.0063
9.221	823.3	573.7	112922655.	.0086	836.5	576.7	113511017.	.0063
9.170	865.5	567.4	111689894.	.0092	879.4	570.5	112291114.	.0063
9.119	895.6	563.3	110885623.	.0097	909.9	566.4	111496917.	.0063
9.068	913.7	561.0	110431303.	.0099	928.2	564.2	111049033.	.0063
9.017	919.8	280.1	110283866.	.0100	934.4	281.7	110903825.	.0063

RADIUS (MM)	T3 (DEG-C)	QDOT (KW/M^2)	QGEN (KW/M^3)	RESIDUAL (DEG-C)	T4 (DEG-C)	QDOT (KW/M^2)	QGEN (KW/M^3)	RESIDUAL (DEG-C)
9.525	275.5	373.6	147068642.	.0013	270.3	373.3	146956022.	.0000
9.475	418.9	683.6	134560606.	.0014	414.4	682.3	134310798.	.0064
9.424	536.6	644.3	126833137.	.0014	532.4	642.8	126521037.	.0064
9.373	634.9	618.2	121689788.	.0015	631.0	616.5	121343994.	.0064
9.322	717.4	600.1	118132364.	.0027	713.6	598.3	117766114.	.0064
9.271	785.8	587.4	115630332.	.0038	782.1	585.5	115250641.	.0064
9.221	841.1	578.5	113871799.	.0046	837.5	576.5	113482851.	.0064
9.170	883.8	572.3	112661436.	.0053	880.3	570.3	112266044.	.0064
9.119	914.3	568.3	111873590.	.0058	910.8	566.3	111473892.	.0064
9.068	932.7	566.1	111429371.	.0061	929.2	564.0	111027179.	.0064
9.017	938.8	282.7	111285367.	.0061	935.3	281.7	110882353.	.0064

RADIUS (MM)	T5 (DEG-C)	QDOT (KW/M^2)	QGEN (KW/M^3)	RESIDUAL (DEG-C)
9.525	276.9	373.2	146928781.	.0012
9.475	420.1	683.1	134470962.	.0014
9.424	537.7	644.0	126768806.	.0014
9.373	636.0	618.0	121640338.	.0014
9.322	718.4	599.9	118092497.	.0027
9.271	786.7	587.3	115596979.	.0037
9.221	842.0	578.4	113842989.	.0046
9.170	884.8	572.2	112635780.	.0053
9.119	915.3	568.2	111850021.	.0058
9.068	933.6	566.0	111406998.	.0060
9.017	939.7	282.6	111263386.	.0061

TEMP DISTRIBUTION DID NOT CONVERGE IF "1" APPEARS

NP	STATION	1	2	3	4	5
0		0	0	0	0	0
1		0	0	0	0	0
2		0	0	0	0	0
3		0	0	0	0	0
4		1	0	0	0	0
5		0	0	0	0	0
6		0	0	0	0	0
7		0	0	0	0	0
8		0	0	0	0	0
9		0	0	0	0	0
10		0	0	0	0	0
11		0	0	0	0	0
12		0	0	0	0	0
13		0	0	0	0	0
14		0	0	0	0	0

VOLTAGE CORRECTION DID NOT CONVERGE IF "1" APPEARS

NP	STATION	1	2	3	4	5
0		0	0	0	0	0
1		0	0	0	0	0
2		0	0	0	0	0
3		0	0	0	0	0
4		0	0	0	0	0
5		0	0	0	0	0
6		0	0	0	0	0
7		0	0	0	0	0
8		0	0	0	0	0
9		0	0	0	0	0
10		0	0	0	0	0
11		0	0	0	0	0
12		0	0	0	0	0
13		0	0	0	0	0
14		0	0	0	0	0

H CORRECTION DID NOT CONVERGE IF "1" APPEARS; IF "2" APPEARS THE TC MEASUREMENT IS SUSPECT - Q INSTEAD OF H CORRECTION PERFORMED;
Q CORRECTION DID NOT CONVERGE IF "3" APPEARS

NP	STATION	1	2	3	4	5
0		0	0	0	0	0
1		1	1	1	1	1
2		1	1	1	1	1
3		1	1	1	1	1
4		1	1	1	1	1
5		1	1	1	1	1
6		1	1	1	1	1
7		1	1	1	1	1
8		1	1	1	1	1
9		0	0	0	0	0
10		0	0	0	0	0
11		0	0	0	0	0
12		0	0	0	0	0
13		0	0	0	0	0
14		0	0	0	0	0